Nuclear Spectroscopy with Neutrons

Carlos Granja

Institute of Experimental and Applied Physics

Czech Technical University in Prague

www.utef.cvut.cz

Thanks to the organizers

Questions

Lecture available on request:

carlos.granja@utef.cvut.cz

Outline

- Introduction & terms
- Neutron sources & detectors
- Nuclear spectroscopy

break

- Example of complete nuclear spectroscopy

Neutrons in Nuclear Physics & Applications

Neutrons are a powerful tool to probe

- **nuclear motion, nuclear matter and structure**
- **the stability of matter and their fundamental role**
- **neutron-induced reactions: resonances & reaction mechanisms**
- astrophysical objects & stellar nucleosysnthesis (element abundancies)
- basic neutron properties and interactions

Neutron induced reactions

are a **rich source of data in nuclear spectroscopy**.

Use of the neutron as a probe to obtain **information on nuclear properties (nuclear structure and nuclear reaction mechanisms)**.

As such a tool, neutron reactions have advantages over other reactions (e.g., methods available for **gamma-ray spectroscopy** provide high presicion and accuracy unmatched by other techniques).

Applications

- reactor design
- nuclear waste & spent fuel transmutation
- nuclear fusion & energy production (d,t) → *n* 's [14 MeV]
- (not only in) energy applications → demand for presice nuclear data
- radiochemistry
- medicine: diagnosis, radiotherapy
- industrial uses: materials production, testing and analysis, radiation damage
- analytical methods (Activation Analysis, ...)
- biology, materials science, archeology, enviromental studies, condensed matter (diffraction studies)

Glossary of Terms I *

• **SPECTROSCOPY** The branch of physics concerned with the **production**, **measurement**, and **interpretation** of (radiation) **spectra** arising from either **emission** or **absorption** of **radiant energy** by various substances (nuclei).

• **NUCLEAR SPECTROSCOPY** The **measurement** of the **energy spectrum, angular distribution, etc...** of **particles emitted** or **scattered** in a **nuclear reaction or decay** to obtain **information about the target and the residual nuclei**.

• **NEUTRON SPECTROSCOPY**

  • **Measurement** of **transmission curves** from which **neutron** and **total widths of resonances** can be deduced.

  • Part of Neutron Physics studying the **energy dependence of effective cross sections of different neutron – nuclei interactions** and the **characteristics of formed excited states** in nuclei [BAI-2002].

  • Collection of **instruments and techniques for neutron detection and measurement**.

• **STATISTICAL NUCLEAR PHYSICS** the application of both **statistical spectroscopy** and the **statistical theory of nuclear reactions** (e.g., **compound nucleus reactions**).

• **THEORY** An **attempt to explain a class of phenomena** by deducing them as necessary consequences of other phenomena regarded as more primitive and less in need of explanation. More general & more weight!.

• **MODEL** A **mathematical or physical system**, obeying certain specified conditions (**parameters**), whose behaviour is used to understand a **particular physical system** to which is analogous in some way. Used to describe nuclear reactions. More specific, less weight!

There are both **Theories** and **Models** of both **Nuclear Structure** and **Nuclear Reactions**.

* *Glossary of terms of the International Union of Pure and Applied Physics IUPAC*

Glossary of Terms II*

CLASSIFICATION OF NEUTRONS BY KINETIC ENERGY*

• **COLD** *Neutrons* have a ***temperature*** **considerably lower than normal room temperature**.

• **DELAYED** *Neutrons* **emitted by *fission products*** formed by nuclear decay (the observed delay is due to the lifetime of the preceding nuclear decay or decays.

• **EPICADMIUM** *Neutrons* of **kinetic energy greater than the effective cadmiun cut-off (~0.5 eV)** for neutrons.

• **EPITHERMAL** *Neutrons* of **kinetic energy greater than that of thermal agitation**. The term is often restricted to energies just above thermal (generally 25 meV).

• **FAST** *Neutrons* of **kinetic energy greater than** some specified value (**≥ 0.1 MeV**). This value may vary over a wide range and will be dependent upon the application, such as reactor physics, shielding or dosimetry.

• **FISSION** *Neutrons* **originating in the *fission* process** which have retained their original energy.

• **INTERMEDIATE** *Neutrons* of **kinetic energy between the energies of *slow* and *fast neutrons*** . In reactor physics, the range might be **1 eV to 0.1 MeV**.

• **PROMPT** *Neutrons* **accompanying the *fission* process** without measurable delay.

• **RESONANCE** *Neutrons* , the energy of which corresponds to the ***resonance energy*** **of a specified *nuclide*** or *element* . If the nuclide is not specified, the term refers to resonance neutrons of ^{238}U.

• **SLOW** *Neutrons* of **kinetic energy less than** some specified value (**≤ 1 eV**). This value may vary over a wide range and depends on the application. In reactor physics, the value is frequently chosen to be 1 eV; in dosimetry, the effective cadmium cut-off is used.

• **THERMAL** *Neutrons* in **thermal equilibrium with the medium in which they exist** (generally, but not necessarily, 25 meV – room temperature)

* *Glossary of terms of the International Union of Pure and Applied Physics IUPAC*

Neutrons by kinetic energy

Neutrons called	$E_{kinetic}$	T, K	velocity	Wavelength, λ
UCN	~250 neV	~0.003	~ 7 m/s	~ 600 Å
Cold	<3 meV	<35	~ 760 m/s	~ 5 Å = $5 \cdot 10^{-8}$ cm
Thermal	~25.9 meV	300	~ 2,224 m/s	~ 1.8 Å
Resonance	~1 eV	~10^4	~$1.4 \cdot 10^4$ m/s	~ 0.3 Å
Slow	~100 eV	~10^6	~$1.4 \cdot 10^5$ m/s	~ 0.03 Å
Intermed. energy	~10 keV	~10^8	~$1.4 \cdot 10^6$ m/s	~ 0.003 Å
Fast	~ 1 MeV	~10^{10}	~ 0.046 c	~ 0.0003 Å
High energy	~ 100 MeV	~10^{12}	~ 0.43 c	~ 3 fm= $3 \cdot 10^{-13}$ cm
Relativistic	>1 GeV	>10^{13}	> 0.875 c	< 0.9 fm

→ **Ultra Cold Neutrons** are reflected from the surface of most substances like ping pong balls and can thus exist in hollow vessels for long times (**neutron bottles**)

Neutron Sources

According to

- technique of production
- application
- neutron energy
- beam intensity, purity, pulsed/continuous

Technique of production

- radioisotope
- accelerator
- reactor

NUCLEAR REACTIONS

- (α,n)
- (p,n)
- (d,n)
- (γ,n)
- (γ,2n)
- (γ,pn)
- (t,n)

Q > 0: **exothermic**

Q < 0: **endothermic** (threshold)

Direct radioisotope sources of neutrons (as direct radioactive decay) are not practically available. The specific beta decay with the longest half life that leads to an excited state that does de – excite by neutron emission is

$$^{87}Br \rightarrow {}^{87}Kr^{*} + \beta^{-} \qquad \tau = 55\ s \ \text{(too short!)}$$
$$\hookrightarrow {}^{87}Kr + n$$

The possible choices for **radioisotope neutron sources** are based either on **spontaneous fission** or on **nuclear reactions** for which the incident particle is the product of a conventional decay process using an **α – or γ – radioisotope source**.

Fission neutron sources

Many transuranic heavy nuclides have an appreciable **spontaneous fission decay** probability. **Several fast neutrons are promptly emitted** in each fission event, so a sample of such a radionuclide can be a simple and convenient isotopic neutron source.

However, there are additional **products of the fission process**:

- heavy **fission products**
- **prompt fission gamma rays**
- **beta** and **gamma activity** of of the **accumulated fission products**

Used as neutron source, the isotope is encapsulated in a suficiently thick container so that only the **fast neutrons** and the **gamma rays** emerge from the source

neutron yield
- 0.116n/s per Bq.
- 4.3 x 10^9 n/s per *Ci*
- 2.3 x 10^{12} n/s per *g*.

each fission
- 3.8 neutrons
- 9.7 emiited γ photons

combined activity ! α + f.

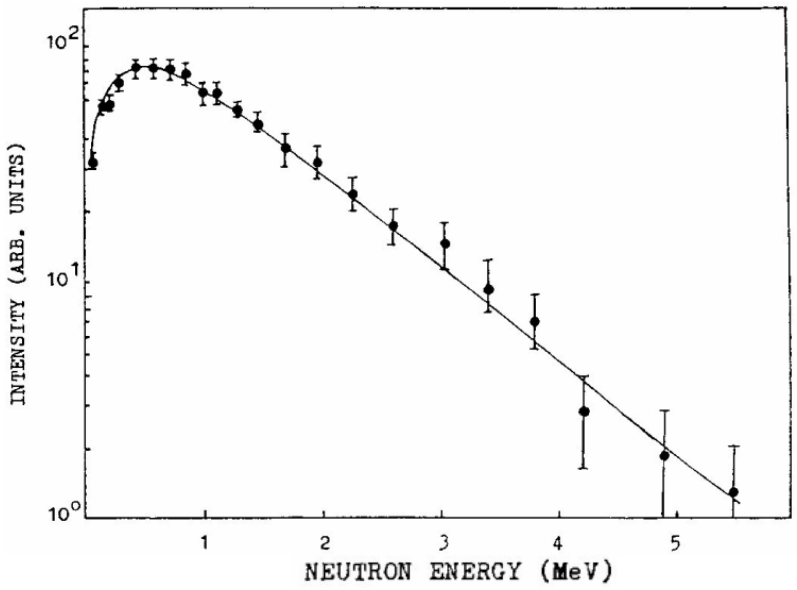

Measured neutron energy spectrum from the spontaneous fission of ^{252}Cf.

The **most common spontaneous fission source** is ^{252}**Cf** (other include ^{235}**U**, ^{239}**Pu**). Its half life of **2.65 years** is convenient, and the isotope is one of the most widely produced of all transuranics. The **dominant decay mechanism is alpha decay** - the alpha emission rate is about 32 times that for spontaneous fission (i.e. ~ only **3 % of all decays through fission**).

Fission neutron sources

In fission of heavy elements:

235U (92p + 143n) + $n \rightarrow$ X + Y + 2.5n + Q
X, Y nuclei with atomic mass ~ 95 and 140 u
~2.5n produced per fission:
1n used to maintain the fission reaction and
1.5n can be utilized as a n-source
99% of neutrons are *prompt* (<10–14 sec),
but *delayed* neutrons (in seconds and minute range) are most essential for maintaining controlled chain reaction

Q ~ 210 MeV per fission released:

~ 175 MeV - kinetic energy of fission fragment;
~ 7 MeV - prompt gamma-rays
~ 5 MeV - kinetic energy of fission n's
~ 7 MeV - betas from fission products
~ 6 MeV - gammas from fission products
~ 10 MeV - neutrinos (invisible)

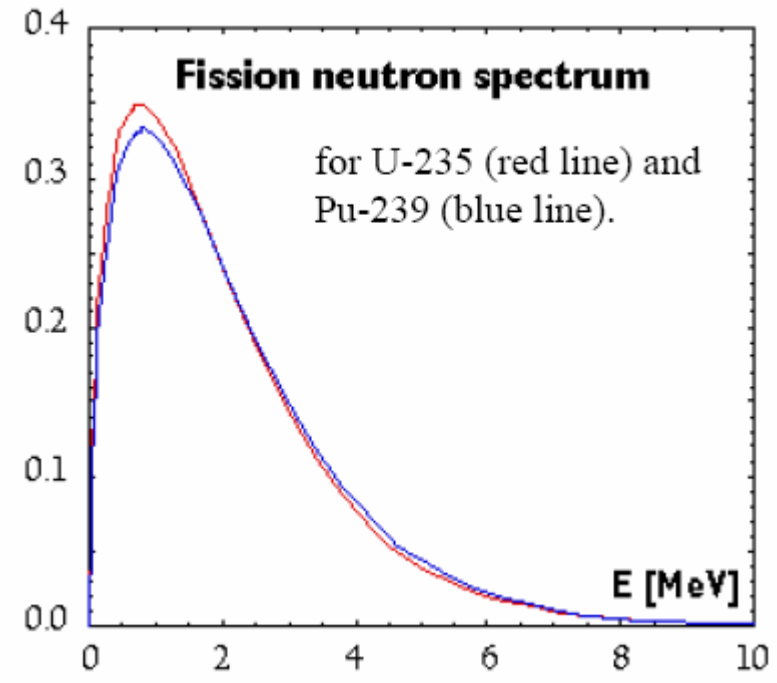

Radioisotope photoneutron sources

Radioisotope gamma – ray emitters can be used to produce neutrons when combined with an appropiate target material. The resulting **photoneutron sources** are based on the **absorption of a gamma – ray photon** to allow the **emission of a free neutron**. Only two reactions are of practical significance:

$$^{9}_{4}Be + \gamma \rightarrow {}^{8}_{4}Be + {}^{1}_{0}n \qquad Q = -1.666 \text{ MeV}$$

$$^{2}_{1}H + \gamma \rightarrow {}^{1}_{1}H + {}^{1}_{0}n \qquad Q = -2.226 \text{ MeV}$$

If gamma rays are monoenergetic, then the produced neutrons are also monoenergetic

Small spreading (few %) from angle kinemetics & neutron scattering (in large sources)

Large gamma – ray activities are required to produce neutron sources of meaningful intensity. About only

1 gamma ray per 10^5 – 10^6 generates a neutron.

Most **common gamma emitters**:

^{226}Ra, ^{124}Sb, ^{72}Ga, ^{140}La and ^{24}Na.

The half lives of the common gamma – ray sources are usually short → reactivation in a nuclear reactor between uses.

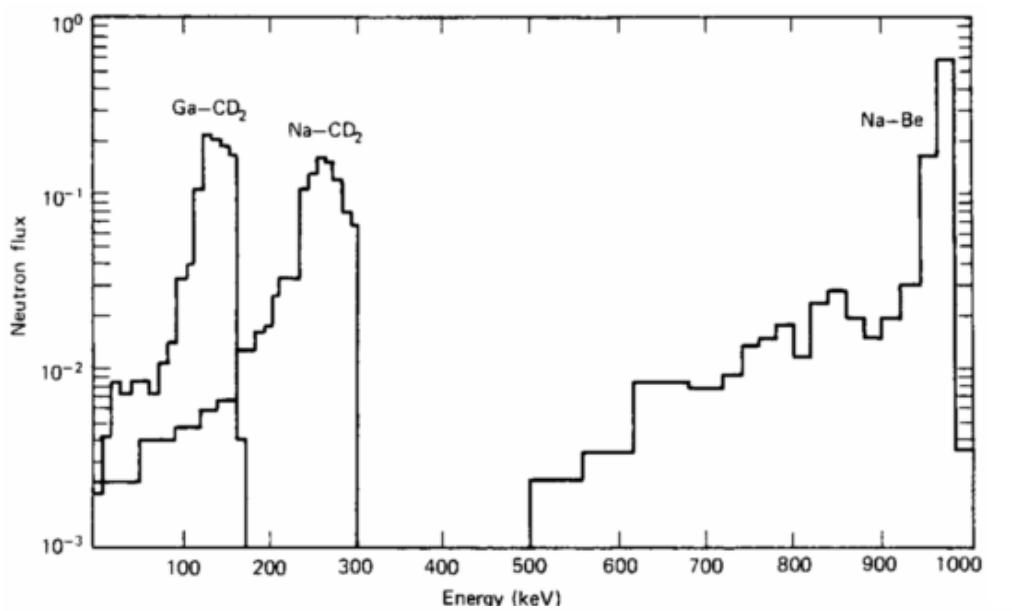

Neutron spectra calculated for the photoneutron source dimensions shown The gamma emitters are either ^{72}Ga or ^{24}Na. The outer shells are either deuterated polyethylene (CD_2) or beryllium (Be).

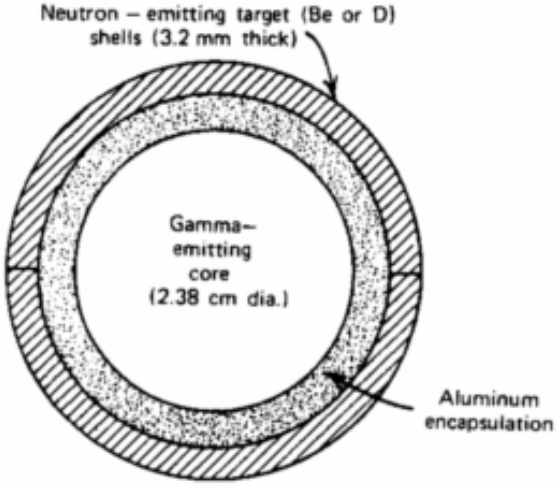

Construction of a simple spherical photoneutron source.

Radioisotope photoneutron sources

Photoneutron Source Characteristics

Gamma-Ray Emitter	Half-Life[a]	Gamma Energy[a] (MeV)	Target	Neutron Energy[b] (keV)	Neutron Yield (n/s) for 10^{10} Bq Activity[c]
^{24}Na	15.0 h	2.7541	Be	967	340,000
		2.7541	D	263	330,000
^{28}Al	2.24 min	1.7787	Be	101	32,600
^{38}Cl	37.3 min	2.1676	Be	446	43,100
^{56}Mn	2.58 h	1.8107	Be	129	91,500
		2.1131		398	
		2.9598		1,149	
		2.9598	D	365	162
^{72}Ga	14.1 h	1.8611	Be	174	64,900
		2.2016		476	
		2.5077		748	
		2.5077	D	140	25,100
^{76}As	26.3 h	1.7877	Be	109	3,050
		2.0963		383	
^{88}Y	107 d	1.8361	Be	152	229,000
		2.7340		949	
		2.7340	D	253	160
^{116m}In	54.1 min	2.1121	Be	397	15,600
^{124}Sb	60.2 d	1.6910	Be	23	210,000
^{140}La	40.3 h	2.5217	Be	760	10,200
		2.5217	D	147	6,600
^{144}Pr	17.3 min	2.1856	Be	462	690

Radioisotope (α,n) sources

Energetic α particles are available from the **direct decay** of several convenient **radionuclides** which allow to fabricate **small self – contained neutron portable sources** by **mixing an α – emitting isotope with a suitable target material**.

Various target materials can lead to (α,n) reactions for the α – particle energies available in radioactive decay. The **maximum neutron yield is obtained when berylium is chosen** as target through the reaction:

α – berillium sources: $^{4}_{2}\alpha + {}^{9}_{4}Be \rightarrow {}^{12}_{6}C + {}^{1}_{0}n$ Q = + 5.7 MeV

^{9}Be has a relatively loose neutron (B_n=1.7 MeV)

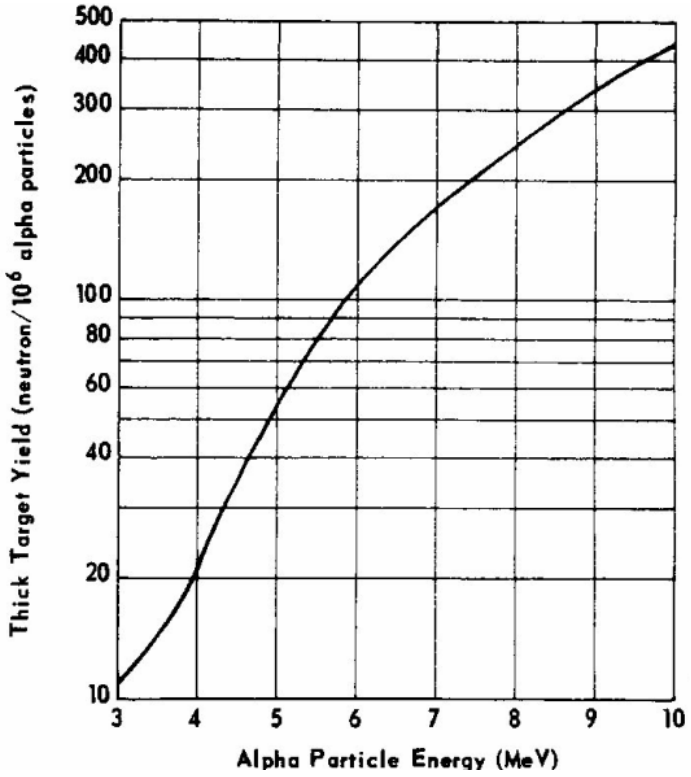

Thick target yield of neutrons for alpha particles on beryllium.

In **common (α,n) sources only about 1 in 10^4 α's reacts with a Be nucleus** (most α's are stopped in the mixed source material). Some isotopes,notably **^{226}Ra** and **^{227}Ac**, lead to long chains of daughter products that add to the α – particle yield, but also contribute a large gamma – ray background. Such sources can present intense gamma – ray background interferences and can require elaborate handling procedures (due to added bilogical hazard).

For large – size sources, **secondary processes** such as **neutron scattering**, **Be(n,2n)** and **Pu(n,f)** can occur.

Radioisotope (α,n) sources

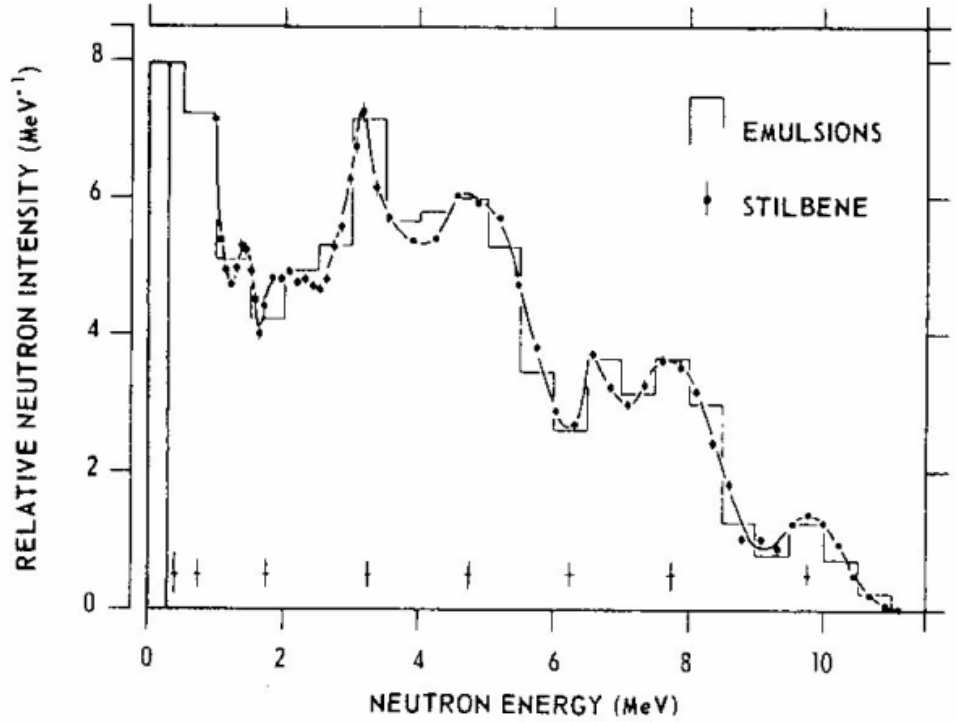

Measured energy spectra for neutrons from a $^{239}Pu/Be$ source

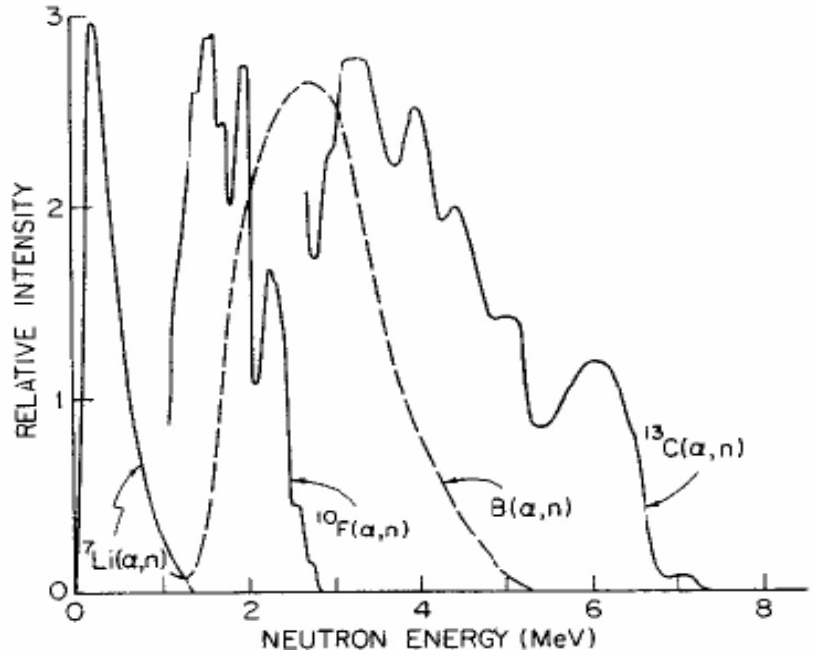

Neutron energy spectra from alternative (α, n) sources.

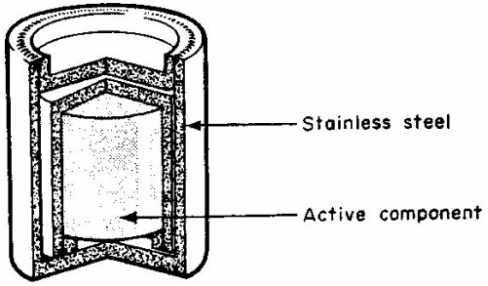

Typical double-walled construction for Be (α, n) sources.

Radioisotope (α,n) sources

Characteristics of Be(α, n) Neutron Sources

Source	Half-Life	E_α (MeV)	Neutron Yield per 10^6 Primary Alpha Particles		Percent Yield with $E_n < 1.5$ MeV	
			Calculated	Experimental	Calculated	Experimental
^{239}Pu/Be	24000 y	5.14	65	57	11	9–33
^{210}Po/Be	138 d	5.30	73	69	13	12
^{238}Pu/Be	87.4 y	5.48	79[a]	—	—	—
^{241}Am/Be	433 y	5.48	82	70	14	15–23
^{244}Cm/Be	18 y	5.79	100[b]	—	18	29
^{242}Cm/Be	162 d	6.10	118	106	22	26
^{226}Ra/Be + daughters	1602 y	Multiple	502	—	26	33–38
^{227}Ac/Be + daughters	21.6 y	Multiple	702	—	28	38

Alternative (α, n) Isotopic Neutron Sources

Target	Reaction	Q-Value	Neutron Yield per 10^6 Alpha Particles
Natural B	^{10}B (α, n) ^{11}B(α, n)	+1.07 MeV +0.158 MeV	13 for ^{241}Am alpha particles
F	^{19}F(α, n)	−1.93 MeV	4.1 for ^{241}Am alpha particles
Isotopically separated ^{13}C	^{13}C(α, n)	+2.2 MeV	11 for ^{238}Pu alpha particles
Natural Li	^{7}Li(α, n)	−2.79 MeV	
Be (for comparison)	^{9}Be(α, n)	+5.71 MeV	70 for ^{241}Am alpha particles

Selection of source

- n yield (typ. $10^{7\text{-}8}$ n/s)
- background
- half life
- cost & availability

Neutrons from charged particle reactions

Many nuclear reactions can produce neutrons but they require an **accelerator to provide a beam of particles** to initiate the reaction. They may not be as convenient (simple, portable) as radioactive sources, but by selecting the incident energy and angle, **monoenergetic neutron beams of almost any desired energy** can be obtained.

Alpha particles are the only heavy charged particles with low *Z* conveniently available from radioisotopes.

(d,n) $^{2}_{1}H + {}^{2}_{1}H \rightarrow {}^{3}_{2}He + {}^{1}_{0}n$ Q = 3.3 MeV **D – D** reaction E_n = 3 MeV

(d,n) $^{2}_{1}H + {}^{3}_{1}H \rightarrow {}^{4}_{2}He + {}^{1}_{0}n$ Q = 17.6 MeV **D – T** reaction E_n = 14 MeV

(α,n) $^{9}_{4}Be + {}^{4}_{2}He \rightarrow {}^{12}_{6}C + {}^{1}_{0}n$ Q = 5.7 MeV

(p,n) $^{7}_{3}Li + {}^{1}_{1}H \rightarrow {}^{7}_{4}Be + {}^{1}_{0}n$ Q = – 1.6 MeV

Also: ^{9}Be(d,n), ^{3}H(p,n) Q negative

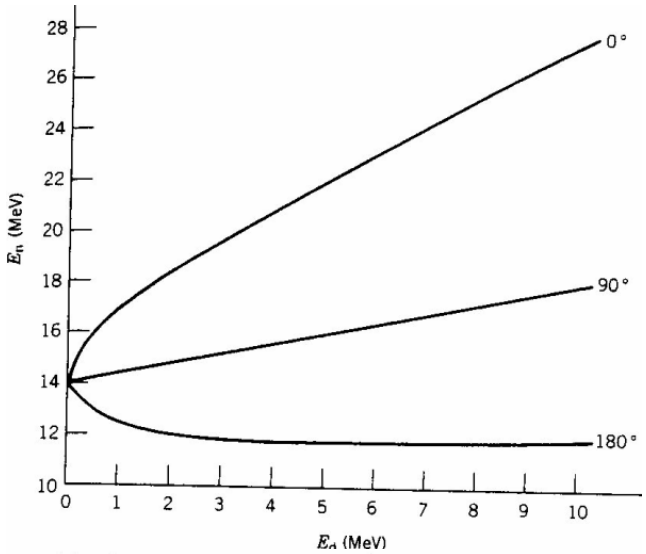

Neutrons emitted in the ^{3}H(d, n)^{4}He reaction

Coloumb barrier between incident d and the light target nucleus is relalively small

↓

d 's need <u>not</u> be accelerated to very high energies to create a significant n yield.

↓

NEUTRON GENERATORS

d are accelerated by U = 100 – 300 kV.

↓

All *n*'s produced have essentially the same energy (incident particle energy << Q)

A **1 mA *d* beam** produces ~ **10^{9} *n*/s** from a thick ***d*** target.

A **1 mA *d* beam** produces ~ **10^{11} *n*/s** from a thick ***t*** target.

Neutrons from charged particle reactions

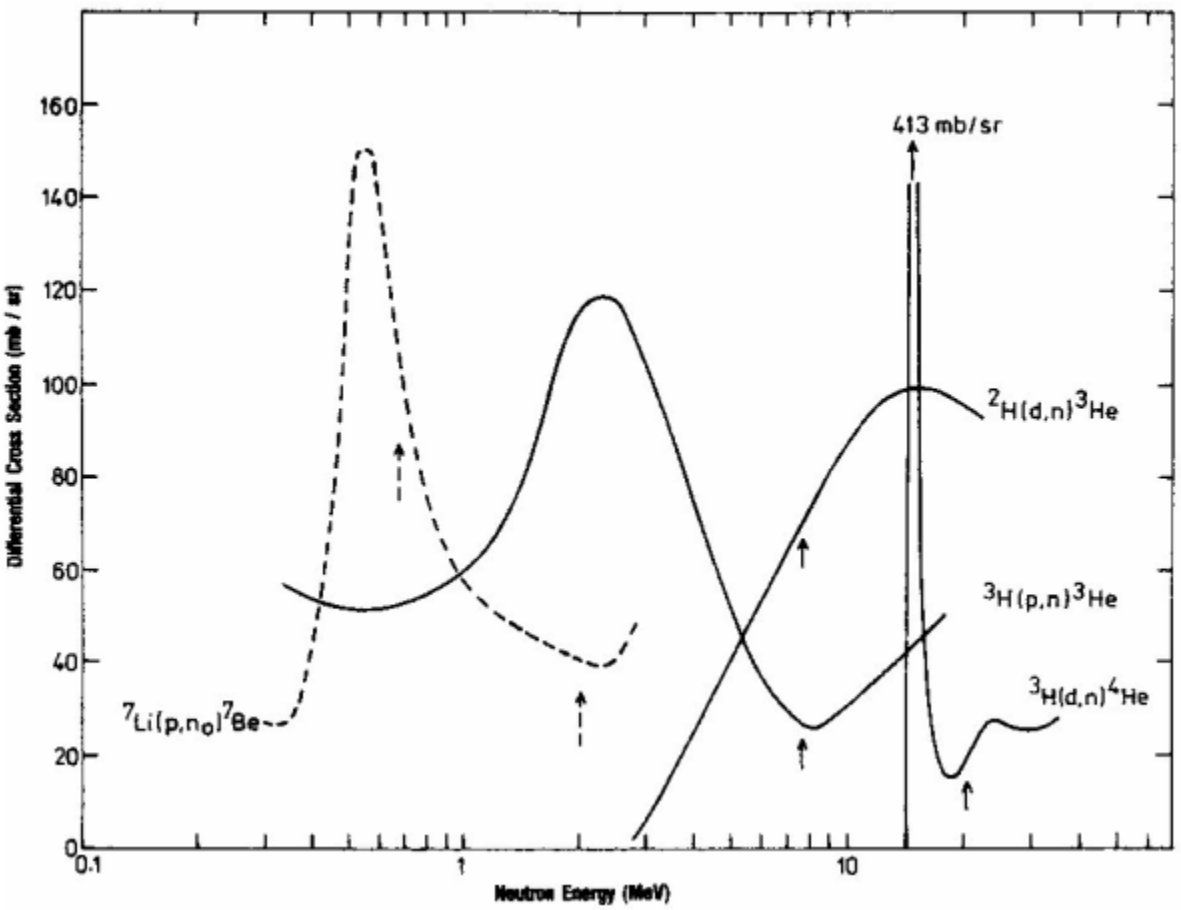

The zero-degree differential cross section in the laboratory system, for producing neutrons of energy E_n for the $^{3}H(p,n)^{3}He$, $^{2}H(d,n)^{3}He$ and $^{3}H(d,n)^{4}He$ reactions. The $^{7}Li(p,n_0)^{7}Be$ cross section is shown for comparison, where the arrow indicates the threshold for the $^{7}Li(p,n_1)^{7}Be^{*}$ reaction. The other arrows indicate the maximum neutron energy at the thresholds for three particle break-up.

Reactor and Spallation sources

RESEARCH NUCLEAR REACTORS

The **neutron flux** of a **research nuclear fission reactor** can be quite high – typically ~ **10^{14} *n* /cm^2/s** at the core and ~ **10^7 *n* /cm^2/s** at the extracted beam guides. The energy spectrum at the core extends to 5 – 7 MeV but peaks at 1 – 2 MeV. These neutrons are generally reduced to **thermal energies** within the reactor, but there are also **fast neutrons** present in the core. Through small holes in the shielding of the reactor vessel permits a **beam of neutrons** to be extracted into the laboratory for experiments. The high neutron reactor fluxes are particularly useful for **low – cross – section reactions** (and *e.g.*, **production of radioisotopes** by neutron capture or **neutron activation analysis** of trace elements).

- **Steady – state** ← Fermi @ Chicago (1942)
- **Pulsed** ← Frisch @ Los Alamos (1945)

BEAMS: ***Continuous, Pulsed, Filtered***

Fast **~ μs *n* 's bursts** (IBR @ Dubna), ***Thermal*** (Triga)

SPALLATION NEUTRON SOURCES

Spallation neutron sources consist of an **accelerator** providing a beam of **high – energy (≤ 1 GeV) protons** or **heavier ions** and a suitable **target of heavy – element material**.

Initially known from **cosmic – ray** studies (mass distributions), the **spallation reaction is the breaking off of nucleons, singly and in clusters, from a nucleus by an energetic bombarding particle**.

Cosmic rays produce **spallation reaction products** in collision with interstellar matter

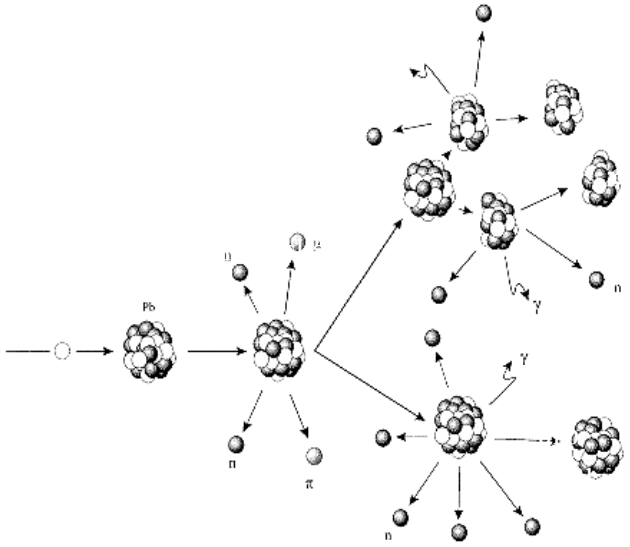

In the laboratory E. O. Lawrence observed secondary *n* 's from a U target bombarded by 90 MeV *p* 's. When the **energy of the incident particle or nucleus exceeds about 100 MeV→ spallation reaction**.

Spallation reactions can serve as intense source of neutrons.

Time – of – flight

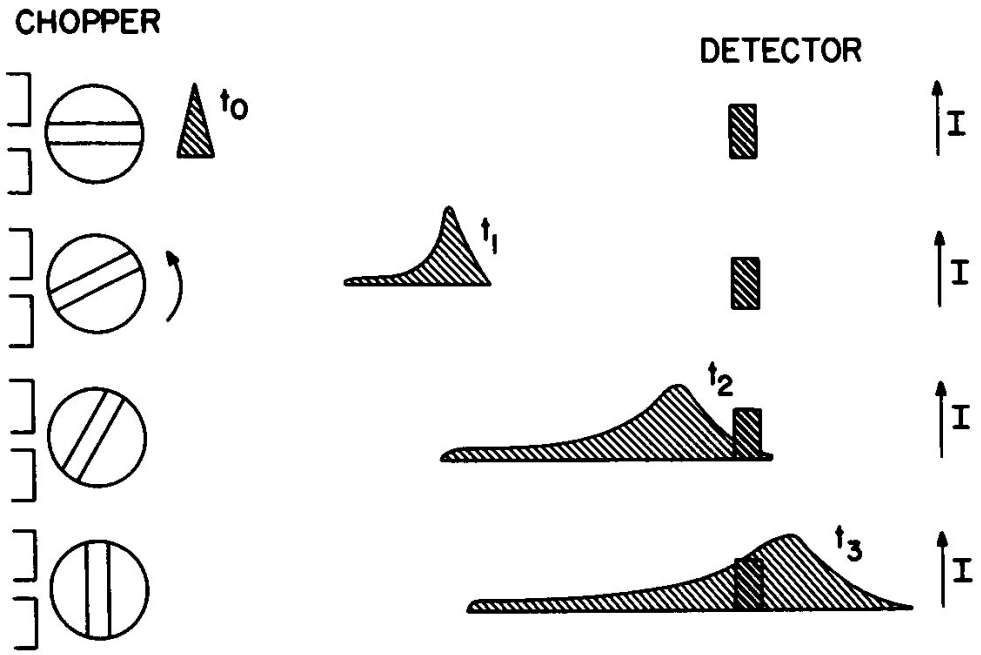

Illustration of the time-of-flight principle.

$$l \rightarrow t \rightarrow v \rightarrow E_n \longrightarrow T_n = \frac{1}{2} E_n^o \frac{l^2}{t_n^2 c^2}$$

Time – of – flight

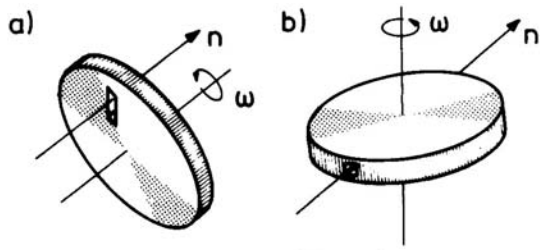

The two basic rotor configurations.
a) The beam and rotor axes are parallel.
b) The beam and rotor axes are perpendicular.

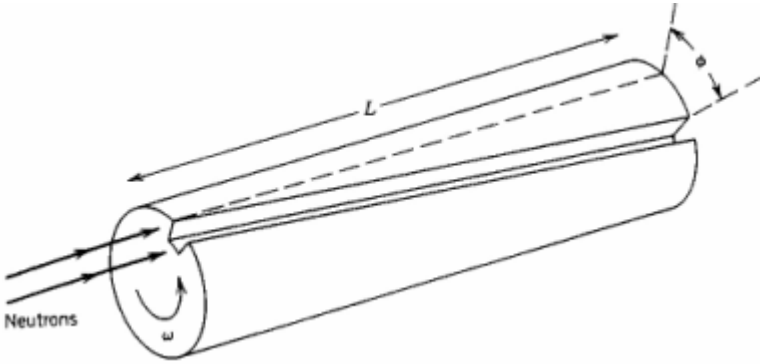

Neutron velocity selector, consisting of a rotating cylinder with one or more helical slots cut into its surface. The cylinder is made of a material, such as cadmium, with a high absorption for neutrons. The selector will pass neutrons of velocity v that travel the length L of the cylinder in the time that it takes it to rotate through the angle ϕ; that is, $t = L/v = \phi/\omega$, so that $v = L\omega/\phi$. Changing the angular speed ω permits selection of the neutron velocity.

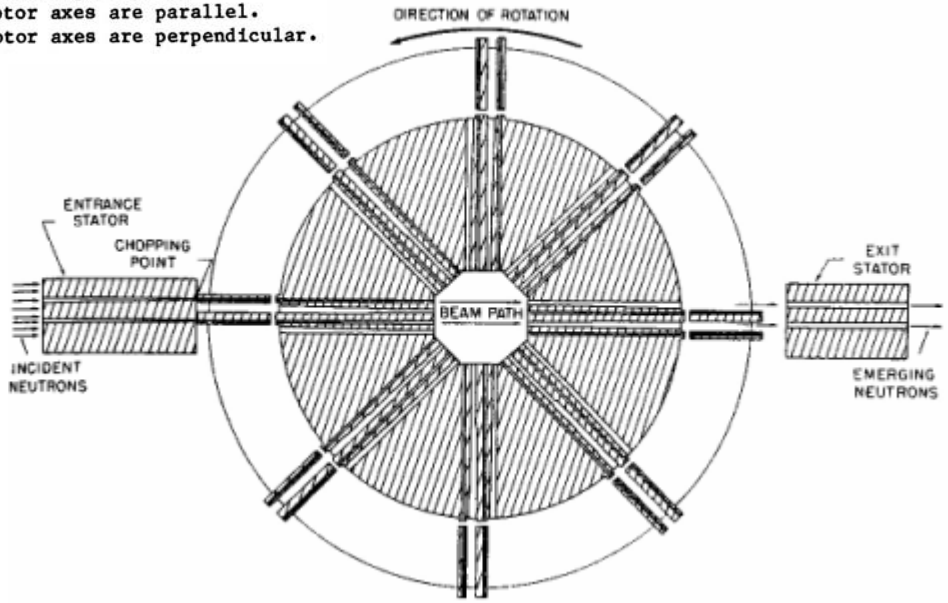

Rotating shutter or "chopper" for producing pulses of neutrons. A continuous stream of neutrons enters from the left and a pulse of neutrons emerges at right if the rotor slits line up with the entrance slits. The rotor is made of stainless steel with phenolic slits.

Time – of – flight

$$E_n \geq 1\text{MeV} \Rightarrow \quad E_n = E_n^{\circ}\left[\left(1-\frac{l^2}{t^2c^2}\right)^{-1/2}\right]$$

$$E_n \leq 1\text{MeV} \Rightarrow \quad E_n = E_n^{\circ}\frac{l^2}{t^2c^2}$$

ΔE_n=0.16% @ 1 MeV

Flight time = 1 / v

$$f = \frac{t_n}{l} = \frac{1}{c}\left[1-\left[\frac{E_n^{0}}{E_n + E_n^{0}}\right]^2\right]^{-1/2} \qquad 1\text{eV} \rightarrow t = 70\mu s/\text{m}$$

Typical Specific Flight Times of Fast Neutrons at a Few Energies

E_n (MeV)	t_n/l (ns/m) Relativistic	Non-Relativistic
0.1	228.65	228.63
0.5	102.29	102.25
1	72.356	72.299
5	32.462	32.333
10	23.045	
50	10.428	
100	7.795	

1/v [ns/m]	En [MeV]
25	8
50	2
100	0.5

Time – of – flight

Cross-sections of H, C, N, and O (Time – of – flight spectra) as function of normalized flight time, or 1/v (ns/m)

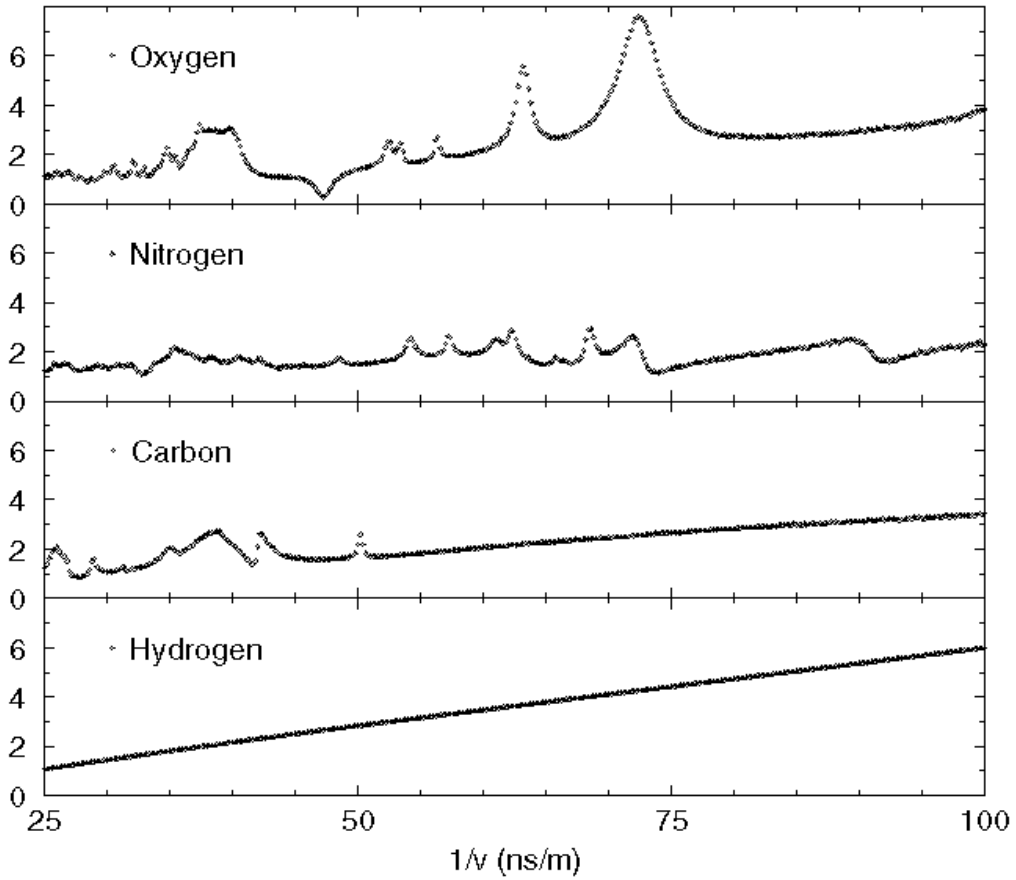

Neutron Filtered Beams

Transmission of tailored ^{56}Fe neutron filter

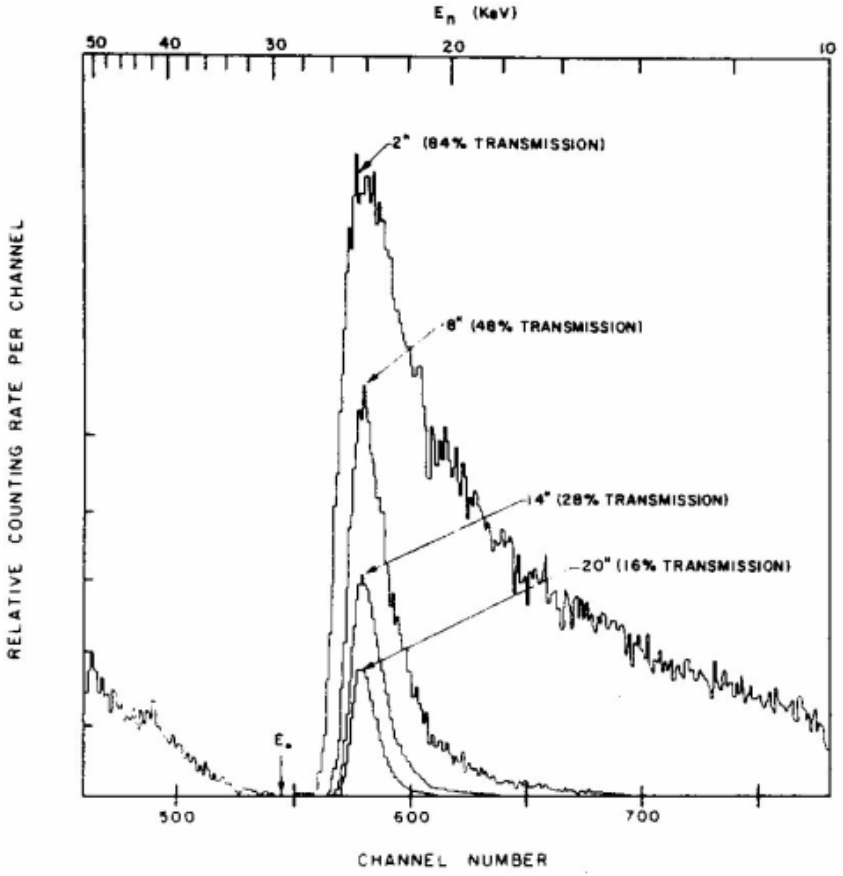

The neutron counting rate at a 25.5-m flight path versus time-of-flight for neutrons passing through Fe filters of thickness 5.1, 20.3, 35.6 and 50.8 cm (2, 8, 14 and 20 inches). The neutron transmission at the 24.3-keV peak is shown in parentheses. The curve shown above 28 keV is for the 5.1-cm thick filter.

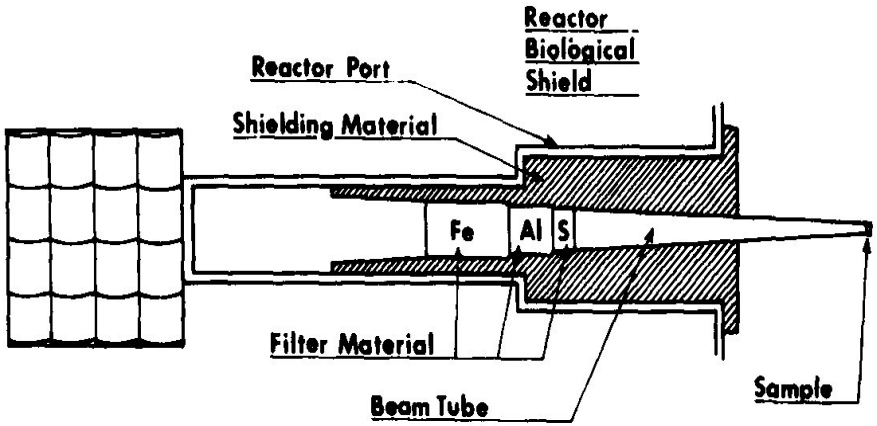

Example of filtered beam arrangement: in a re-entrant beam tube.

Neutron Filtered Beams

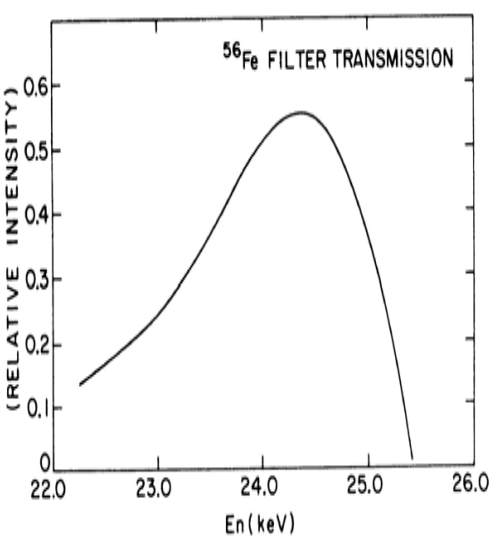

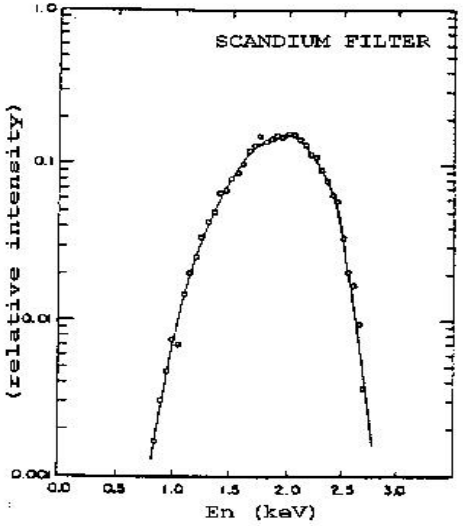

Transmission of tailored ^{56}Fe neutron filter

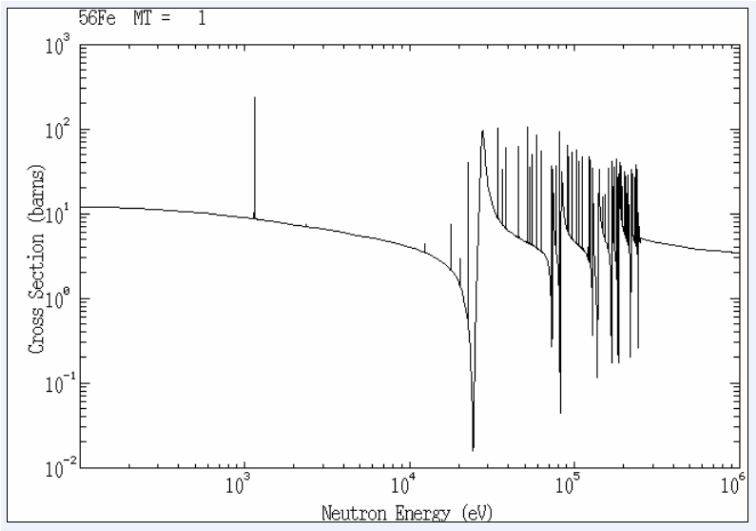

Neutron Filtered Beams

Filtered neutron beams in ARC: beam composition, mean energy, width, flux and purity [13]

Beam	Filter composition	E_n (keV)	FWHM (keV)	ϕ_n (n/sec/cm^2)	Purity (%)
24 keV	^{56}Fe + Al + Cd	24.3	1.7	4.2×10^7	95
2 keV	Sc + Cd	2.0	0.9	7.1×10^7	70
Non-thermal	Al + Cd	~ 0.001	~ 1	$\sim 10^7$	~ 70
Thermal	Bi	thermal	Maxwell	$\sim 10^9$	~ 70

Filter	Beam Energy	Width (FWHM)	Size (cm^2)	Intensity (n/sec)	Purity (%)
22.86 cm Fe 36.20 cm Al 6.35 cm S	24.3 keV	2.0 keV	7.27	9.30×10^6	98
68.58 cm Fe-56 (99.87%)	24.3 keV	1.0 keV	7.27	10^8	80
30.48 cm Fe-56 17.78 cm Al	24.3 keV	1.7 keV	7.27	2.80×10^7	95
71.1 cm Sc (188 gms/cm^2)	2.0 keV	0.9 keV	7.27	4.75×10^7	70
Bi single crystal	thermal	Maxwellian	$\leq$7.27 (variable)	10^9	

186 eV,	55 & 144 keV,	2.35 MeV
^{238}U,	Si,	O

Neutrons from crystal monochromator

Monochromator for producing a beam of monoenergetic neutrons.

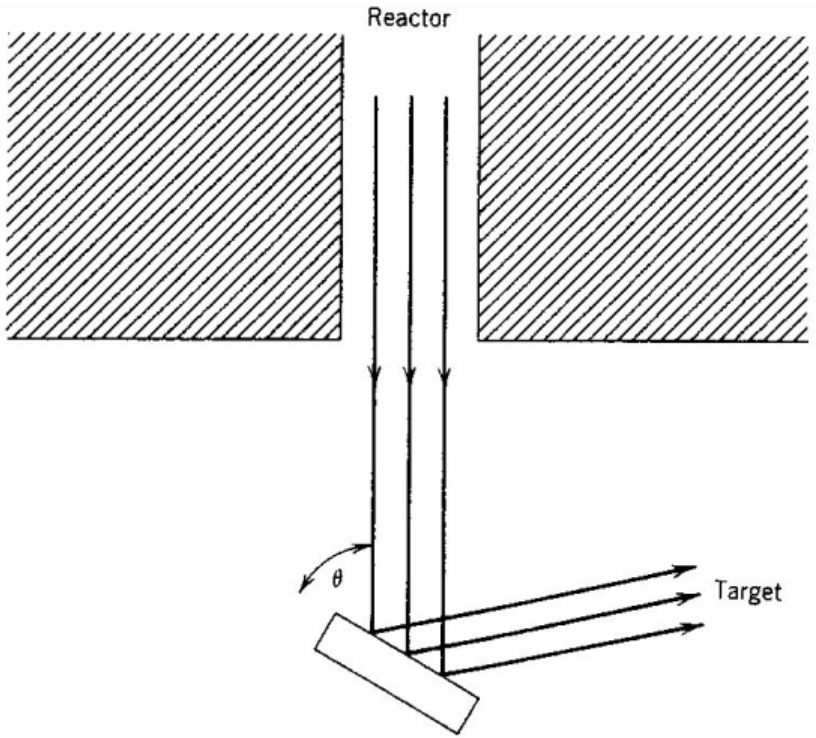

A collimated beam of reactor neutrons with a broad spectrum of wavelengths is Bragg reflected from a single crystal. For a particular value of θ, there will be an interference maximum for a certain wavelength, and thus by varying θ we can choose the wavelength.
there may be other Bragg reflected peaks at other angles, which are not shown.

Interaction of neutrons with matter

Neutrons (in common with gamma rays) **carry no charge** and therefore **cannot interact in matter by means of the Coulomb force** – which dominates the energy loss mechanism for charged particles (e,p,α,μ,...).

Neutrons can also **travel through many *cm* of matter without any type of interaction** and thus can be totally invisible to a detector of common size. When a neutron undergoes **inteaction** it is **with the nucleus** (and not with the atomic electrons) of the absorbing material. As a result of the interaction, **the neutron may either totally disappear and be replaced by one or more secondary radiations, or else the energy or direction of the neutron is changed significantly**.

In constrast to gamma rays, the **secondary radiations** resulting from neutron interactions are almost always **heavy charged particles**. These particles may be produced either as a result of neutron- induced nuclear reactions or they may be the nuclei of the absorbing material itself, which have gained energy as a result of a neutron collision.

The **relative probabilities** of the various types of neutron interactions **change dramatically with neutron energy**.

→ **Slow** & **Fast neutron interactions**. Dividing line @ ~ **0.5 eV** (*Cd* cutoff energy)

SLOW NEUTRON INTERACTIONS

Elastic scattering with absorber nuclei whereby neutrons are **thermalized** with the absorber (@ room temperature → **25 meV**).

Large number of **neutron – induced reactions**: can create **secondary radiations** of sufficient energy (to be detected). Because E_n is so low, all such reactions must have ***+Q***. In most materials the **radiative neutron capture** is the most probable and plays an essential role in the **attenuation or shielding of neutrons**.

The **most efficient moderator is hydrogen** because the neutron can lose **up to all its energy** in a single collision with a H nucleus.

Neutron Shielding & Dosimetry !

FAST NEUTRON INTERACTIONS

The probability of most neutron – induced reactionsdrops off rapidly with encreasing neutron energy. However, the importance of **scattering becomes greater** as the neutron can transfer an appreciable amount of energy in one collision.

The **secondary radiations** in this case **are recoil nuclei**. At each scattering event, the **neutron loses energy** and is thereby **moderated or slowed** to lower energy.

If E_n is sufficienty high, **ineslastic scattering** with nuclei can take place in which the recoil nucleus is elevated to one of its excited states during the collision. The nucleus quickly de – excites, **emitting a gamma ray**, and the neutron loses a greater fraction of its energy. This interaction plays an important role in the **shielding of high energy neutrons**.

Neutron detectors

Neutrons are generally detected through nuclear reactions that result in prompt energetic charged particles such as protons, α and so on. Every neutron detector involves the **combination of a target material** designed to carry out this **conversion** together with a **conventional radiation detector**.

→ Target nucleus + n →

- recoil nucleus
- p, α, γ,
- fission fragment

DETECTION

identification, energy, momentum, position.

DETECTORS

gas chambers, proportional counters, solid, liquid.

Because the **cross section for neutron interactions** in most materials is a **strong function of neutron energy**, different techniques exist for neutron detection in different energy regions.

→

- **slow neutron** detection & spectroscopy
- **fast neutron** detection & spectroscopy

SLOW NEUTRON DETECTION

Suitable nuclear reaction for neutron detection:

- large cross section
- large Q value → energy for charged products
- discrimination against intense γ background

→

g.s. (exc. s.)

BF$_3$ tubes

$^{10}_{5}B + {}^{1}_{0}n \rightarrow {}^{7}_{3}Li^{(*)} + {}^{4}_{2}\alpha$ Q = 2.8 (2.3) MeV σ = 4000 *b*

$^{6}_{3}Li + {}^{1}_{0}n \rightarrow {}^{3}_{1}H + {}^{4}_{2}\alpha$ Q = 4.8 MeV σ = 940 *b*

$^{3}_{2}He + {}^{1}_{0}n \rightarrow {}^{3}_{1}H + {}^{1}_{1}p$ Q = 0.8 MeV σ = 5300 *b*

Gd neutron capture detector: ^{157}Gd σ = 2.5 x 10^5 b. → γ 's, *e* 's [72 keV *IC* e$^-$]

Neutron induced fission reactions: have *Q* ~ 200 MeV. ^{233}U, ^{235}U, ^{239}Pu.`

E$_n$* << *Q → not possible to measure E$_n$.

Neutron detectors

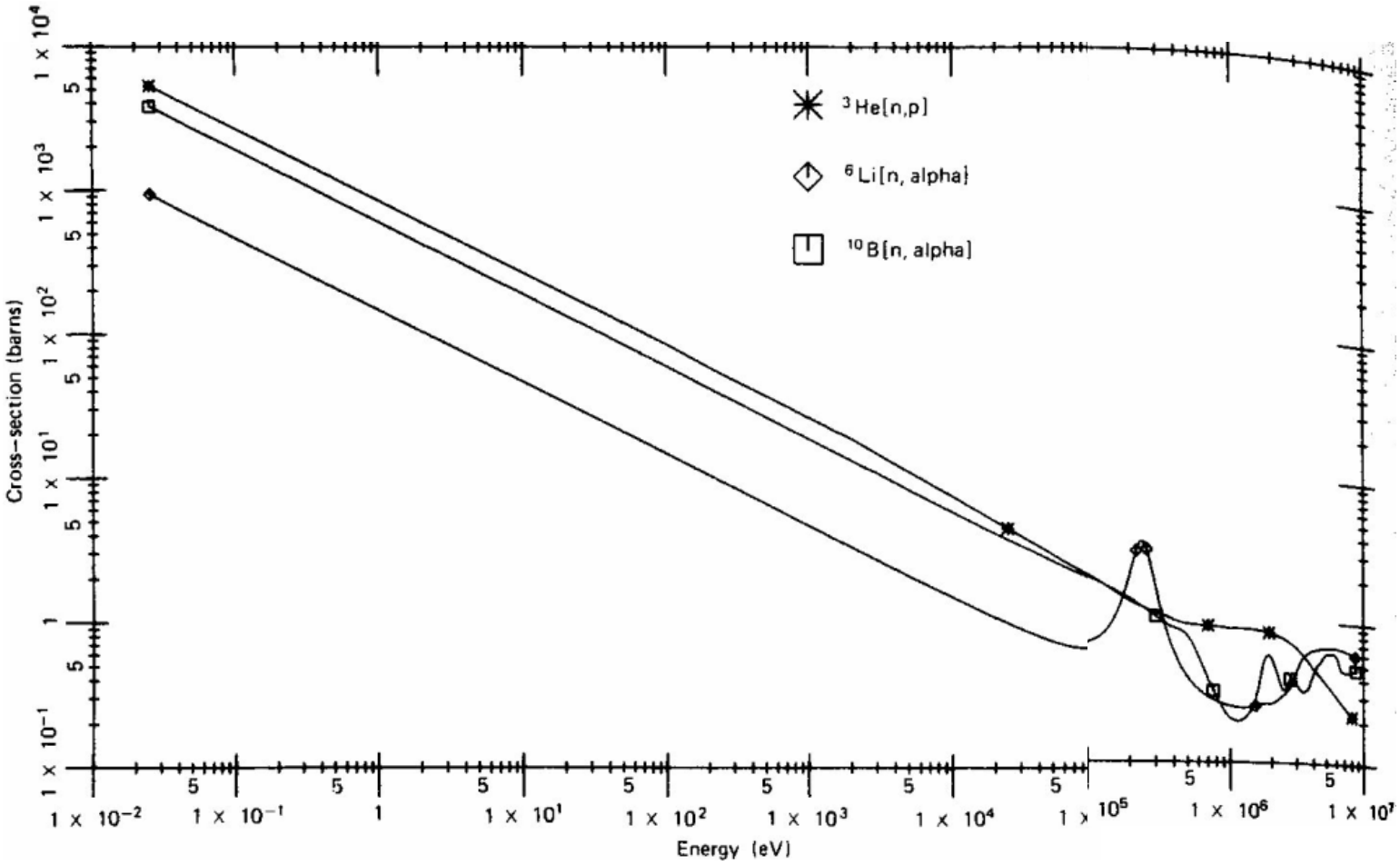

Cross section versus neutron energy for some reactions of interest in neutron detection.

Neutron detectors

The cross sections for the reactions for slow – neutron detection decrease with energy. Only the **^{3}He** proportional counter may serve for **both thermal neutron detection and fast neutron spectroscopy**. With fast neutrons, **elastic scattering** is used to produce recoil nuclei (generally hydrogen). When **E_n > 10 – 100 keV → the reaction products carry information on E_n**

FAST NEUTRON DETECTION

• **Neutron moderation**: the inherently low detection efficiency for fast neutrons of slow neutron detectors can be improved by surrounding the detector with **moderating material** (Hydrogen: paraffin, polyethylene). Information on E_n is lost.

• **Fast neutron – induced reactions**: The loss of En information and the long detection time of moderating detectors are avoided in **direct nuclear reaction detection**. However, the cross sections are low exhibiting low detection efficiency.

^{3}He(n,p): ^{3}He proportional counter, ionization chamber, scintillator, semiconductor

^{6}Li(n,α): Li Iodide scintillator, Li glass and glass fiber scintillators

Fast neutron scattering: the most common method of fast neutron detection is based on **elastic scattering of neutrons by light nuclei**. The **recoil nucleus** (H, d, He) carries part (or even all) of the E_n. Detectors based on hydrogen, which result in **recoil protons**, are called **proton recoil detectors, proton recoil scintillator, Gas recoil proportional counters**

Fission reactions serve only for counting – the energy of the neutron is lost (<< *Q*) → not of spectroscopic interest. ⟶

Activation counters use the radioactivity induced by neutron capture.

NEUTRON DETECTION BY ACTIVATION

Neutron measurements can be also carried out indirectly through the radioactivity that is induced in some materials by neutron interactions. Such **activation detector** is exposed to a flux of neutrons for a period of time and then removed so that the induced radioactivity may be counted and yield information about the number and energy of *n*'s.

Activator materials such as ^{55}Mn, ^{59}Co, ^{63,65}Cu, ^{164}Dy, ^{197}Au are generally used for **slow – neutron detection**. There are also **threshold activator materials** using **threshold reactions** such as (n,2n), (n,p), (n,α).

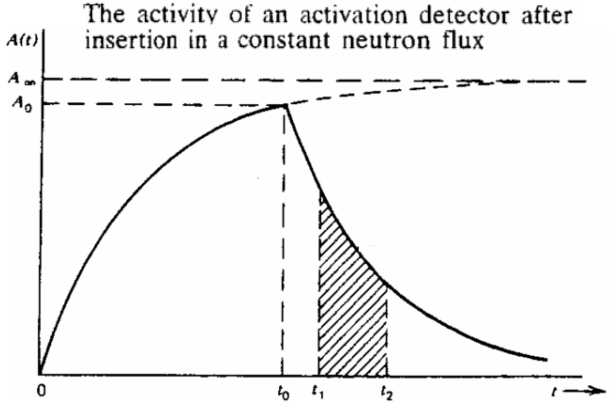

Neutron detectors

FISSION CHAMBERS

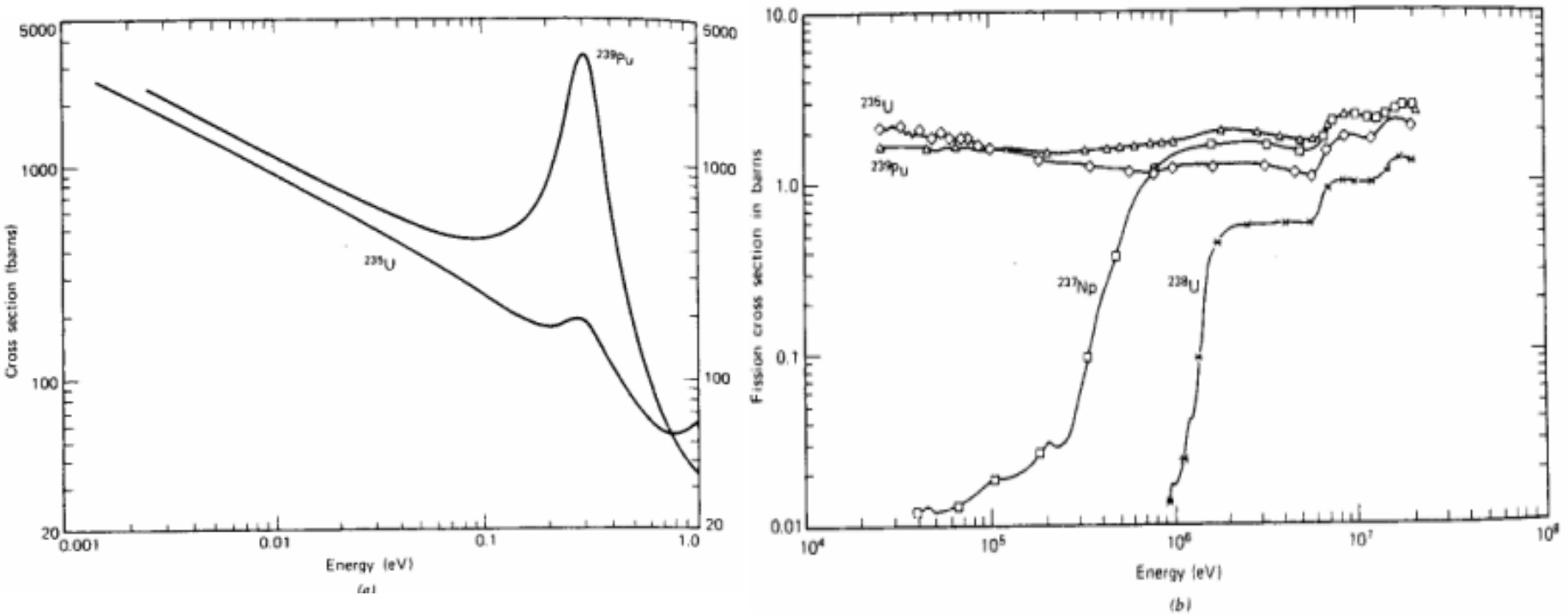

Fission cross sections of some common target nuclides used in fission chambers. (*a*) Slow neutron region where the cross sections shown are relatively large. (*b*) Fast neutron region. Chambers with ^{237}Np or ^{238}U are used as *threshold detectors* sensitive only to fast neutrons.

Nuclear Spectroscopy with Neutrons

- Introduction & terms
- Neutron sources & detectors
- **Nuclear spectroscopy**

break

- Example of complete nuclear spectroscopy

Nuclear Reactions

$$N = \phi_n \cdot \sigma \cdot n_T$$

[#/s] = [#/cm^2/s • cm^2 • #]

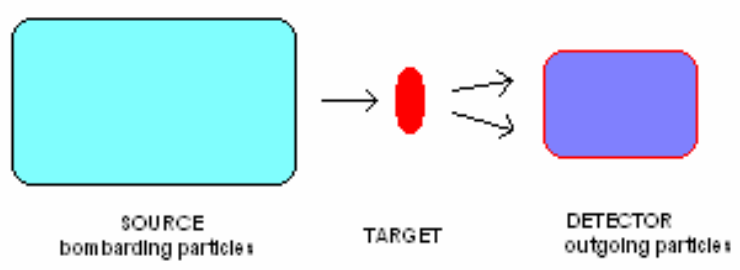

N	number of events (count rate)
ϕ_n	neutron flux
σ	cross section
n_T	number of target nuclei

Conservation laws

- energy
- momentum (linear, angular)
- parity, baryon number, ...

!

- background identification (supression)
- energy calibration
- intensity calibration

$A =$	152	154	155	156	157	**158**	160
$\eta_{\text{target}}[\%]$	< 0.05	< 0.05	0.6	0.7	1.7	**95.8**	1.1
$\eta_{\text{natural}}[\%]$	0.2	2.2	14.8	20.5	15.6	**24.8**	21.8
$\sigma_{n\gamma}[barn]$	1100	85	61000	1.5	254000	**2.5**	0.8

1 barn = 10^{-24} cm^2

10^3 [~ 0.1 μCi] = 10^7 • 10^{-24} • 10^{20} ← sealed source [~ mCi]

10^{10} [~ Ci] = 10^{14} • 10^{-24} • 10^{20} ← int. target @ high flux reactor core

Neutron reactions

- radiative neutron capture (n,γ)
- elastic scattering (n,n)
- inelastic scattering (n,n')
- exchange reactions (n,p)
- transfer reactions (n,d), (d,p), (d,t), ...
- fission (n,f)
- other (n,2n)

In non-fissile nuclei, absorption ↔ radiative capture

THE FREE NEUTRON

The ultimate fate of a free neutron is either **absorption** (by a nucleus, after slowing down) or **beta decay** (neglible)

Investigate the **lifetime of the free neutron**, estimate the lower limit of a **possible electric charge** and **magnetic dipole moment**.

DIRECT REACTION: when the reaction proceeds from one state to another (i.e., through a **two-body channel**) without formation of a compound system. It is considered as a **single** (or few – body) process.

The **optical model** is used to describe DR and the channel wave function by **distorted waves**.

If more the reaction proceeds through more than one – step, then **multistep direct reaction theory** is used.

When the final channel is strongly coupled to the initial channel (e.g., a **resonance** with large cross section) and when **multi – step processes** occur, then **Coupled – Channel** theory is used.

In the case of weak coupling can be treated pertubatively, i.e. **Born Approximation** i.e. **DWBA** can be used.

In the **continuum** (large number of final states are involved with no dominance of single final state). CCBA is not suitable.

COMPOUND NUCLEUS REACTIONS: statistical process where the initial particle energy and momentum are shared among many nucleons and the system lives for a **long time**. It is considered as a **collective** (or many – body) process.

BREAKUP REACTIONS: If, for example, in a (d,p) reaction *Ed* – *Ep* exceeds 10 MeV or so, the neutron cannot be accomodated in **a bound orbit**. It must stay in the **continuum**; i.e. the final state of the reaction under consideration is of a **three – body nature** or so called breakup process. Neutron induced reactions do not induce breakup processes.

DWBA Distorted Waves Born Approximation

PWBA Plane Waves BA

CCBA Coupled Channels BA

Nuclear spectroscopy with neutrons

The **interaction character of neutrons** with nuclei depends on **neutron energy**. That is, the **reaction cross section** depends on the incident particle (neutron) energy, but also on the target level density and individual level characteristics.

At $E_n < E_x$, where E_x is the lowest target nucleus excited level, only **elastic scattering** of neutrons on nuclei and some exothermal nuclear reactions, most of all **neutron radiative capture**, are possible.

On some **light nuclei**, reactions with **outgoing charged particles** exhibit large cross sections. e.g.,

$^{3}He(n,p)^{3}H$, $^{6}Li(n,\alpha)^{3}H$, $^{10}B(n,\alpha)^{7}Li$

The **heaviest nuclei** (U and transuranium elements) neutron capture can cause **nuclear fission**.

Polarized fast neutrons

allow to investigate a variety of **nuclear interactions – phenomena**:

- nucleon – nucleus spin – orbit interaction.
- spin – spin interaction or charge – symmetry violating mechanisms.
- resonance parameters and phase shifts.
- nucleon – nucleon and fe – nucleon systems.
- sensitive tests of models for nuclear reaction mechanisms.

$^{7}Li(\vec{p},\vec{n})^{7}Be$ @ $\theta = 50 \rightarrow P \sim 0.2 - 0.6$

$^{2}H(d,\vec{n})^{3}He$

$^{3}H(d,\vec{n})^{4}He$

Neutron Reaction Cross Section

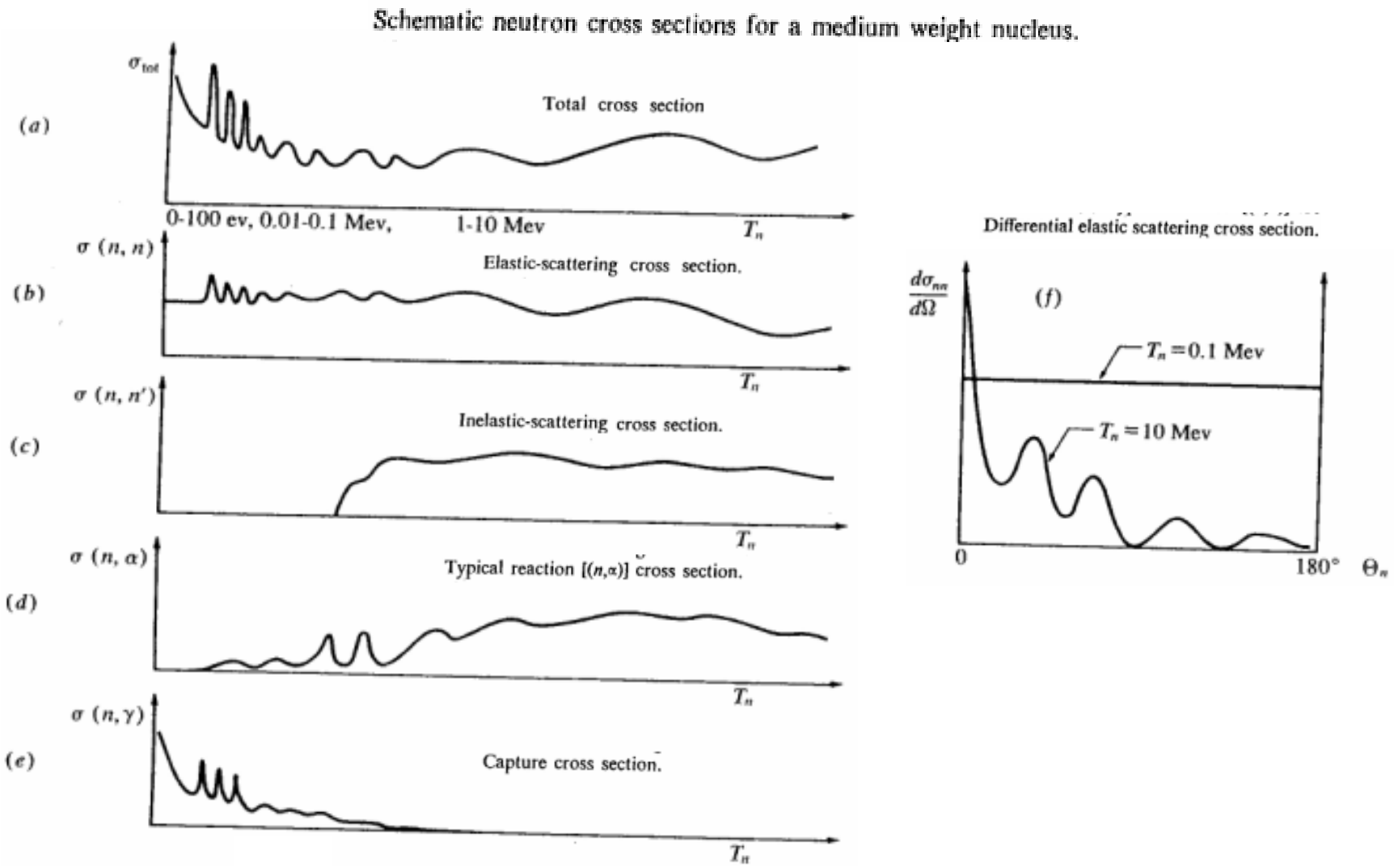

Neutron & Proton Reaction Cross Section

Schmatic neutron (left) and proton (right) cross sections for a medium weight nucleus.

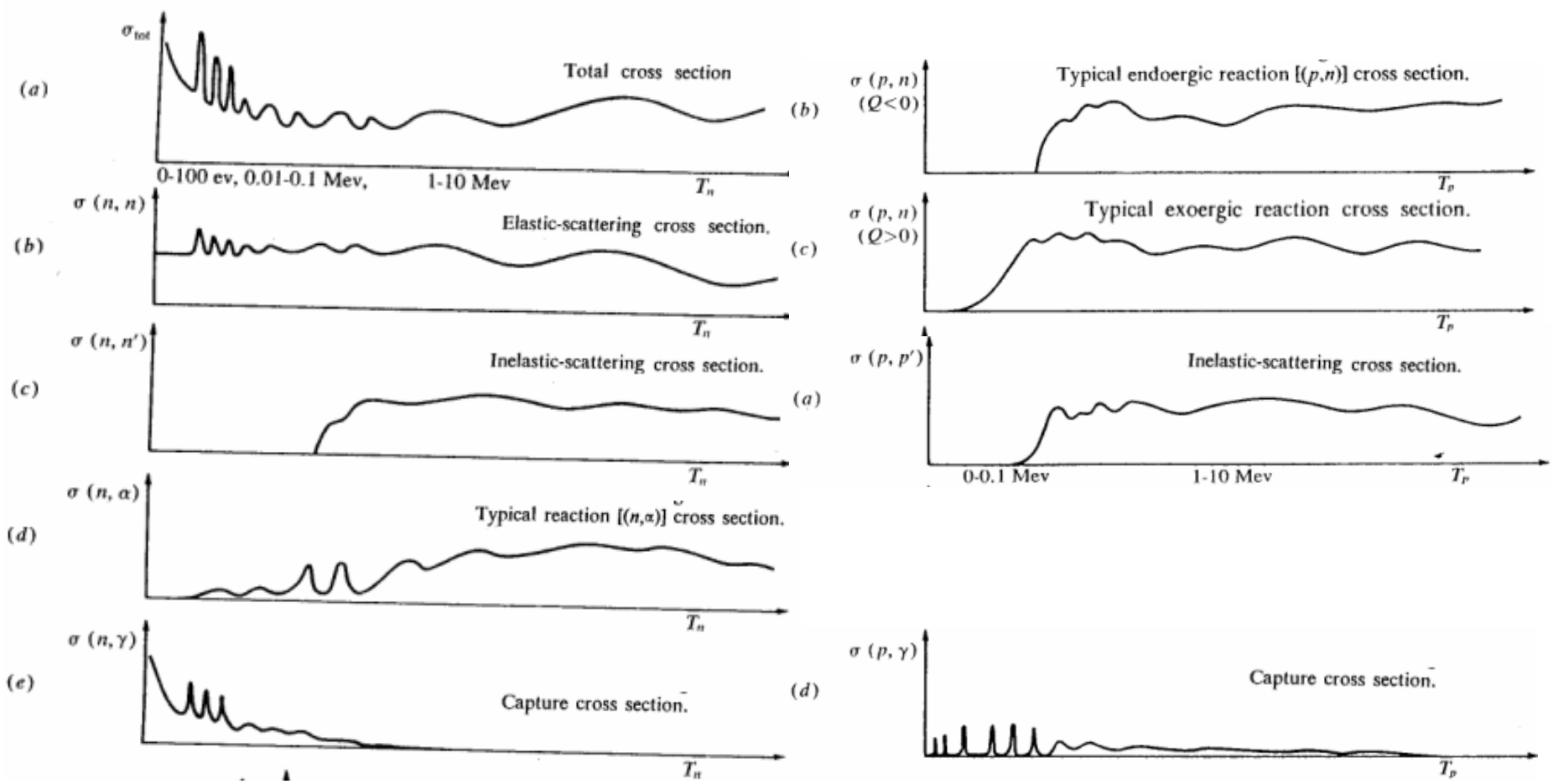

For charged particles the concept of total cross section is not meaningful because the integrated elastic-scattering cross section is theoretically infinite

Neutron & Proton Reaction Cross Section

Schmatic neutron (left) and proton (right) cross sections for a medium weight nucleus.

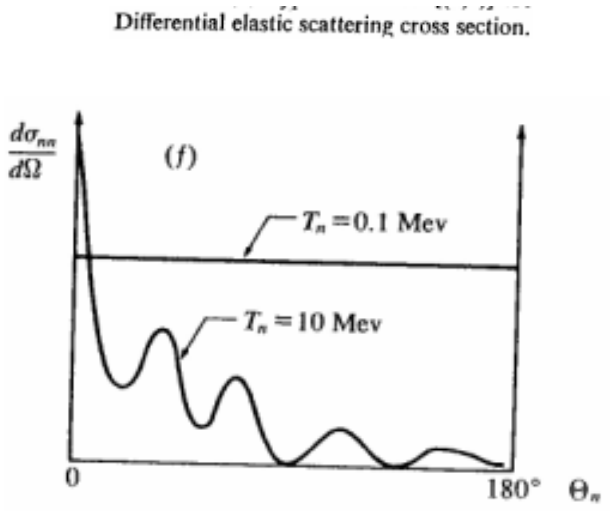

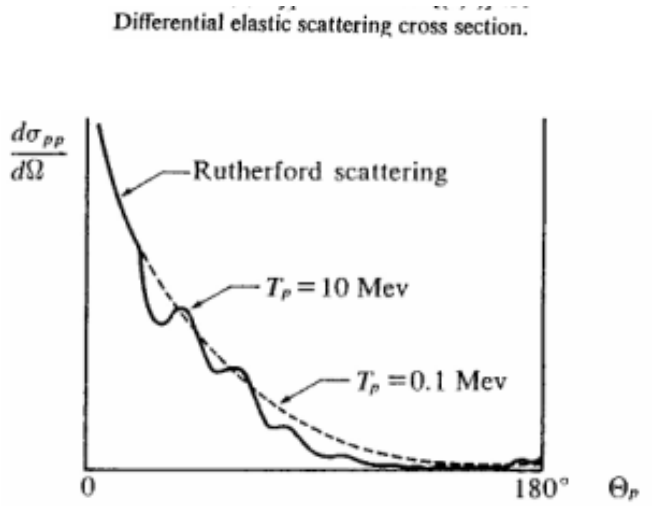

Neutron Cross Section

neutron induced reactions

$$\sigma_{tot} = \sigma_{capture} + \sigma_{elastic} + \sigma_{inelastic} + \sigma_{fission} + \ldots$$

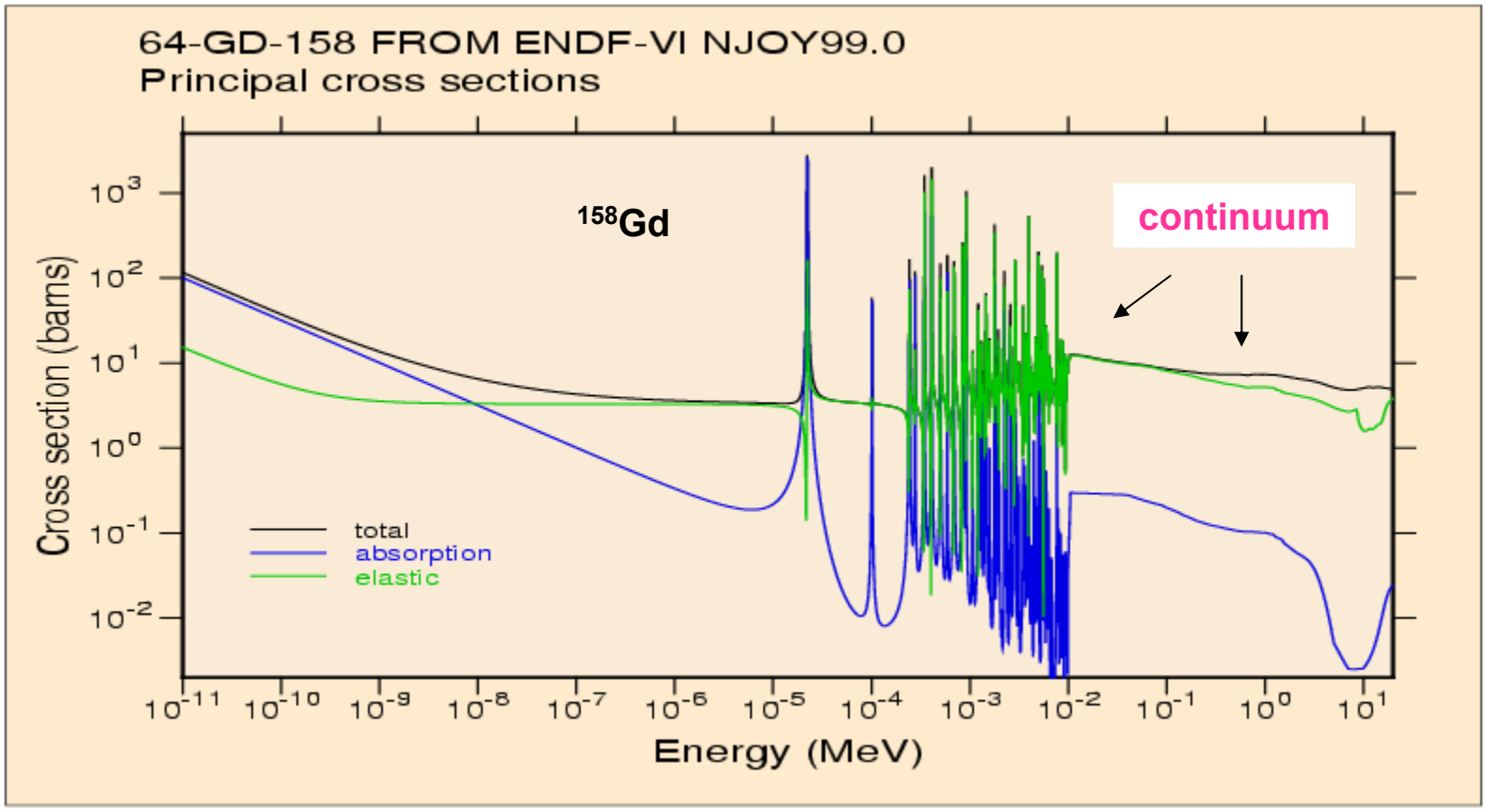

Neutron Cross Section

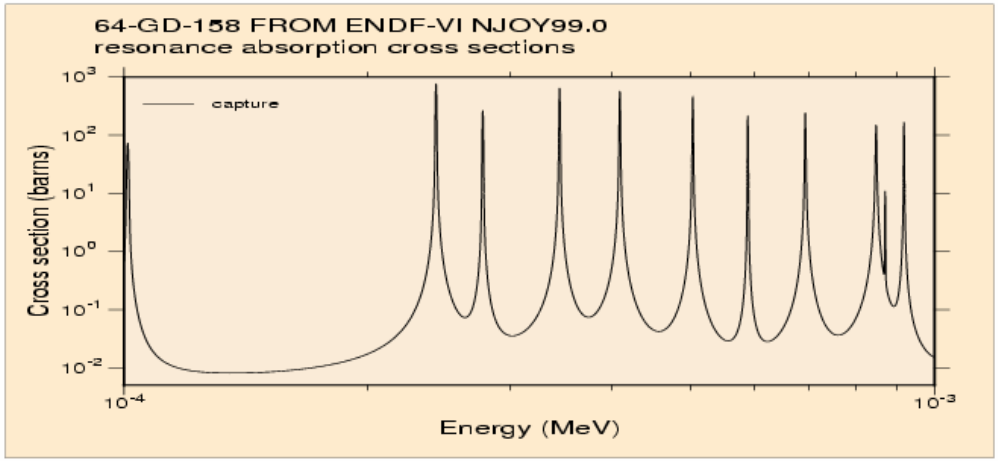

Radiative capture neutron cross section in ^{158}Gd in the region from 100 eV to 1 keV.

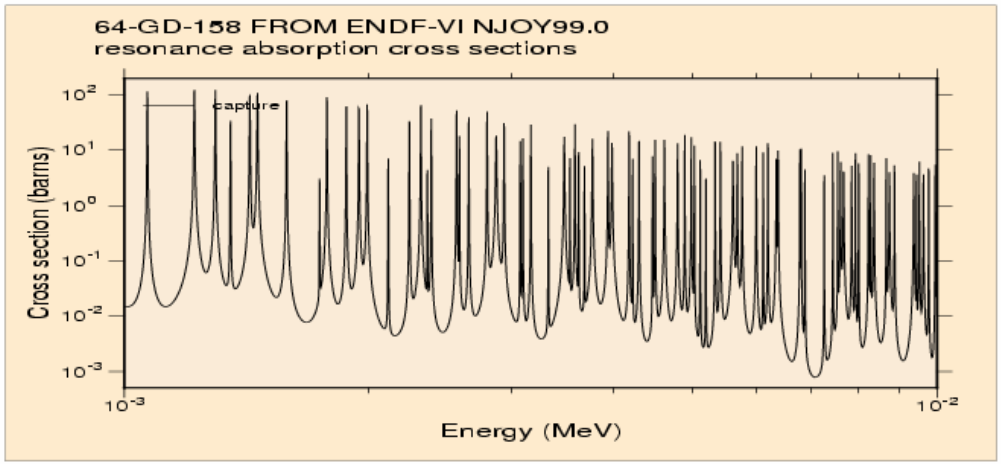

Radiative capture neutron cross section in ^{158}Gd in the region from 1 keV to 10 keV.

Neutron Cross Section

^{235}U

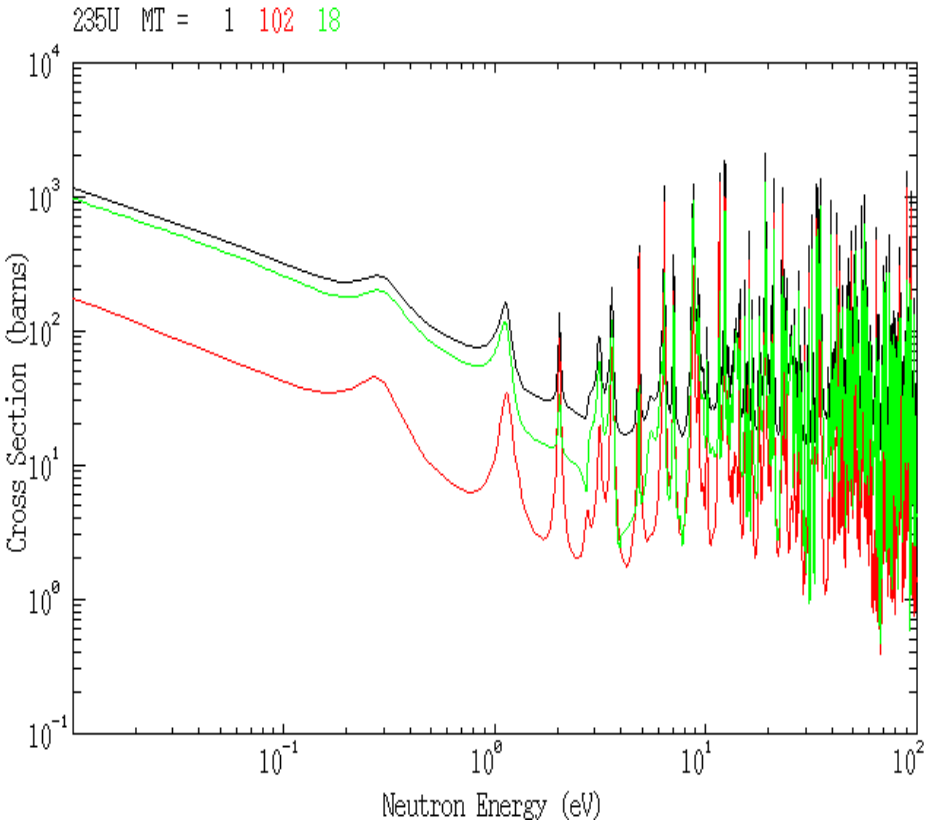

^{238}U

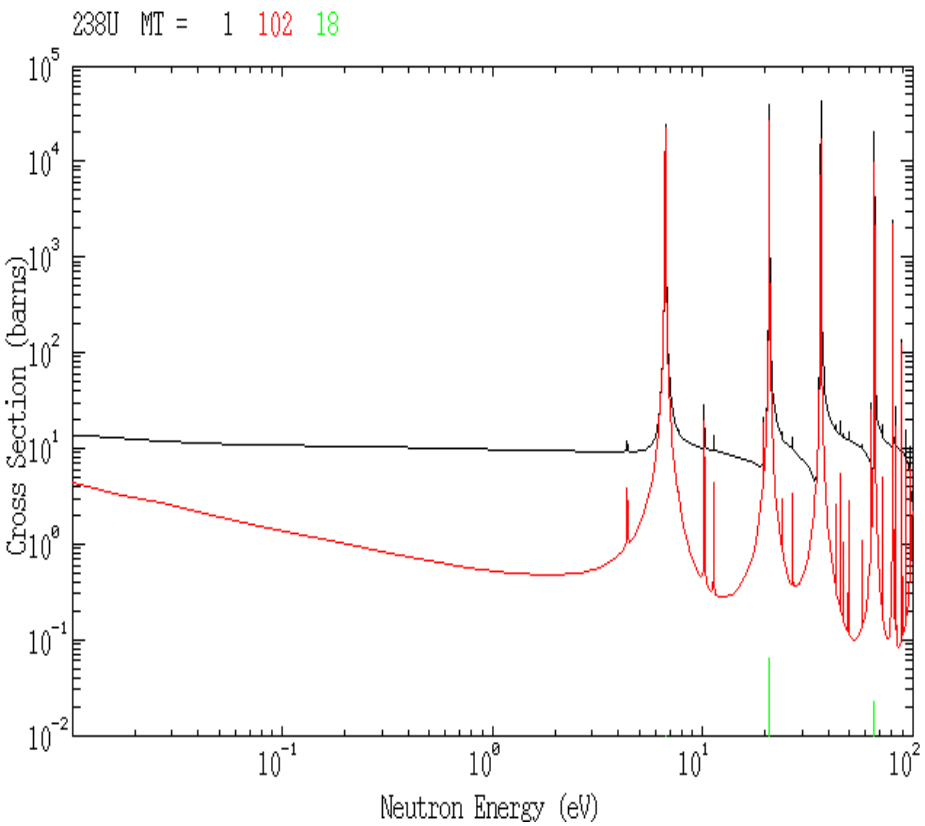

Neutron Cross Section

^{157}Gd

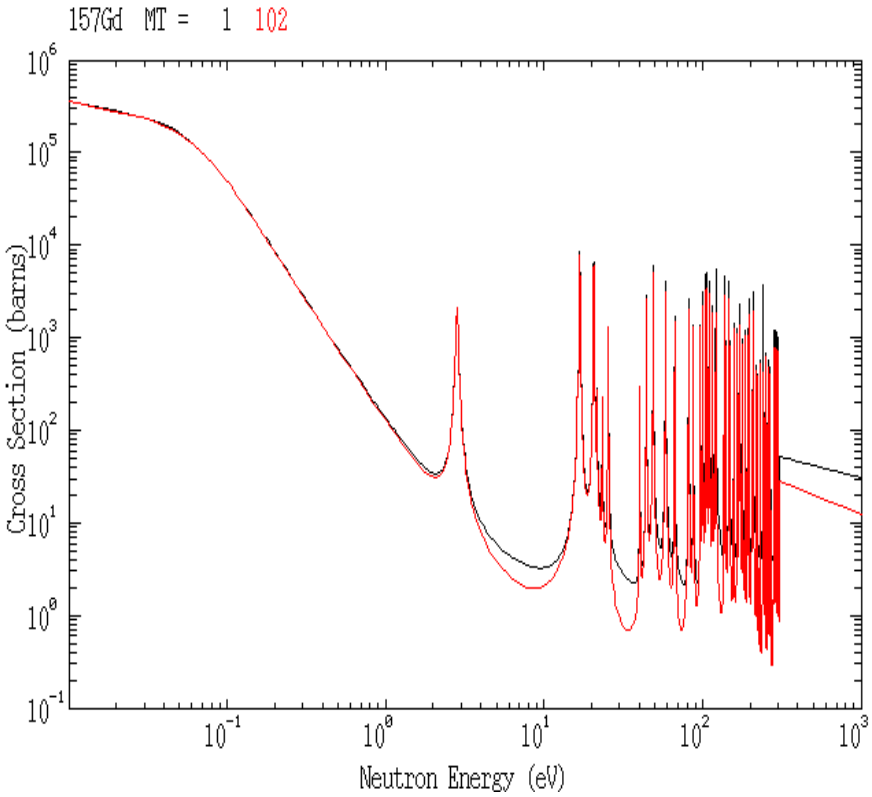

^{158}Gd

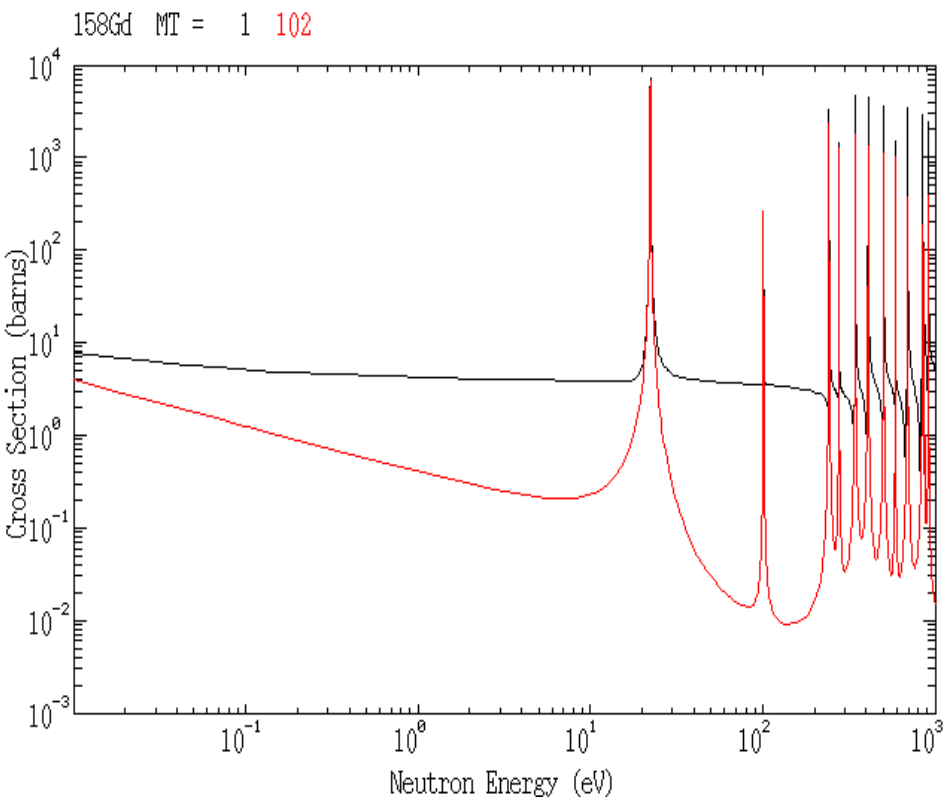

Radiative neutron capture

NEUTRON CAPTURE A nuclear reaction in which a ***neutron*** **is absorbed by a target nucleus** producing an isotope one mass number greater in its ground or excited states.

Neutron capture γ-ray measurements extend over 9 orders of magnitude of neutron energy: from cold and thermal neutron fluxes to the d(t,n) reaction near 14 MeV.

In this large energy scale, the **capture cross section varies from well separeted resonances with complex configurations to the unresolved resonance regions where giant resonance structures** may be found.

Radiative neutron capture reactions are observed in almost every nuclide and are often the dominant reaction near thermal neutron energy.

The exothermic absorption of a neutron by a target nucleus (Z,A) forms a **compound nucleus** (Z,A+1) at exitation energies in the range 4 to 10 MeV (determined namely by the rest-mass energy difference Q – i.e, **neutron binding energy**, of the final and initial nuclides plus the center-of-mass neutron kinetic energy.

When the energy of the compound nucleus corresponds to that of an excited state, a **resonance** is observed. This **captured state** then (after a "long" time ~ 10^{-15} -10^{-12}) decays by the emission of electromagnetic radiation (**primary γ ray**) leaving the compound nucleus in a lower energy state.

The subsequent (**secondary γ ray**) decay of this state to lower energy states, i.e., a **cascade of γ-rays**, leaves the compound nucleus in its ground state which may or may not be stable against α or β decay.

Gamma rays from inelastic scattering or fission are also present – when those processes are energetically allowed.

Test of inverse reaction: **photonuclear reaction** (γ,n).

Radiative neutron capture

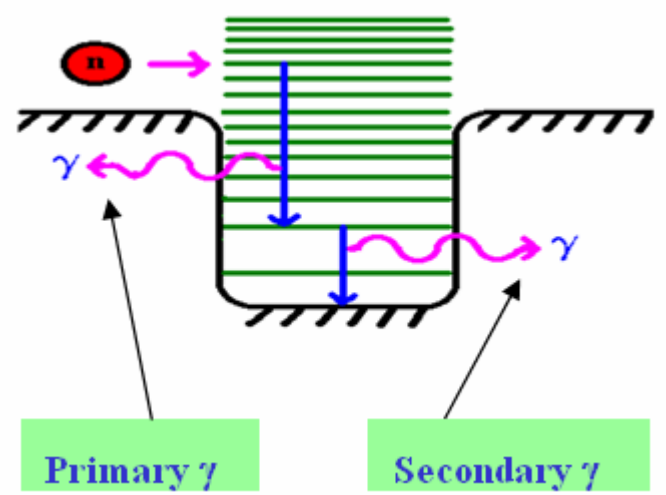

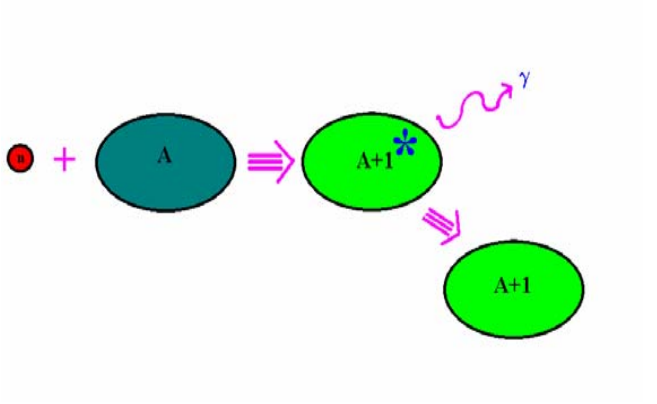

- non-selective population of nuclear excited states (within a given spin and parity range)
- γ-transitions: **electric × magnetic**
- population of collective states
- observation of transitions among low-lying excited states
- branching ratios of depopulation

Radiative neutron capture

The (n, γ) method uses the **neutron separation energy** to form a highly excited (~7 MeV) state that subsequently **decays by electromagnetic radiation**. The energy brought in by a thermal or a slow neutron is so small that particle emission does not compete. The **capturing states** manifest as quasi-stable states with long lives ($\tau \sim 10^{-14}$ s).

The **compound nucleus** is a system with remarkable stability. Its decay is to be considered as a separate process with no inmediate connections with the formation stage (Bohr 1936)*:

$$\sigma(a,b) = \sigma_{CN}(a) \cdot \frac{\Gamma_i}{\Gamma}$$

& no correlations between the entrance and exit channels

The energy dependence of the compound nucleus cross section formation near the resonance is described by the **Breit – Wigner formula**:

$$\sigma_{CN} = \pi \lambda_n^2 \frac{g\Gamma_n\Gamma}{(E_n + E_r)^2 + \Gamma^2/4}$$

λ_n = De Broglie neutron wave length

g = statistical factor

The **total resonance width**: $\Gamma = \Gamma_n + \Gamma_\gamma + \Gamma_f + \Gamma_\alpha + \Gamma_{...} + ... = \hbar w$

Level **lifetime**: $\tau = \hbar / \Gamma$

Transition probabilty $w \sim w(\lambda, E_\gamma, B)$

Multipole order λ

Reduced Transition Probability $B \sim \Psi_i, \Omega, \Psi_f$

The **neutron** and **radiative strength functions** define some properties of states lying near the neutron binding energy. The generally accepted picture is **statistical**, although **non – statistical effects** are known.

Single – Particle **Weisskopf Estimates** Γ_W & hindrance factors [V. Plujko lecture]

**Assumptions violated by direct and valence capture*

Radiative neutron capture

SPECTROSCOPIC INFORMATION

- energy levels and cascade schemes
- electromagnetic transitions (primary, secondary)
- spins and parities of low – lying states
- absolute transition rates (lifetimes)
- branching ratios
- angular correlations
- non-selective population of nuclear excited states (J^{π} range)
- branching ratios of nuclear level depopulation
- resonance spectroscopic information: cross section, spectroscopic factors, energy, total and partial widths, spins, parity, resonace level spacing
- scattering lengths, nuclear potential radii

HIGH RESOLUTION GAMMA SPECTROSCOPY: Detailed and precise information on electromagnetic transitions. Energies, Intensities, spins, parities, lifetimes, correlations.

POLARIZED REACTION STUDIES: Information on angular momenta & phase shift between partial waves

FAST NEUTRON RADIATIVE CAPTURE: Study of nuclear **giant multipole modes** & interference of between the dominating dipole and higher multipole radiations. Study of the competition between **Compound Nucleus** and **Direct – Semi – Direct Capture** mechanisms.

Radiative neutron capture

$^{158}Gd(n,\gamma)^{159}Gd$

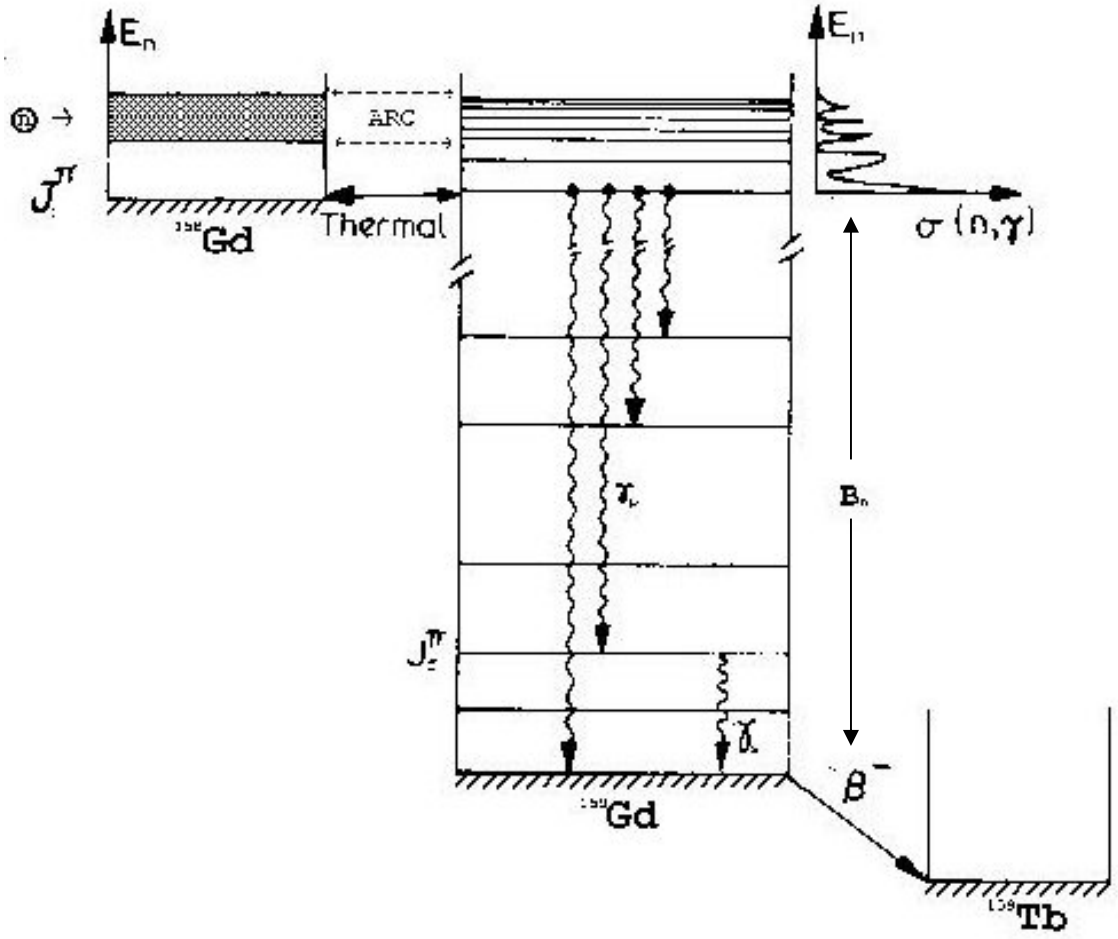

Radiative neutron capture

CROSS SECTION

The statistical description of radiative transition strengths based on the spreading of electric – dipole giant resonance results into a broad range of **compound nucleus states**.

For many light and near – closed – shell nuclei a **direct capture mechanism** dominated by single – particle transitions from the entrance channel is observed namely for off – resonance capture cross sections.

Resonance capture cross section [Lane, Lynn 1960]:

$$\sigma_{res\ cap} = \sigma_{CN} + \sigma_{channel} + \sigma_{dir\ cap}$$

resonance external — hard sphere potential

single particle final states

Direct capture is a direct form of radiative capture observed far away from resonances not involving the compound nucleus. The neutron-target interaction is represented in zero order by a potential well, and the neutron that is initially in an *s*-orbit simply falls into a *p*-wave orbit in the final nucleus resulting in the emission of a primary *E1* transition. Theoretical analysis of this process requires knowledge of the coherent scattering length, the binding energy and (d,p) spectroscopic factors. When all internal contributions can be ignored this process is known as **channel capture**.

Slow – neutron direct capture, known as **potential capture**, is described in terms of the optical model.

Radiative neutron capture

KINEMATICS $\sigma = \sigma_{CN} \cdot \frac{\Gamma_f}{\Gamma}$

formation **I** and decay **II** $n + A \xrightarrow{\mathbf{I}} (A+1)_{CN} \xrightarrow{\mathbf{II}} (A+1)^* + \gamma$

excitation energy **I**: $E^* = B_n + \tilde{T_n} + \tilde{T_A} = B_n + \frac{1}{2}\left(\frac{m_n m_A}{m_n + m_A}\right) v_n^2$

$$E^* = B_n + \frac{m_A}{m_{A+1}} T_n = B_n + T_n\left(1 - \frac{m_n}{m_{A+1}}\right) = B_n + T_n - T_r$$

spin and parity $\vec{J_\lambda} = \vec{J_0} + \vec{l}$

capture state λ $\pi_\lambda = \pi_0 \times (-1)^l$

Recoil energies

T_n (eV)	T_r (eV)
0.025	2×10^{-4}
2000	12
24000	150

excitation energy **II**: $E^* = E_f + E_\gamma + \frac{E_\gamma^2}{2m_{A+1}c^2}$

populated level f $E_f = B_n + T_n - \underbrace{T_n \frac{m_n}{m_{A+1}}}_{\mathbf{I}} - E_\gamma - \underbrace{\frac{E_\gamma^2}{2m_{A+1}c^2}}_{\mathbf{II}}$

neutron binding energy $B_n = E_f + E_\gamma\left(1 + \underbrace{\frac{E_\gamma}{2m_{A+1}c^2}}_{\mathbf{II}}\right) - T_n\left(1 - \underbrace{\frac{m_n}{m_{A+1}}}_{\mathbf{I}}\right)$

secondary gamma–ray $E_{f'} = E_f - E_{\gamma'}\left(1 + \frac{E_{\gamma'}}{2m_{A+1}c^2}\right)$

Primary Gamma – ray & Populated levels

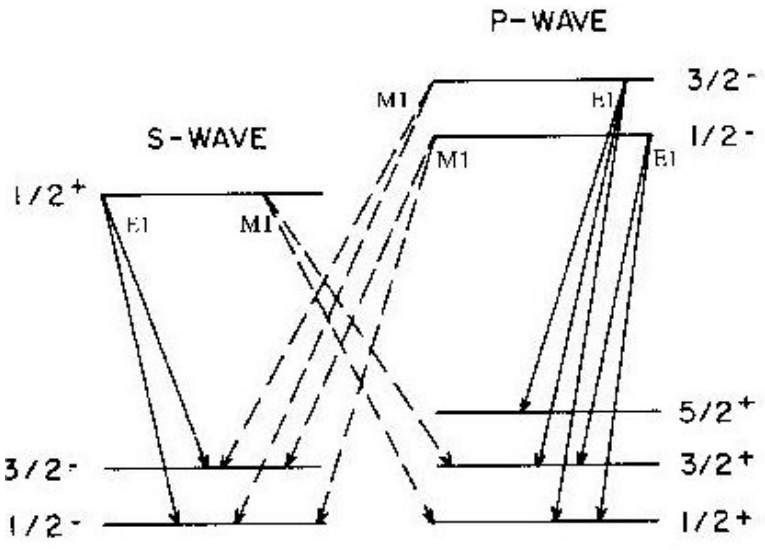

Population of low – lying states by *E1* and *M1* transitions from *s* and *p* – wave capture stares

multipole	*L*	$\Delta\pi$	ΔJ	rel. strength
E1	1	-	-1,0,1	1
M1	1	+	-1,0,1	10^{-1}
E2	2	-	-2,-1,0,1,2	10^{-1}
M2	2	+	-2,-1,0,1,2	10^{-1}

Selection Rules

$$\begin{aligned} \vec{J}_f &= \vec{J}_\lambda + \vec{L} \\ \pi_f &= \pi_\lambda \times (-1)^L \quad \ldots \text{ electric transitions} \\ \pi_f &= \pi_\lambda \times (-1)^{L+1} \quad \ldots \text{ magnetic transitions} \end{aligned}$$

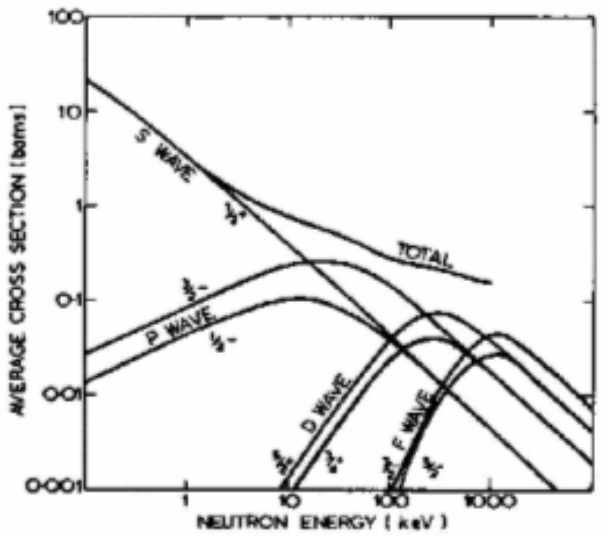

Partial neutron cross sections for *s, p, d, f* – capture on a medium heavy nucleus

Primary gamma – ray intensity

From the complexity of the compound nucleus states, it follows, according to the central-limit theorem of statistics, that the **reduced-width amplitudes for a set of resonances have a Gaussian distribution centered on a mean of zero**.

The resultant distribution, so-called **Porter-Thomas distribution**, says that the primary gamma-ray intensities have a very wide distribution with most probable value zero.

This distribution applies for any measurement, whether resonant or nonresonant capture is involved, so long as the incident energy is well defined for the captured neutron. Thermal neutron capture may be considered as a measurement of a single entry point.

This is a severe limitation of the thermal capture method for direct population of final states, since **the most probable line intensity is zero**. The wide distribution of intensities makes it difficult to assign spins and parities on the basis of intensity alone.

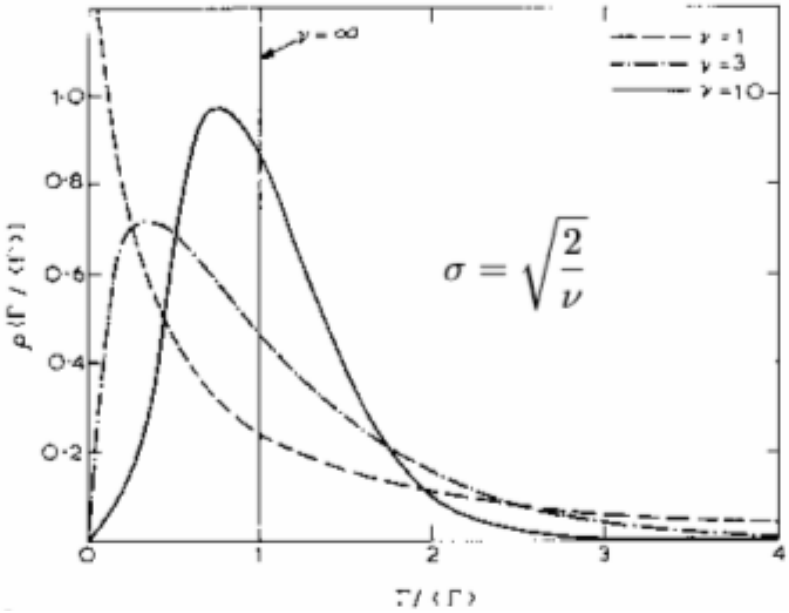

Statistical distribution of partial gamma – widths for various degrees of freedom ν.

Photon Strength

Strengths of electromagnetic transitions between nuclear states provide data for **tests of nuclear models, radiative capture reaction mechanisms, nuclear potentials and nucleon – nucleon interactions**.

The interpretation and compatibility with **photo – absorption** data that involve transitions between the ground state and higher excited states are based on the asumption that the **excitation function in the contiunuum region is independent of the initial target state**.

In medium and heavy nuclei on each low – lying state a **Giant Dipole Resonance** is built (Axel – Brink hypothesis).

The strenghts of individual transitions from a region of high density of states have limited usefulness as indicators of average strengths because of the **statistical nature of the decay process**.

Together with the dependencies noted on the average **nuclear level spacing**, **transition energy** and **multipole order**, a better indicator of the features of the distribution of strength is the **gamma – ray strength function**:

$$f_{XL}(E\gamma) = \frac{\Gamma_{\lambda\gamma f}(XL)}{D_\lambda \cdot E_\gamma^{(2L+1)}}$$

Definition analogous to the **neutron strength function**

$$f_{XL}(E\gamma) = \frac{2.6\cdot 10^{-6}}{(2L+1)} \cdot \frac{\sigma_{XL}(E_\gamma)[fm^2]}{E_\gamma^{(2L+1)}[MeV]}$$

$\sigma_{XL}(E_\gamma)$

photo absorption cross section

In the region between 12 – 20 MeV are observed **Giant Resonances** for **E1, M1, E2** radiation that influence the photon strength in radiative neutron capture

$$f_\gamma(E_\gamma) = \frac{1}{3(\pi\hbar c)^2} \sum_{i=1,2} \sigma_{0_i} \frac{E_\gamma \Gamma_{G_i}^2}{(E_\gamma^2 - E_{G_i}^2)^2 + E_\gamma^2 \Gamma_{G_i}^2}$$

E_G peak GR energy

Γ_G peak spreading width

σ_0 peak cross section

Nuclear Spectroscopy with Neutrons: Experimental Techniques

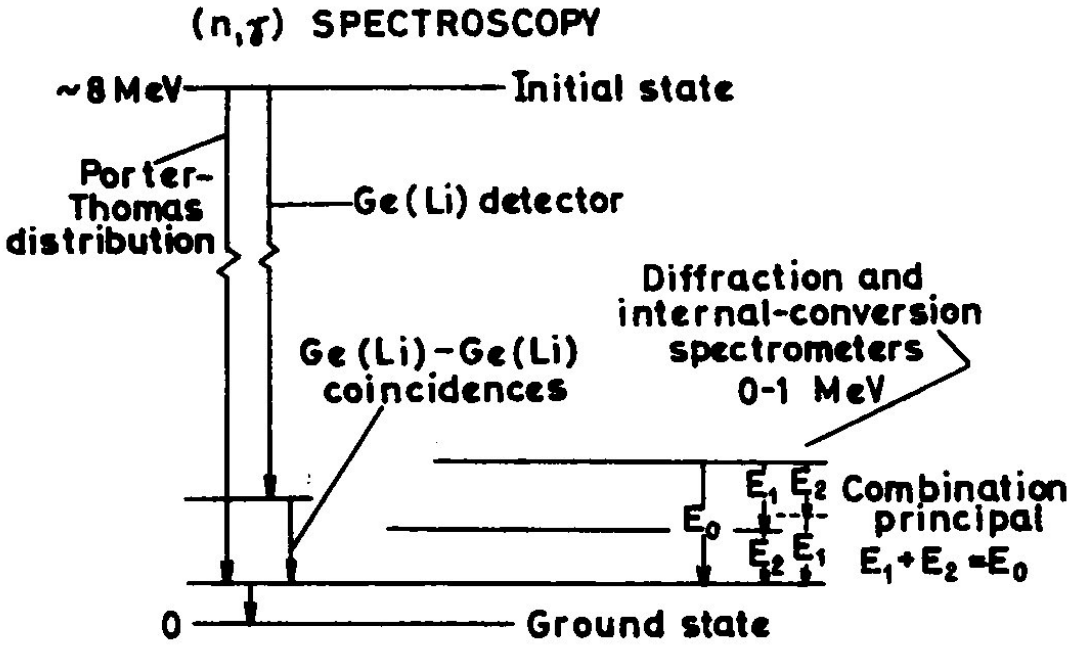

Fig. 2. γ-ray spectrometers

Nuclear Spectroscopy with Neutrons

Outline

- Introduction & terms
- Neutron sources & detectors
- Nuclear spectroscopy

break

- **Example of complete nuclear spectroscopy**

Nuclear spectroscopy of ^{159}Gd

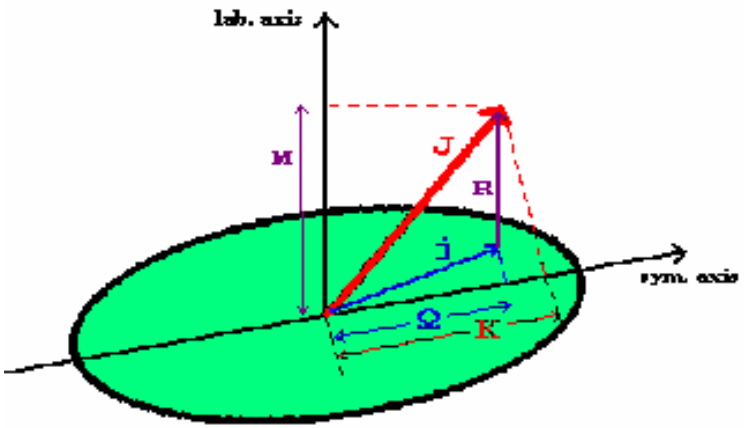

Single particle motion in deformed potential

- Well **deformed odd-A** nucleus with large stable deformation **(ε ~0.3)**
- Splitting of single particle (spherical) strength over many Nilsson (deformed) states which are labelled by the **asymptotic quantum numbers** $K[Nn_z\Lambda]$
- The single particle spectrum for such nuclei in this region exhibits several near-lying states with same parity and $\Delta K = 0, \pm 1$. Such states show strong configuration mixing (Coriolis interaction)
- Major shell *N* orbital crossing near the Fermi surface
- Low-lying **collective vibrational phonons** (quadrupole, octupole,..)

LOW EXCITATIONS

- **One quasiparticle excitations**
- Coupling of single particle motion with collective **rotations**

HIGH EXCITATIONS

- **One and three quasiparticle** excitations
- Coupling of single particle motion with **rotations & vibrations**

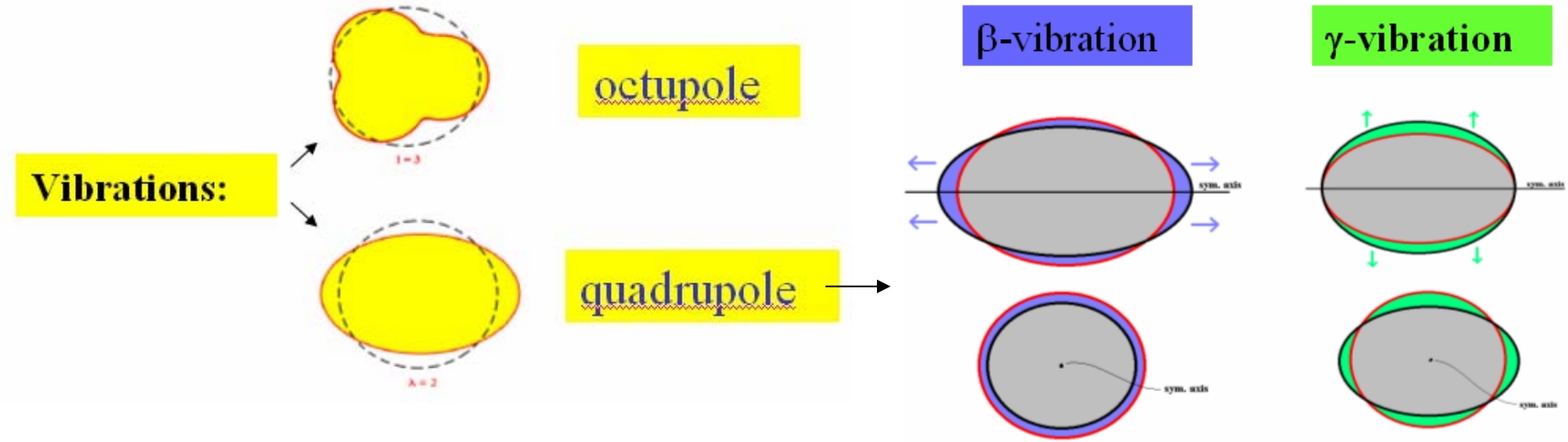

Nuclear spectroscopy of ^{159}Gd

Experiments

Radiative capture	**Neutron transfer**
^{158}Gd(n,γ)^{159}Gd	^{158}Gd(d,p)^{159}Gd
	^{160}Gd(d_{pol},t)^{159}Gd

- **IRC (Dubna), ARC (BNL), TNC & GAMS2/3 (ILL)**
- **Tandem Van de Graaff, Q3D spectrograph (TU-Munich)**

Spectroscopic results

- gamma transitions, levels, gamma decay and branching ratios, spectroscopic factors, photon strength, level density, ...

Model calculations & comparison

- nuclear structure
- nuclear reactions

(n,γ) experiments

EXPERIMENT (laboratory)	E_n	Φ [n/sec cm²]	# of res.	Target [g]	Enrich. [%]	Spectrometer	FWHM ΔEγ
BURN UP & HIGH FLUX (ILL)	thermal ~ 0.025 eV	5 x 10^{14}	thermal	0.055	97.5	Crystal (Quartz) GAMS2/3 + NaI	~ 100's eV
IRC (IBR-30 & TOF) (DUBNA)	epithermal 22 – 1000 eV	Pulsed	12	48.5	97.7	Time-of-Flight Ge (Li)	~ 5 keV
ARC (Sc filter) (BROOKHAVEN)	2 keV	7.7 x 10^{7}	~ 12	80.0	95.8	Pair spectrometer Ge (Li) + NaI(Tl)	~ 6 keV
ARC (Fe filter) (BROOKHAVEN)	24 keV	4.2 x 10^{7}	~ 25	80.0	95.8	Pair spectrometer Ge (Li) + NaI(Tl)	~ 6 keV

Time – of – flight spectra

^{159}Gd

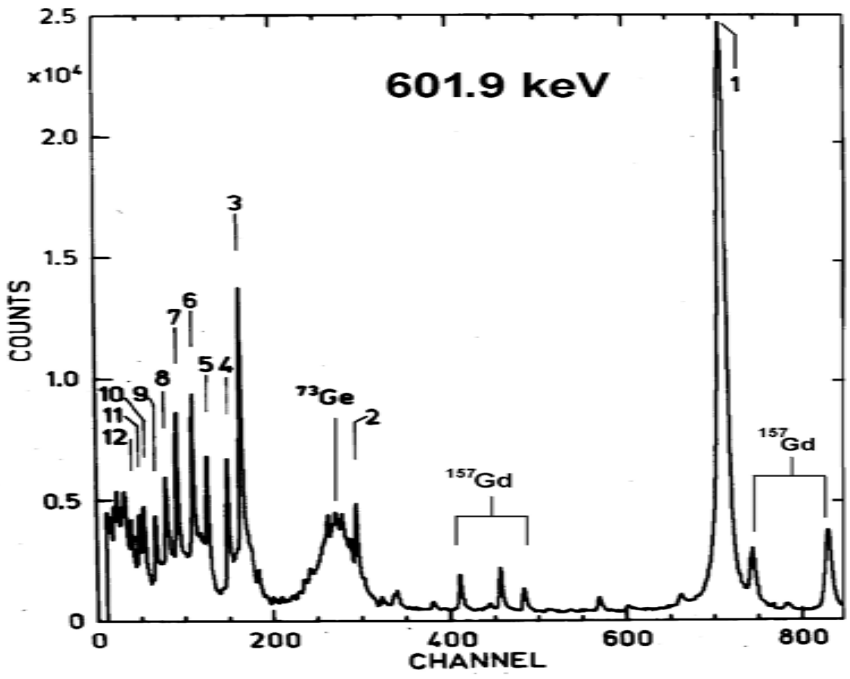

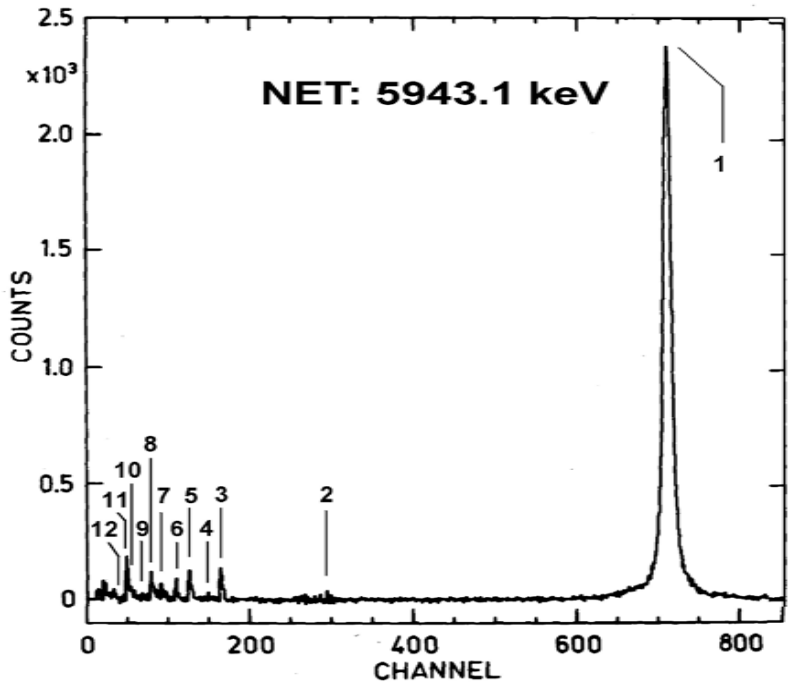

Time – of – flight spectra

^{174}Yb

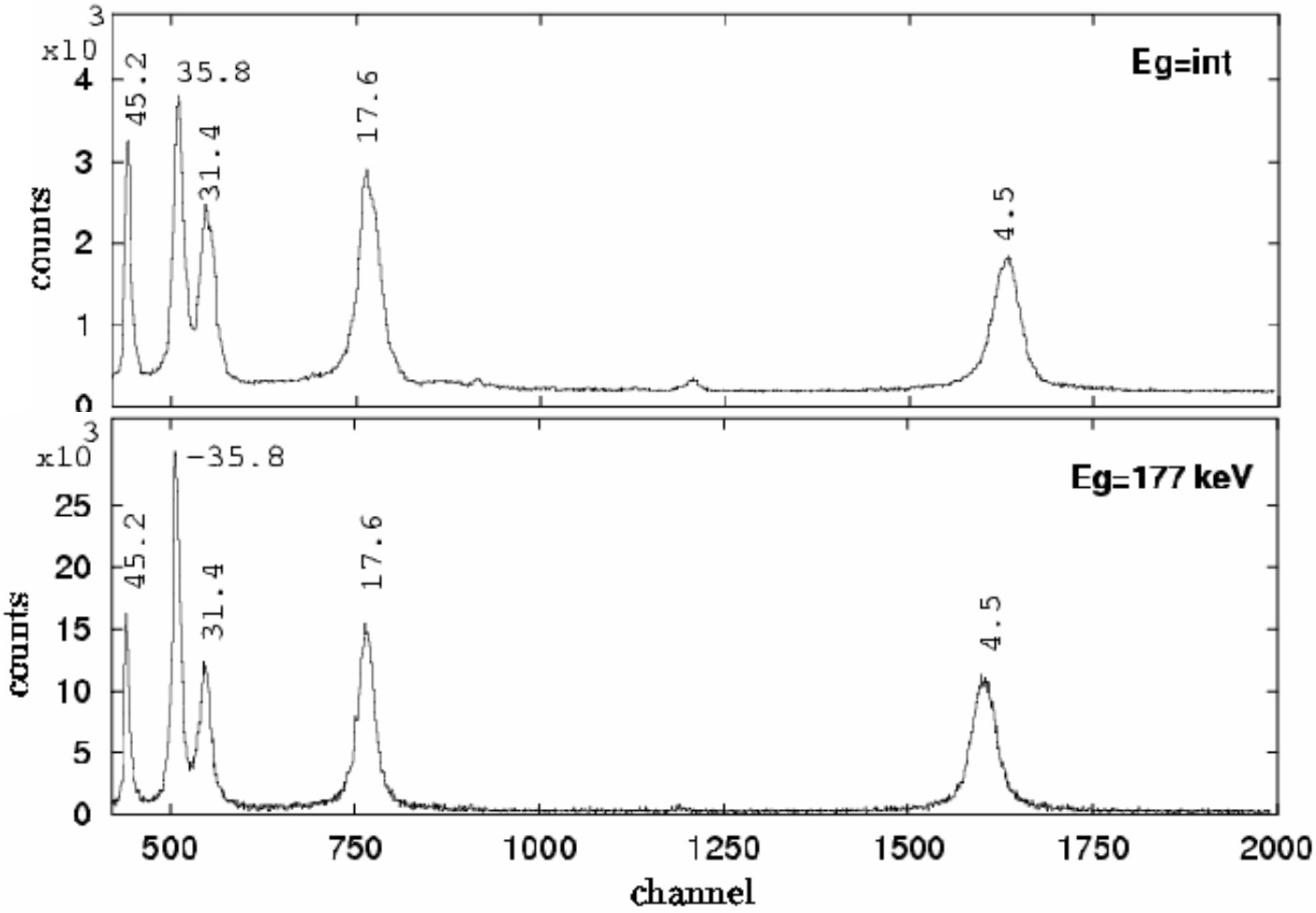

Time – of – flight spectra

^{174}Yb

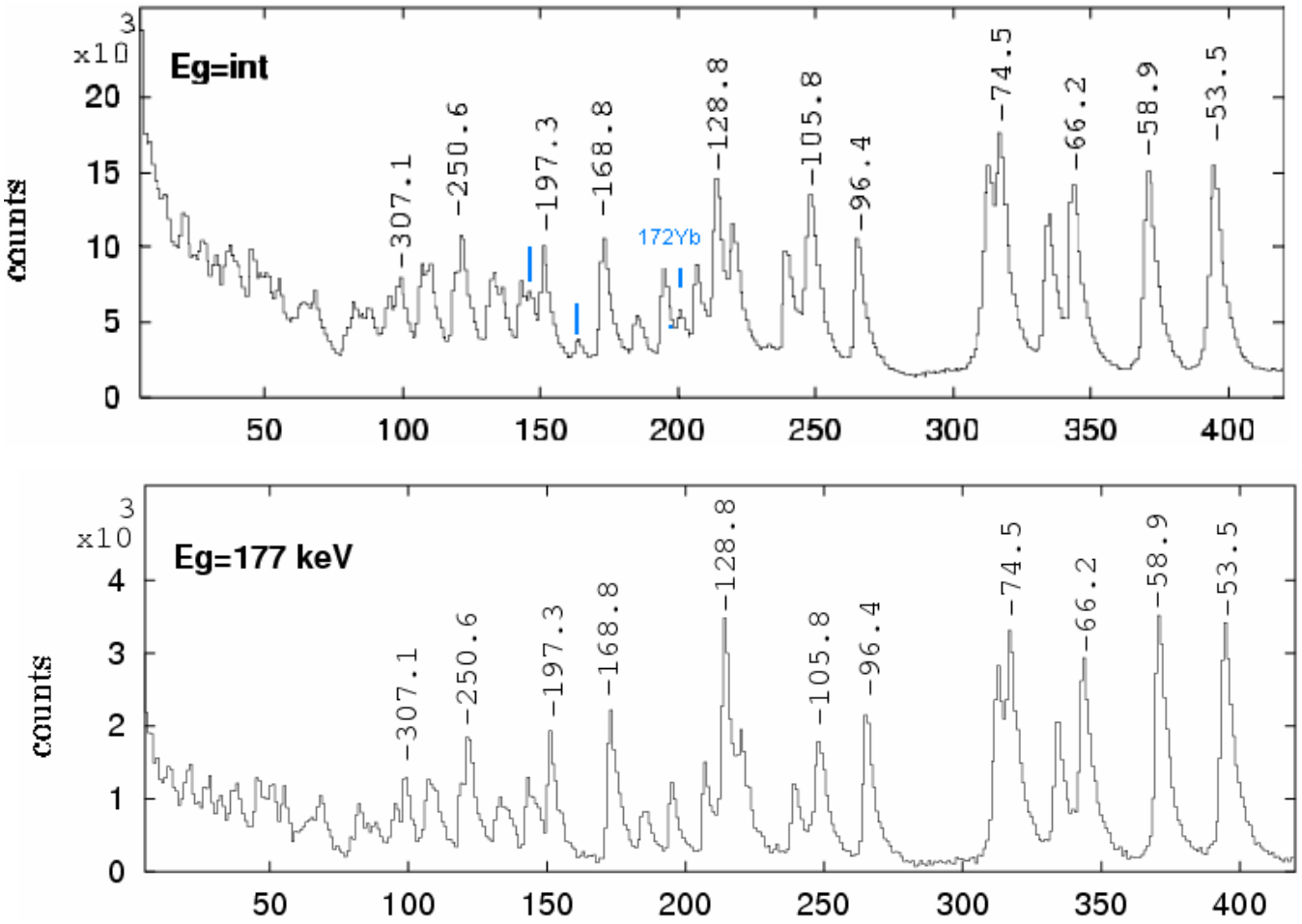

^{172}Yb: 140, 180, 202 eV

Generated gamma – ray spectra

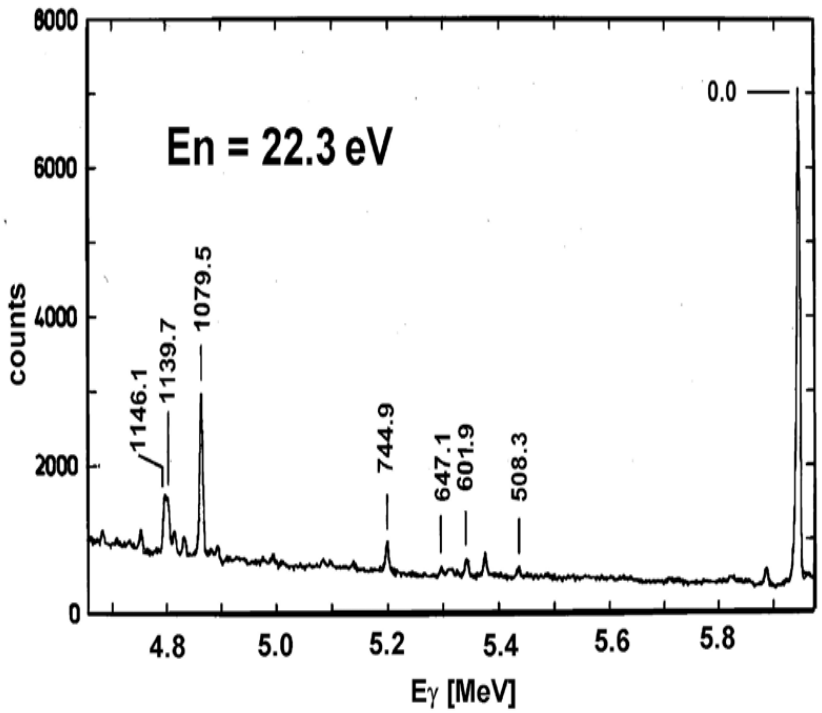

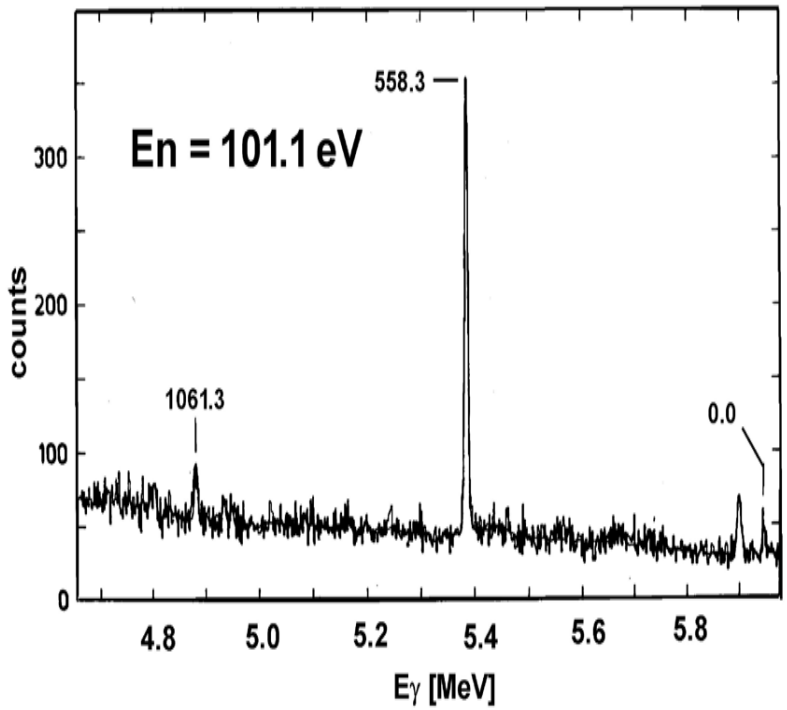

Generated gamma – ray spectra

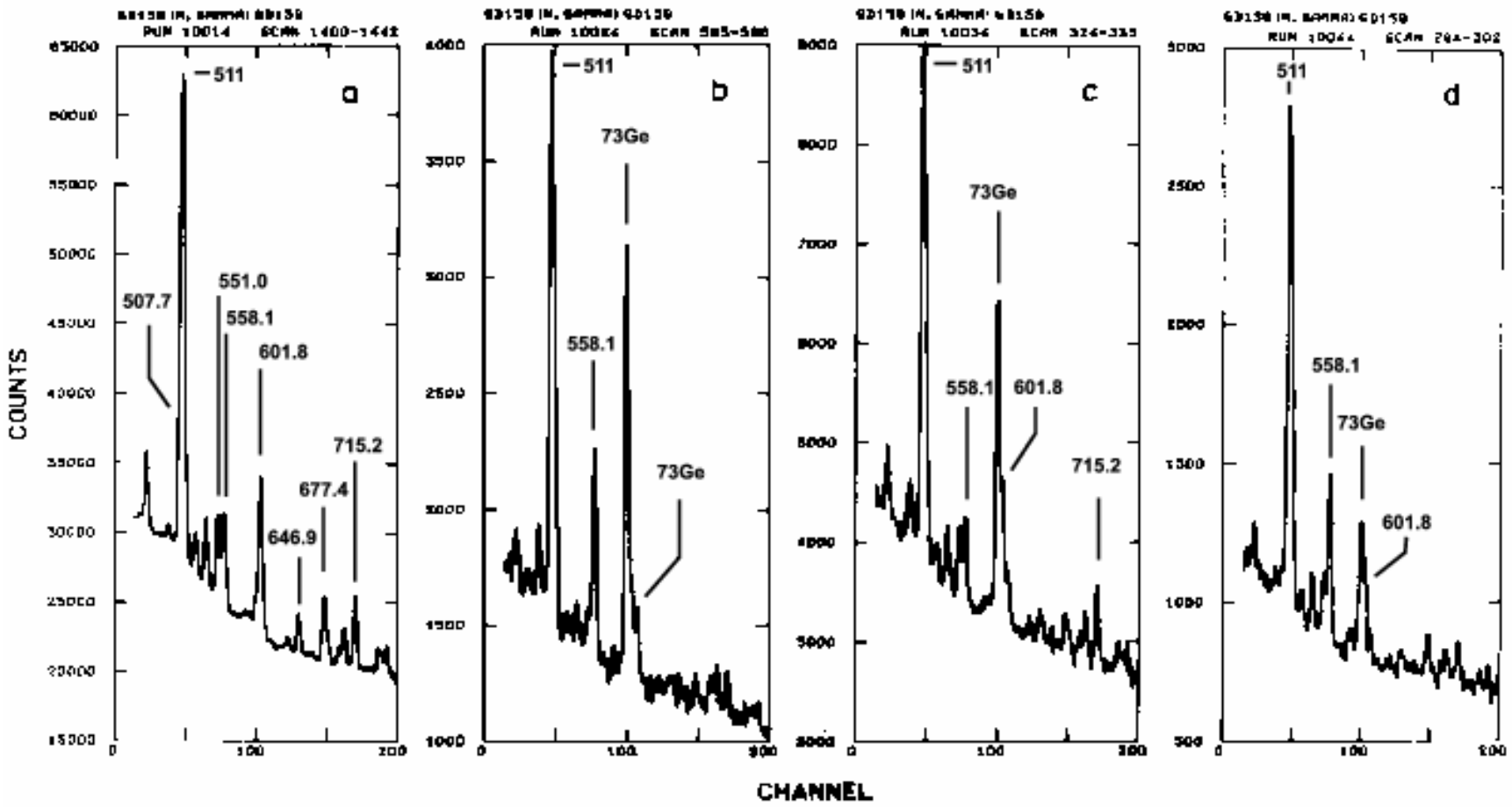

Figure 11: Gamma–ray spectra in the region 500 keV< E_γ <750 keV in IRC. Spectra were produced for neutrons with energies E_n at 22 eV (a), 101 eV (b), 242 eV (c), 277 eV (d),

Generated gamma – ray spectra

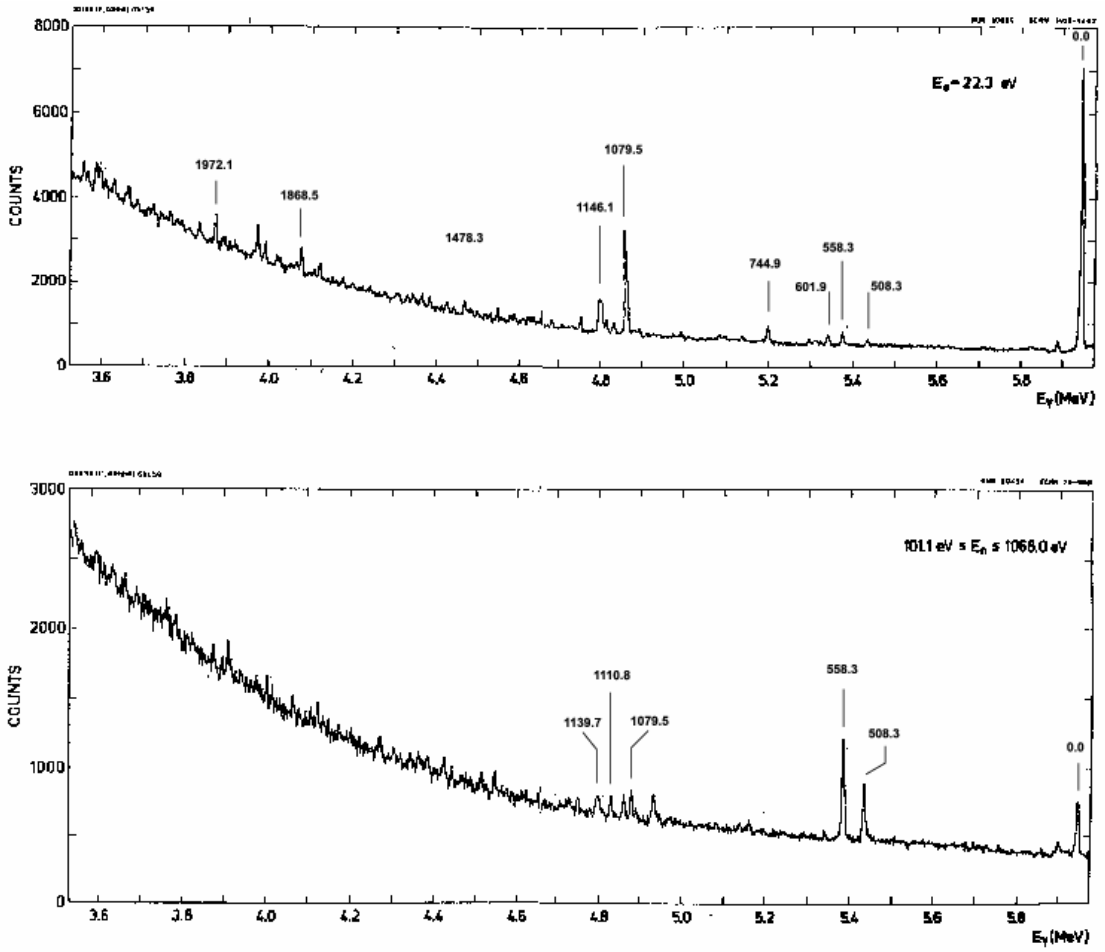

Figure 43: Gamma–ray spectra in the region between 3.6 MeV and 6 MeV of the reaction ^{158}Gd(n,γ)^{159}Gd in IRC. Figures are produced for neutrons with energies at the 22.3 eV resonance (top) and with energies in the range from 101.1 eV through 1068.0 eV (bottom). Some peaks are indicated by the energy of the corresponding populated state (in keV).

Gamma – ray: energy & intensity

Table 1
Intensities of primary γ-ray transitions in the ^{158}Gd(n,γ)^{159}Gd reaction at 12 isolated resonances. Values are given in absolute units (i.e., per 100 neutrons captured) with statistical errors only. Neutron resonance energies E_λ are indicated in eV

$E_{\gamma f}$ [keV]	E_f [keV]	$I_{\lambda\gamma f}$ [a]											
		$E_\lambda = 22.3$	101.1	242.7	277.2	344.8	409.1	503.3	588.5	692.9	847.3	917.1	1068.0
5943.0(2)	0.0	10.00(7)	0.9(2)	1.13(10)	0.8(2)	3.7(4)	0.32(17)	1.04(17)	3.0(3)	0.52(16)	1.8(3)	8.5(8)	−0.1(3)
5434.7(2)	508.3	0.16(3)	0.2(2)	2.55(15)	0.4(2)	2.8(4)	5.1(4)	2.3(3)	0.41(17)	0.4(2)	0.4(2)	0.4(3)	0.5(3)
5384.7(2)	558.3	0.04(2)	13.8(9)	0.35(7)	10.1(7)	0.5(2)	1.2(2)	0.79(16)	2.6(3)	4.6(4)	3.6(4)	0.7(3)	1.9(4)
5341.1(3)	601.9	0.31(3)	0.0(2)	0.10(7)	−0.08(15)	0.13(19)	0.13(18)	−0.11(13)	0.12(14)	0.00(16)	0.08(18)	0.0(3)	0.2(3)
5295.9(5)	647.1	0.15(2)	0.4(2)	−0.13(7)	−0.13(15)	0.3(2)	0.35(18)	−0.05(14)	−0.12(14)	0.09(16)	0.09(18)	0.4(3)	−0.1(3)
5198.1(2)	744.9	0.54(3)	0.2(2)	−0.02(7)	0.38(16)	−0.12(19)	−0.07(16)	−0.23(13)	0.11(14)	0.08(16)	0.14(19)	0.2(3)	0.3(3)
5161.0(5)	782.0	−0.06(2)	0.3(2)	0.05(7)	0.31(17)	0.4(2)	0.34(19)	0.25(15)	0.16(15)	−0.12(16)	0.1(2)	0.2(3)	1.4(4)
5083.0(6)	860.0	0.13(2)	0.3(2)	0.32(8)	−0.25(15)	0.2(2)	0.30(19)	−0.05(14)	−0.01(14)	−0.18(16)	0.3(2)	0.1(3)	1.0(4)
4971.0(13)	972.0	−0.04(3)	0.2(3)	−0.13(10)	0.3(3)	0.1(3)	0.2(3)	0.2(2)	−0.1(2)	0.1(3)	0.2(3)	0.8(5)	0.2(4)
4939.7(10)	1003.3	0.03(3)	0.1(2)	0.13(8)	−0.05(17)	0.1(2)	0.3(2)	0.36(17)	0.03(16)	−0.18(17)	0.5(3)	0.6(4)	0.8(4)
4881.7(3)	1061.3	0.16(3)	1.7(3)	0.21(8)	0.23(18)	0.9(3)	3.3(4)	0.13(16)	0.04(16)	0.34(19)	2.7(4)	1.7(4)	0.6(4)
4863.5(2)	1079.5	2.96(4)	0.1(2)	0.79(10)	0.9(2)	2.74(4)	−0.23(18)	0.09(16)	0.59(18)	0.21(19)	1.3(3)	−0.2(3)	0.5(3)
4832.2(3)	1110.8	0.31(3)	0.3(2)	0.88(10)	0.36(17)	0.0(2)	1.3(4)	0.61(18)	0.18(16)	0.21(18)	−0.2(2)	0.2(4)	2.3(4)
4814.4(3)	1128.6	0.44(3)	−0.3(2)	0.05(8)	0.25(17)	0.0(2)	0.9(2)	0.22(16)	0.25(17)	0.11(18)	−0.4(2)	0.2(3)	−0.1(3)
4803.3(2)	1139.7	0.90(3)	0.8(3)	0.13(9)	0.06(18)	0.1(2)	0.3(2)	1.0(2)	1.4(2)	0.6(2)	0.0(2)	0.9(4)	0.3(3)
4796.9(2)	1146.1	1.02(3)	0.4(2)								0.7(3)	0.3(4)	−0.3(3)
4543.7(11)	1399.3	0.21(3)	0.4(3)								0.0(3)	0.7(4)	0.7(4)
4526.1(13)	1416.9	0.14(3)	0.4(3)								0.1(2)	−0.2(4)	−0.2(4)
4513.4(12)	1429.6	0.13(3)	0.6(3)								0.8(3)	0.0(4)	−0.2(4)
4495.2(13)	1447.8	0.12(3)	0.2(2)								−0.5(3)	−0.1(4)	−0.4(4)
4474.4(12)	1468.6	0.15(3)	0.0(3)								0.1(3)	0.4(4)	0.7(4)
4464.7(3)	1478.3	0.47(3)	0.5(3)	0.09(10)	0.0(2)	0.3(3)	0.4(3)	0.06(19)	0.4(2)	−0.3(3)	−0.1(3)	0.1(4)	0.7(4)
4438.6(8)	1504.4	0.14(3)	0.5(3)	−0.01(10)	0.0(2)	0.8(3)	−0.1(2)	0.06(19)	0.09(19)	0.2(3)	0.2(3)	0.2(4)	0.1(4)
4421.7(5)	1521.3	0.33(3)	0.7(3)	−0.01(11)	0.1(2)	2.2(4)	0.4(3)	0.0(2)	0.6(2)	0.9(3)	0.3(3)	0.5(4)	0.7(4)
4385.9(10)	1557.1	0.00(4)	−0.3(3)	0.32(13)	0.0(3)	0.6(4)	−0.2(3)	−0.2(3)	0.1(3)	−0.2(3)	−0.2(3)	−0.2(5)	0.1(4)
4381.7(5)	1561.3	0.24(4)	0.6(3)	0.07(13)	1.6(4)	0.2(3)	0.4(3)	0.4(3)	−0.1(3)	0.5(3)	0.3(3)	0.7(5)	0.1(5)
4366.0(14)	1577.0	0.16(4)	−0.1(3)	0.06(12)	0.0(3)	0.7(3)	0.4(3)	0.0(2)	0.1(2)	0.2(3)	0.4(3)	0.2(4)	0.5(4)
4360.7(9)	1582.3	0.32(4)	0.3(3)	0.49(12)	0.5(3)	0.2(3)	0.2(3)	0.2(2)	0.5(3)	−0.3(3)	0.3(3)	0.1(4)	0.6(4)
4348.4(15)	1594.6	0.15(4)	0.2(3)	0.08(12)	0.0(3)	0.1(3)	0.0(3)	−0.3(2)	0.2(2)	0.1(3)	−0.1(3)	0.1(4)	0.4(4)
4340.4(15)	1602.6	0.32(7)	0.1(5)	0.2(2)	0.8(5)	−0.2(6)	0.4(5)	0.3(4)	0.4(5)	−0.4(5)	1.8(6)	−0.5(7)	0.7(7)
4327.9(6)	1615.1	0.27(4)	−0.3(3)	0.10(12)	−0.1(3)	−0.2(3)	0.2(3)	−0.3(2)	0.1(2)	−0.3(3)	−0.1(3)	−0.2(4)	0.3(4)
4308.0(10)	1635.0	0.18(4)	−0.4(3)	0.02(12)	−0.1(3)	0.1(3)	0.1(3)	0.0(2)	−0.1(2)	−0.3(3)	0.1(3)	0.1(4)	0.7(4)
4301.4(8)	1641.6	0.19(4)	0.0(3)	0.18(12)	0.8(3)	1.0(3)	0.3(3)	0.0(2)	−0.3(2)	0.3(3)	0.5(3)	0.6(5)	0.4(4)
4273.2(15)	1669.8	0.13(4)	−0.4(3)	−0.03(13)	0.4(3)	−0.1(3)	0.7(3)	−0.2(3)	0.0(3)	0.1(3)	0.2(3)	0.2(5)	0.1(5)
4268.8(8)	1674.2	−0.01(4)	0.0(3)	0.62(14)	0.0(3)	0.1(4)	−0.1(4)	0.4(3)	0.2(3)	−0.4(3)	0.3(3)	0.7(5)	0.9(5)
4238.4(10)	1704.6	0.15(4)	0.2(3)	0.04(12)	−0.1(3)	−0.1(3)	0.3(3)	0.0(3)	0.5(3)	0.4(3)	−0.3(3)	0.8(5)	−0.3(4)
4197.0(10)	1746.0	0.13(4)	−0.4(3)	0.10(12)	0.4(3)	0.1(3)	0.3(3)	0.2(3)	0.5(3)	0.7(3)	0.0(3)	−0.2(4)	−0.4(4)
4172.7(9)	1770.3	0.16(4)	0.0(3)	0.08(12)	−0.1(3)	0.0(3)	0.1(3)	0.2(3)	0.6(3)	0.4(3)	0.0(3)	0.1(4)	0.6(4)
4118.5(4)	1824.5	0.44(4)	0.5(4)	0.52(14)	0.4(3)	0.1(4)	0.6(3)	0.5(3)	0.9(3)	0.5(3)	0.8(4)	2.5(5)	0.0(4)
4102.1(15)	1840.9	0.09(4)	0.2(4)	0.28(14)	0.8(3)	−0.2(3)	0.7(3)	0.3(3)	0.2(3)	0.0(3)	0.3(4)	0.8(5)	0.4(5)
4074.5(3)	1868.5	0.78(5)	0.5(4)	0.12(13)	0.0(3)	0.4(4)	0.1(3)	0.2(3)	0.1(3)	0.2(3)	0.8(4)	0.1(5)	−0.4(5)
4062.3(10)	1880.7	0.30(5)	0.0(4)	0.18(15)	−0.2(3)	0.3(4)	1.0(4)	0.3(3)	0.1(3)	−0.2(4)	0.7(4)	0.5(5)	0.1(5)

(*continued*)

Experimental uncertainties: statistical & systematical

Siginificant error digits: 1 digit (>29), 2 digits (≤29)

C. Granja et al. / Nuclear Physics A ••• (••••) •••–•••

Gamma – ray intensity & photon strength

Table 3
Photon strength in ^{159}Gd observed at 12 individual neutron resonances. Final assignments of transition multipolarity XL are based on the analysis of *analytically averaged* (a) and of *individual* (b) γ-ray intensities. All observed levels have either spin 1/2 or 3/2 with parity as indicated. Assignments are made within 0.1% significance level (assignments within 1% are indicated in parenthesis)

E_γ	$f_\gamma \times 10^{-8}$	Resonance[a]												Multipolarity[b]			E_f	J^π
[keV]	[MeV^{-3}]													$XL(a)$	$XL(b)$	XL	[keV]	$\frac{1}{2}^\pi$, $\frac{3}{2}^\pi$
5943.0(2)	14.6(5)	1	2	3	4	5		7	8	9	10	11		E1	E1	E1	0.0	−
5434.7(2)	9.3(5)	1		3	4	5	6	7	8					E1	E1	E1	508.3	−
5384.7(2)	24.9(9)	1	2	3	4	5	6	7	8	9	10	11	12	E1	E1	E1	558.3	−
5341.1(3)	0.6(4)	1												M1	M1	M1	601.9	+
5295.9(5)	0.8(4)	1												M1	M1	M1	647.1	+
5198.1(2)	1.0(5)	1			4									M1	M1	M1	744.9	+
5161.0(5)	2.3(5)												12		M1	M1	782.0	+
5083.0(6)	1.5(5)	1		3									12	(M1)	M1	M1	860.0	+
4971.0(13)[c]	1.6(7)				4		6	7				11		(M1)	M1	M1	972.0	+
4939.7(10)	2.1(6)							7			10		12		(M1)	(M1)	1003.3	(+)
4881.7(3)	10.0(8)	1	2	3		5	6				10	11		E1	E1	E1	1061.3	−
4863.5(2)	8.1(7)	1		3	4	5			8		10			E1	E1	E1	1079.5	−
4832.2(3)	5.5(7)	1		3	4		6	7					12	E1	E1	E1	1110.8	−
4814.4(3)	1.4(6)	1					6							(M1)	(M1)	(M1)	1128.6	(+)
4803.3(2)	5.6(7)	1	2					7	8	9		11		E1	E1	E1	1139.7	−
4796.9(2)	5.0(7)	1			4		6	7			10			E1	E1	E1	1146.1	−
4543.7(11)	5.2(9)	1		3				7		9				E1	E1	E1	1399.3	−
4526.1(13)	0.6(9)	1												(M1)	M1	M1	1416.9	+
4513.4(12)	2.8(9)	1	2	3					8		10						1429.6	
4495.2(13)	−0.8(9)	1												M1	M1	M1	1447.8	+
4474.4(12)	1.8(9)	1								9					(M1)	(M1)	1468.6	(+)
4464.7(3)	2.9(9)	1	2												(M1)	(M1)	1478.3	(+)

(*continued*)

Photon Strength: Resonance Neutrons

^{159}Gd

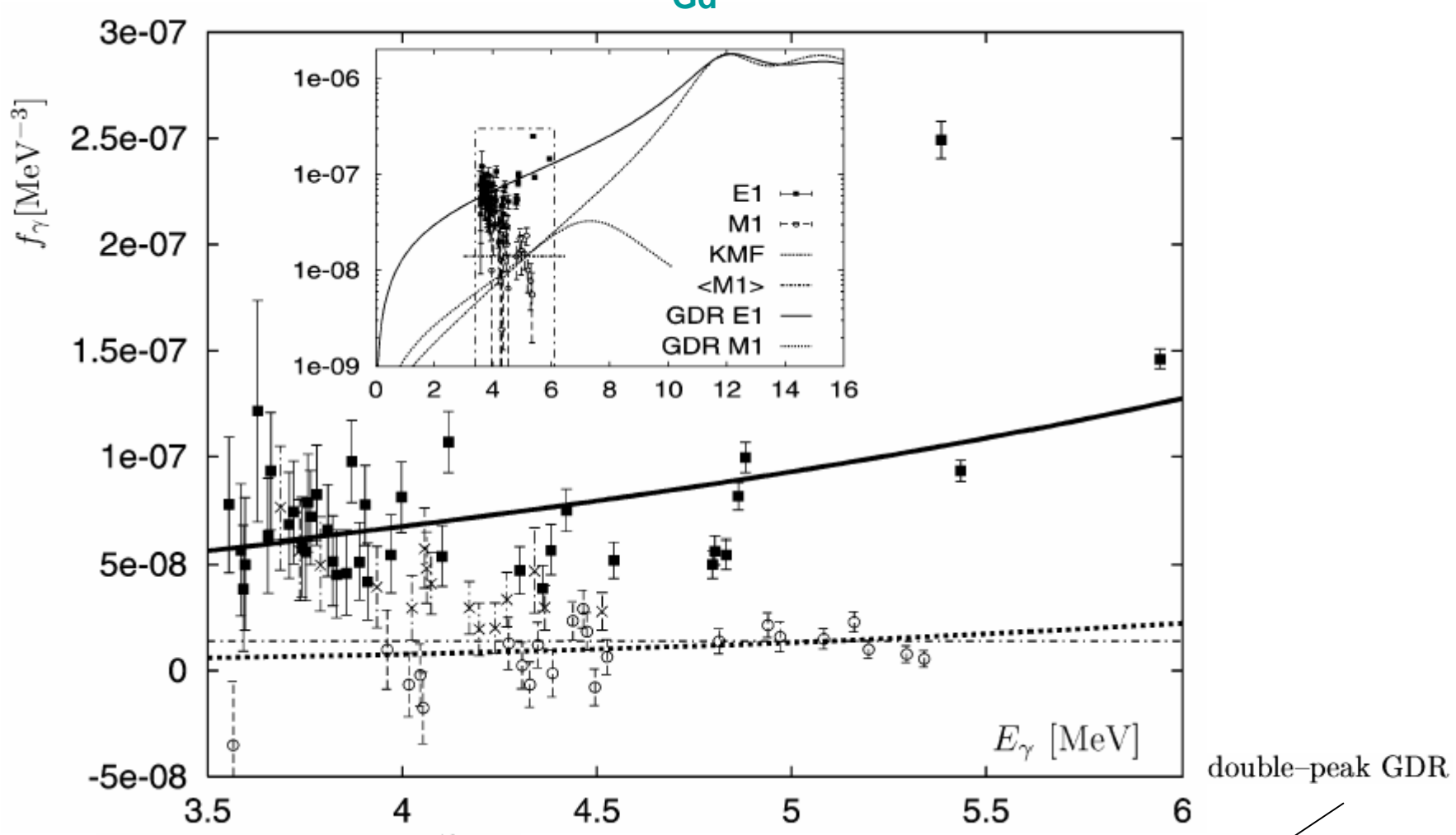

double–peak GDR

$$f_\gamma(E_\gamma) = \frac{1}{12} \times \frac{1}{D_0 E_\gamma^3} \times \sum_{\lambda=1}^{12} \Gamma_{\gamma_\lambda}$$

$$f_\gamma(E_\gamma) = \frac{1}{3(\pi\hbar c)^2} \sum_{i=1,2} \sigma_{0_i} \frac{E_\gamma \Gamma_{G_i}^2}{(E_\gamma^2 - E_{G_i}^2)^2 + E_\gamma^2 \Gamma_{G_i}^2}$$

Nuclear spectroscopy with neutrons

ARTICLE IN PRESS

S0375-9474(03)01474-X/FLA AID:8464 Vol.●●●(●●●)
ELSGMLTM(NUPHA):m1 v 1.158 Prn:16/06/2003; 14:56

npa8464

P.1(1-15)
by:PS p. 1

ELSEVIER

Available online at www.sciencedirect.com

SCIENCE DIRECT®

Nuclear Physics A ●●● (●●●●) ●●●–●●●

NUCLEAR PHYSICS A

www.elsevier.com/locate/npe

Primary gamma transitions in ^{159}Gd after isolated resonance neutron capture

C. Granja [a,b,*], S. Pospíšil [a], J. Kubašta [b], S.A. Telezhnikov [c]

[a] *Institute of Experimental and Applied Physics, Czech Technical University, CZ-12800 Prague 2, Czech Republic*
[b] *Faculty of Nuclear Sciences and Physical Engineering, Czech Technical University, CZ-11819 Prague 1, Czech Republic*
[c] *Joint Institute for Nuclear Research, 141-980 Dubna, M.R., Russia*

Received 22 March 2002; received in revised form 7 February 2003; accepted 29 April 2003

Average resonance capture

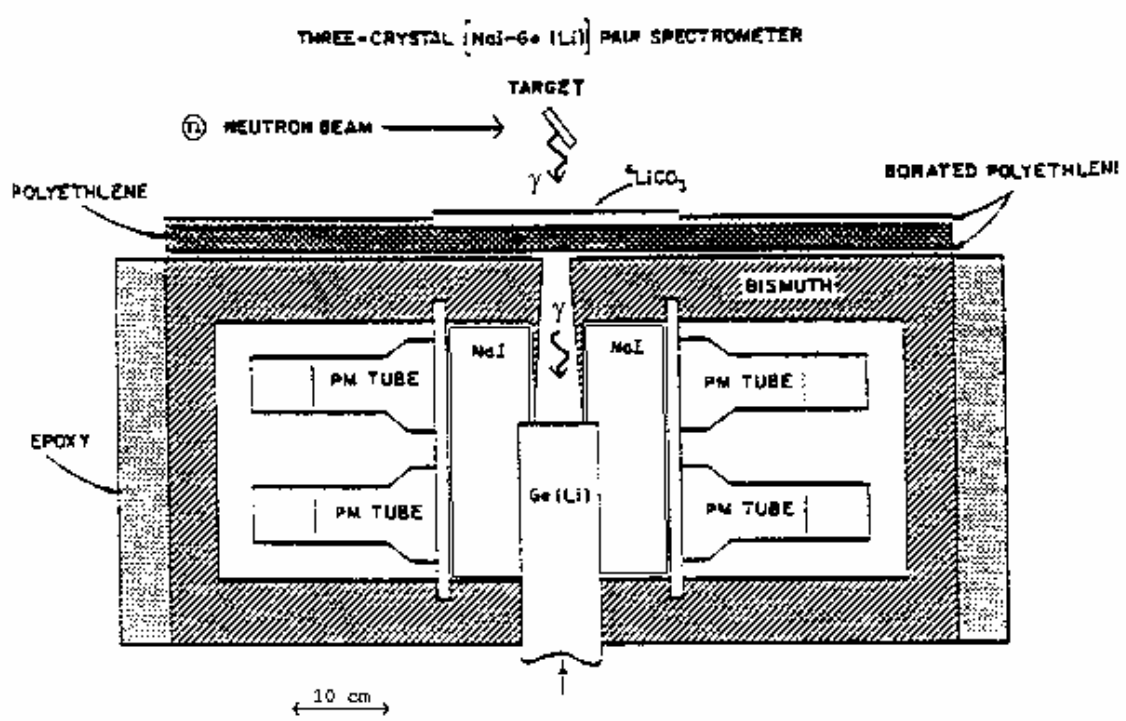

Pair spectrometer in ARC experiments.

Average resonance capture

^{159}Gd:

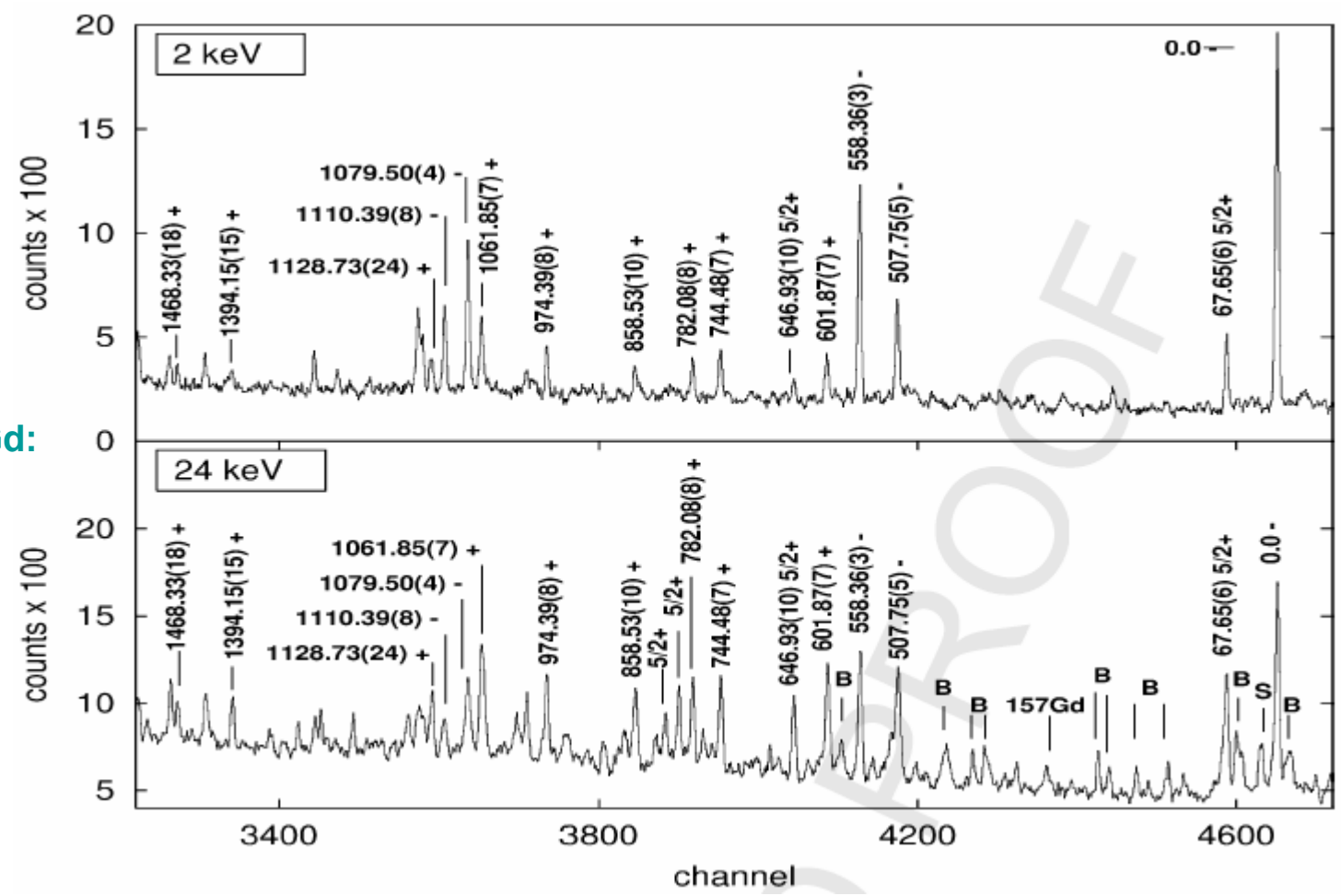

kinematical shift

$$E_{\gamma_a} - E_{\gamma_b} = T_{n_a} - T_{n_b} + \frac{m_n}{m_A}\left(T_{n_b} - T_{n_a}\right)$$

recoil after neutron capture

Average resonance capture

^{159}Gd

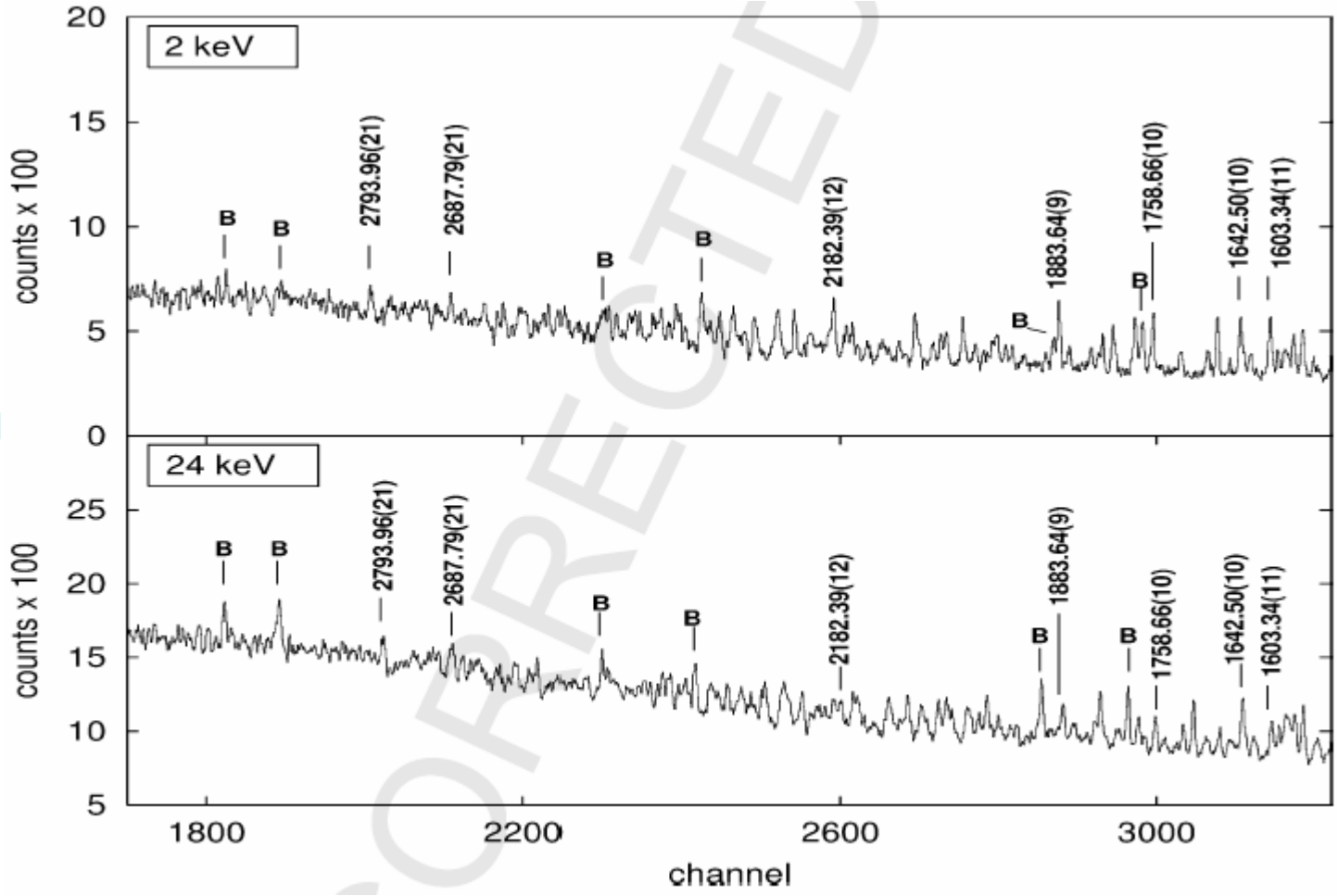

kinematical shift

$$E_{\gamma_a} - E_{\gamma_b} = T_{n_a} - T_{n_b} + \frac{m_n}{m_A}\left(T_{n_b} - T_{n_a}\right)$$

recoil after neutron capture

Average resonance capture

^{159}Gd

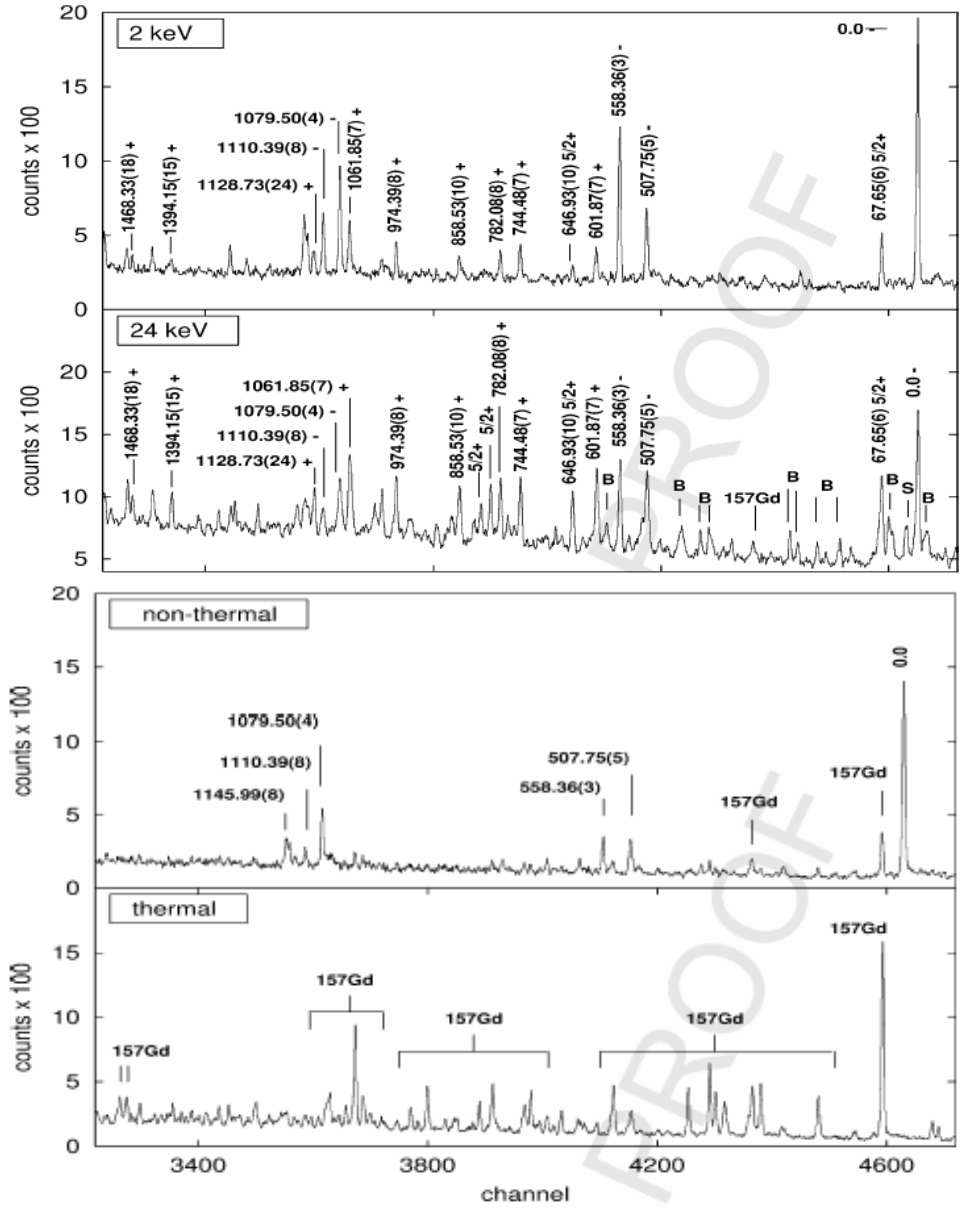

Gamma – rays: energy & intensity

Table 3
Primary γ-rays in ^{159}Gd observed in average resonance capture of 2, 24 keV and non-thermal neutrons. Gamma-ray intensities are given in relative units (normalized to the strongest transitions). Uncertainties of gamma-ray and level energies include systematic errors. Results from isolated resonance capture [21] are included

		2 keV		24 keV		Non-thermal		IRC	
E_x(keV)[a]	J^{π}[b]	E_γ(keV)	I_γ	E_γ(keV)	I_γ	E_γ(keV)	I_γ	E_γ(keV)	I_γ(γs/100n)[c]
0.0[e]	$1/2^-, 3/2^-$	5945.25(3)	100.0(4)	5967.40(5)	100.0(14)	5943.97(3)	100.0(12)	5943.00(20)	1.61(7)
67.65(6)[e]	$5/2^+$	5877.79(8)	19.7(27)	5899.58(8)	56.5(12)				
146.94(23)[e]	$5/2^-$			5820.45(23)	14.2(9)				
507.75(5)[e]	$1/2^-, 3/2^-$	5437.54(7)	26.7(25)	5459.71(9)	47.4(12)	5436.46(13)	16.0(6)	5434.70(20)	1.67(8)
558.36(3)[e]	$1/2^-, 3/2^-$	5386.79(4)	53.6(3)	5409.34(7)	55.2(12)	5385.86(9)	18.4(6)	5384.70(20)	3.05(9)
589.7(6)[e]	$5/2^-$			5377.7(6)	7.0(9)				
601.87(7)[e]	$1/2^+, 3/2^+$	5342.98(14)	12.2(29)	5365.69(8)	51.1(12)	5342.16(21)	7.2(5)	5341.1(3)	0.06(5)
646.93(10)[e]	$5/2^+$	5298.83(23)	6.3(23)	5320.37(11)	33.6(11)	5296.0(8)	2.7(4)	5295.9(5)	0.06(5)
744.48(7)[e]	$1/2^+, 3/2^+$	5200.83(12)	8.9(24)	5222.99(10)	41.0(12)	5199.43(26)	6.9(5)	5198.10(20)	0.04(5)
782.08(8)[e]	$1/2^+, 3/2^+$	5163.49(14)	10.3(23)	5185.18(10)	40.5(12)			5161.0(5)	0.26(5)
800.59(11)[e]	$5/2^+$	5145.2(6)	2.4(10)	5166.80(11)	35.0(12)				
818.59(15)[e]	$5/2^+$	5126.6(6)	2.5(12)	5148.83(16)	23.1(11)				
858.53(10)[e]	$1/2^+, 3/2^+$	5086.28(18)	8.1(22)	5109.17(12)	32.5(12)	5083.1(8)	2.4(4)	5083.0(6)	0.16(5)
872.71(25)	$5/2^-$			5094.70(25)	16.9(11)				
880.4(4)	$1/2^+, 3/2^+, 5/2^+$	5065.2(6)	2.3(10)	5086.7(6)	7.1(10)				
915.3(6)	1/2, 3/2	5030.0(6)	2.8(22)			5029.1(8)	2.2(5)		
974.39(8)[e]	$1/2^+, 3/2^+$	4971.14(12)	12.8(26)	4992.83(10)	38.9(12)	4971.0(5)	3.2(5)	4971.0(13)	0.11(7)
1001.55(12)[e]	$1/2^+, 3/2^+$	4943.66(23)	6.9(21)	4965.92(14)	29.0(12)			4939.7(10)	0.19(5)
1061.85(7)[e]	$1/2^-, 3/2^-$	4884.08(10)	18.2(25)	4904.85(10)	37.0(14)			4881.7(3)	0.86(6)
1079.50(4)[e]	$1/2^-, 3/2^-$	4865.83(5)	38.4(3)	4887.61(12)	34.7(13)	4864.60(8)	30.2(8)	4863.50(10)	0.63(6)
1110.39(8)[e]	$1/2^-, 3/2^-$	4834.94(8)	21.5(28)	4856.90(26)	15.2(12)	4833.38(22)	7.9(6)	4832.2(3)	0.59(6)
1128.59(11)[e]	$1/2^+, 3/2^+$	4816.00(19)	8.5(23)	4839.23(14)	27.0(12)	4814.9(5)	5.6(6)	4814.4(3)	0.11(5)
1140.08(10)[e]	$1/2^-, 3/2^-$	4804.85(13)	13.4(26)	4828.07(25)	15.6(12)	4804.22(18)	10.8(7)	4803.30(20)	0.47(6)
1145.99(8)[e]	$1/2^-, 3/2^-$	4799.11(10)	19.4(28)	4822.56(23)	17.4(12)	4797.99(15)	13.3(7)	4796.90(20)	0.46(6)
1159.59(21)[e]	$5/2^+$	4785.8(6)	2.5(21)	4807.82(23)	18.2(12)				
1178.4(6)[e]	$1/2^+, 3/2^+, 5/2^+$	4768.0(9)	1.7(20)	4788.3(8)	5.2(11)				
1284.45(13)[e]	1/2, 3/2	4660.76(15)	7.2(26)	4683.16(25)	14.9(12)	4661.1(6)	2.8(6)		
1325.3(8)	1/2, 3/2, 5/2	4620.6(10)	2.0(22)	4641.3(13)	4.4(11)				
1344.0(4)	$1/2^+, 3/2^+, 5/2^+$	4601.9(6)	2.6(23)	4623.0(5)	9.1(12)				

(continued)

$$E_x = B_n + T_n\left(1 - \frac{m_n}{m_A}\right) - E_\gamma - \alpha E_\gamma^2.$$

Photon Strength: ARC 2 keV neutrons

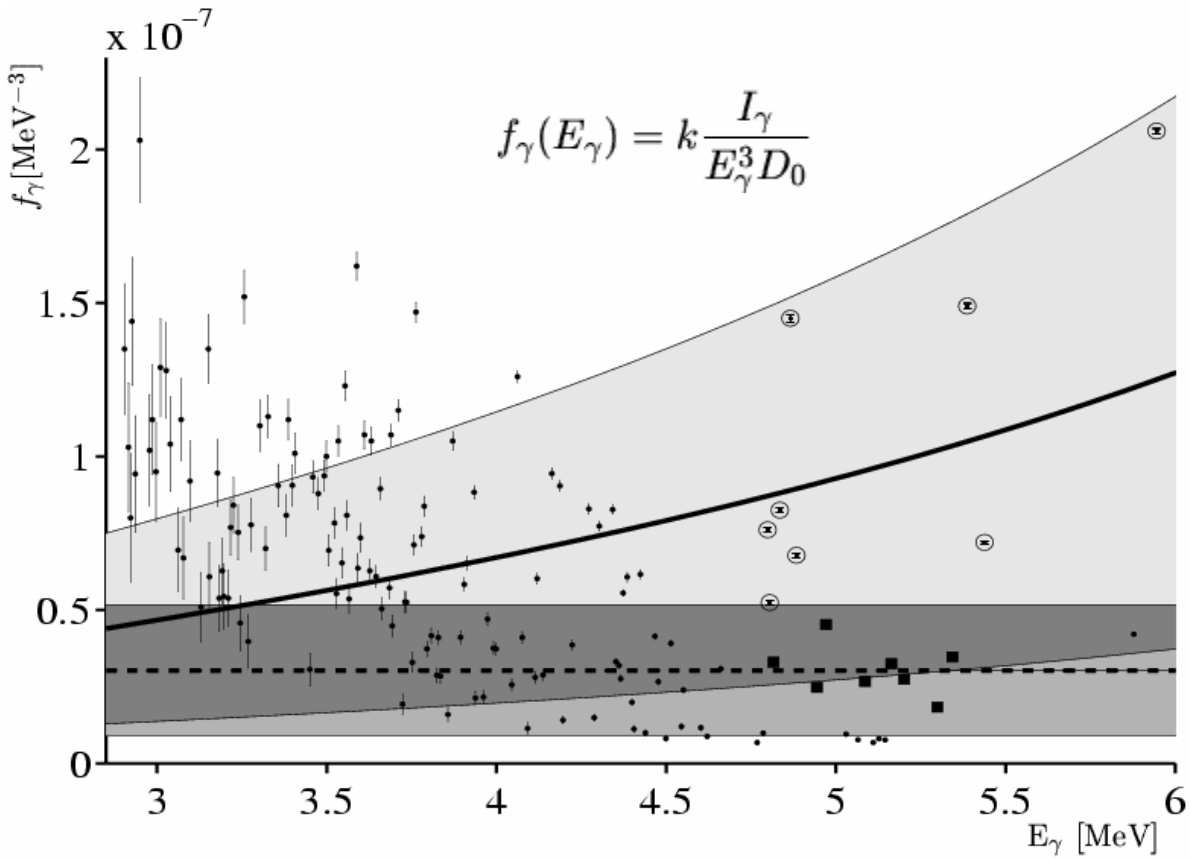

statistical fluctuations

$$\sqrt{\frac{2}{\nu}}$$

effective degrees of freedom

$$\nu \simeq \frac{N}{3}$$

Fig. 3. Photon strength in ^{159}Gd with 2 keV neutrons in ARC. The giant dipole resonance function of standard Lorentzian shape for $E1$–strength (bold solid–line) and a constant value $M1$–strength model (bold dashed line) are included with reduced (by 0.7) Porter–Thomas fluctuations (shadow bands). Previously well–established $E1$ and $M1$ transitions [21] are marked with ◯ and ■, respectively.

Photon Strength: ARC 2 keV neutrons

Target: ^{158}Gd

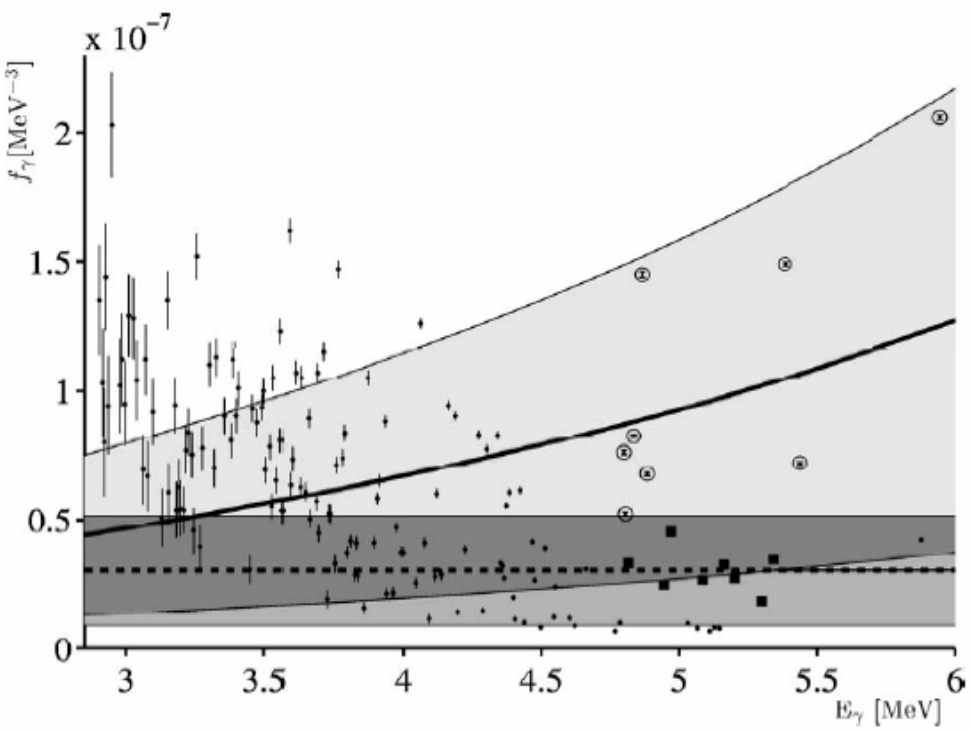

Target: ^{173}Yb

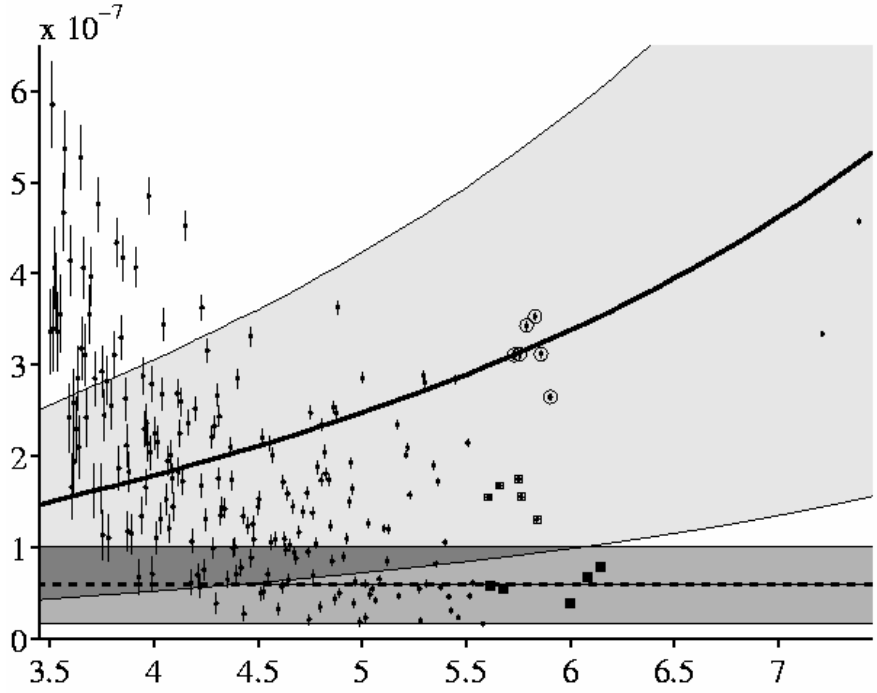

Photon Strength: ratio 24 keV / 2 keV

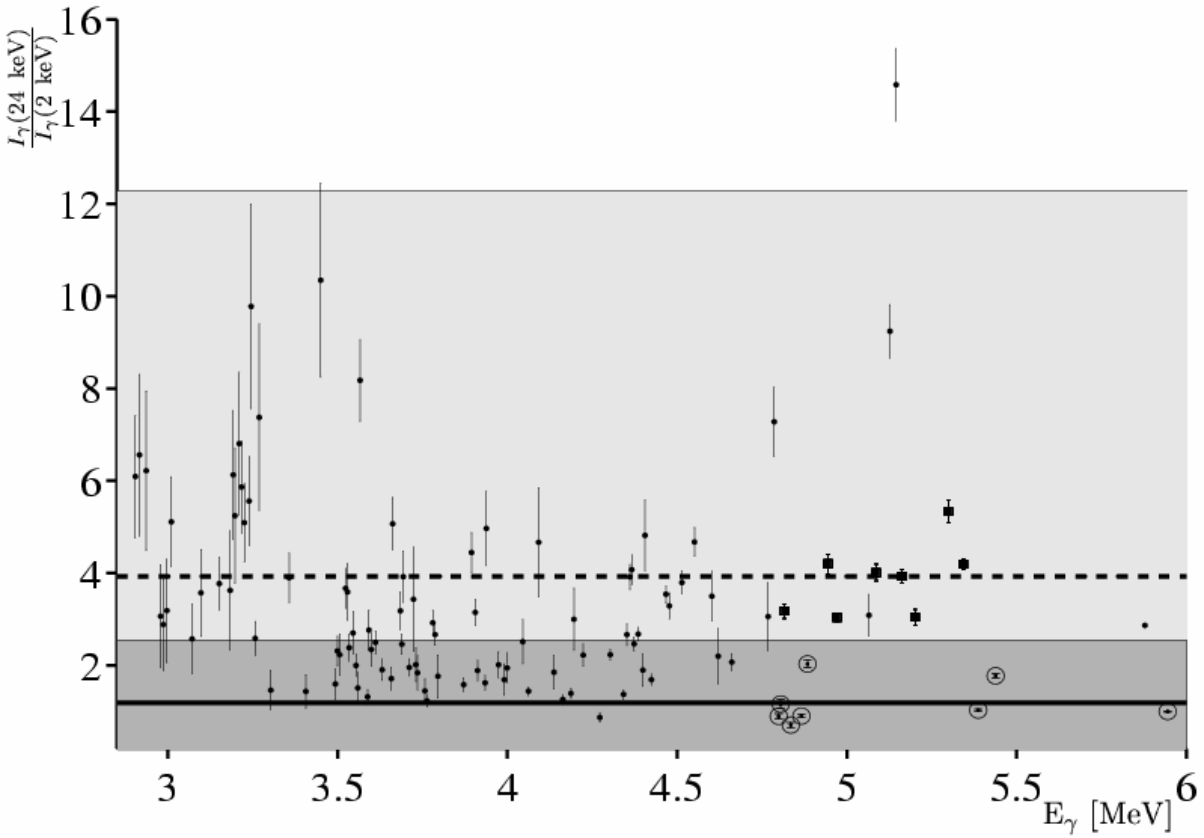

Fig. 4. Ratio of intensity of primary γ–rays in ^{159}Gd between 24 keV and 2 keV neutrons in ARC. The statistical fluctuations (convoluted between these two data sets) are shown as shadow bands around the $E1$ strength (solid–line) and around the $M1$ strength (dashed–line) with 90% confidence levels. The well–established $E1$ and $M1$ transitions [21] at 2 keV (Figure 3) are marked with ◯ and ■, respectively.

Photon Strength: ratio 24 keV / 2 keV

Target: ^{158}Gd

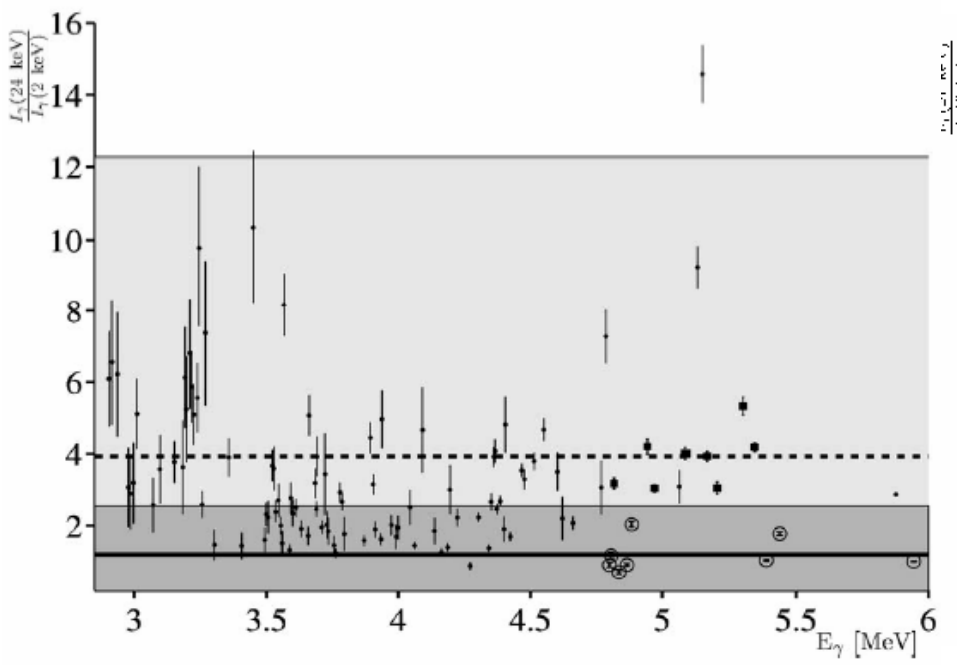

Target: ^{173}Yb

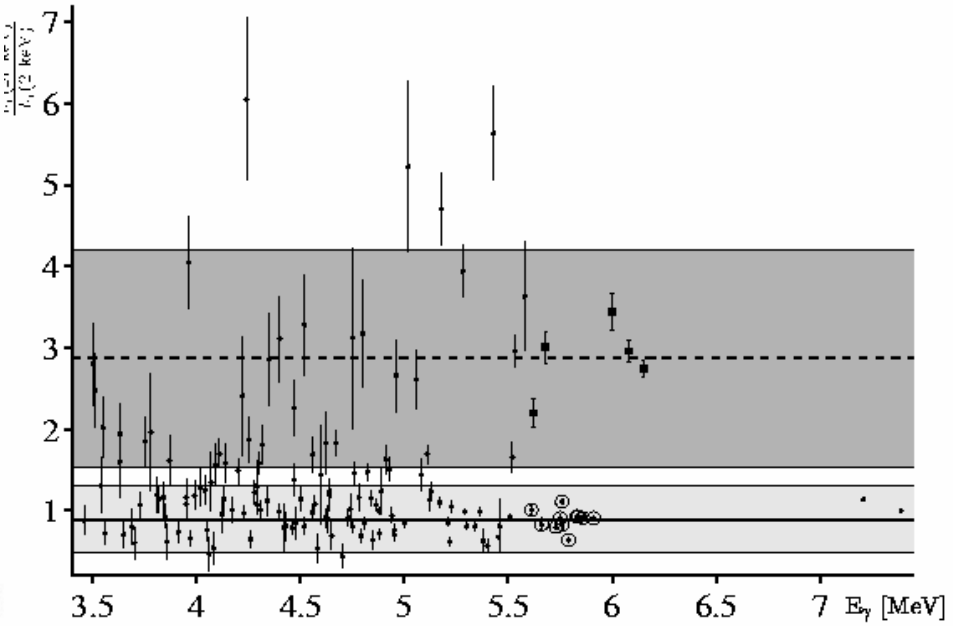

Nuclear spectroscopy with neutrons

ARTICLE IN PRESS

S0375-9474(03)01757-3/FLA AID:8572 Vol.●●●(●●●) npa8572 P.1 (1-20)
ELSGMLTM(NUPHA):m1 v 1.174 Prn:4/11/2003; 9:26 by:Neringa p. 1

Available online at www.sciencedirect.com
SCIENCE DIRECT®

ELSEVIER

Nuclear Physics A ●●● (●●●●) ●●●–●●●

NUCLEAR PHYSICS A

www.elsevier.com/locate/npe

Levels of ^{159}Gd populated in average resonance neutron capture

C. Granja [a,*], S. Pospíšil [a], S.A. Telezhnikov [b], R.E. Chrien [c]

[a] *Institute of Experimental and Applied Physics, Czech Technical University, 128 00, Prague 2, Czech Republic*
[b] *Joint Institute for Nuclear Research, 141-980 Dubna, Moscow region, Russia*
[c] *Brookhaven National Laboratory, Upton, NY 119 73, USA*

Received 1 September 2003; received in revised form 10 September 2003; accepted 16 September 2003

High flux reactor & high resolution γ – ray spectroscopy

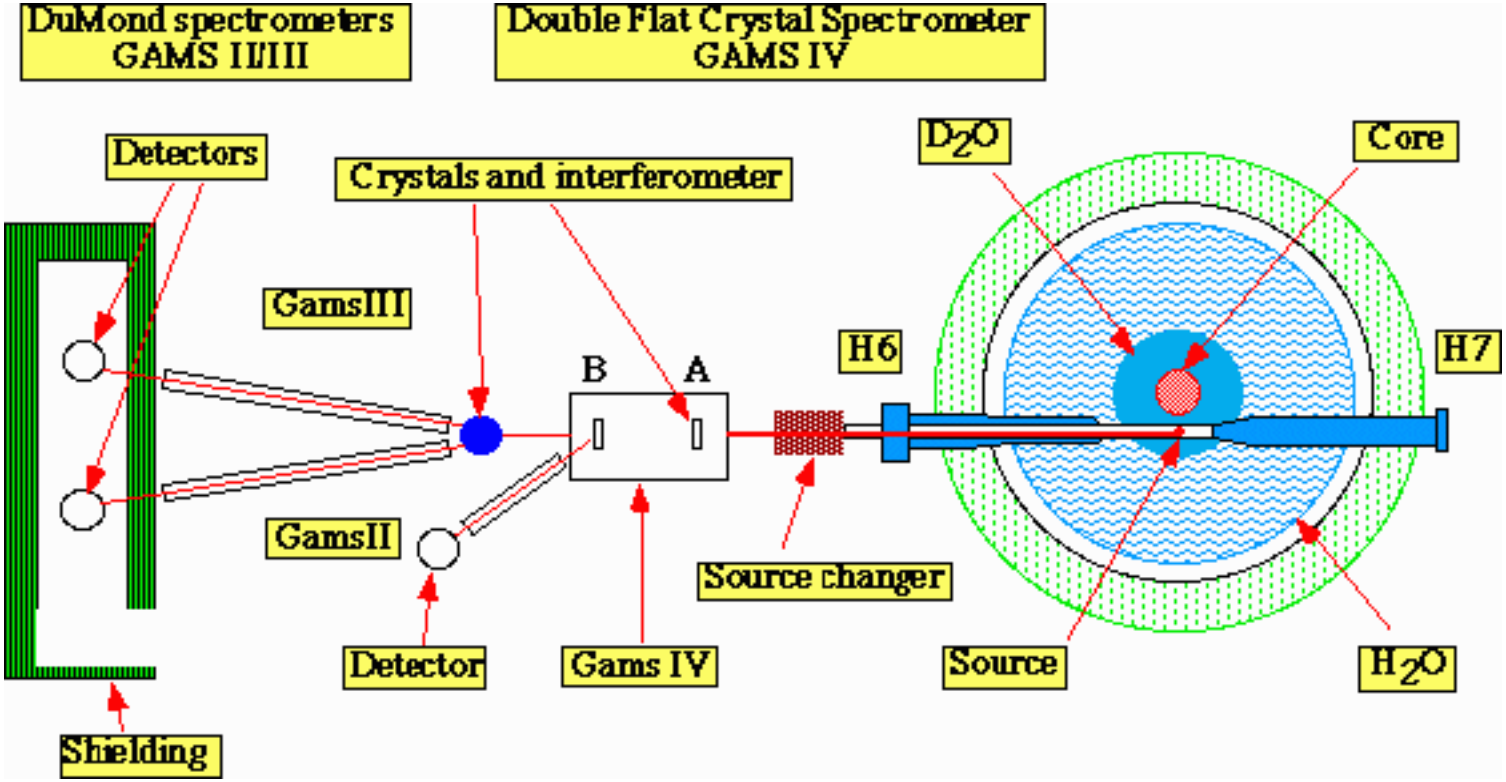

High flux reactor & high resolution γ – ray spectroscopy

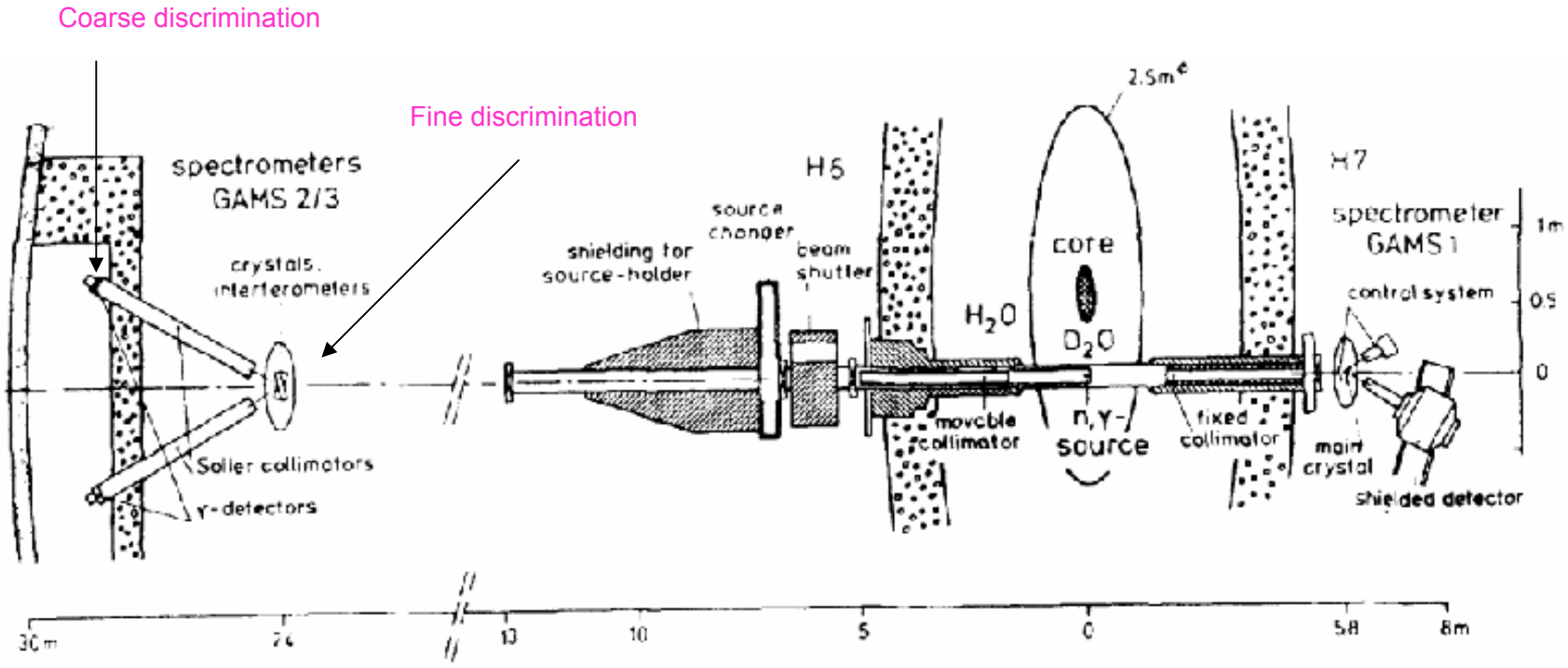

Figure 17: Schematic setup of the high–resolution GAMS2/3 bent–crystal spectrometers at the High Flux Reactor, Institut Laue–Langevin [72].

High flux reactor & high resolution γ – ray spectroscopy

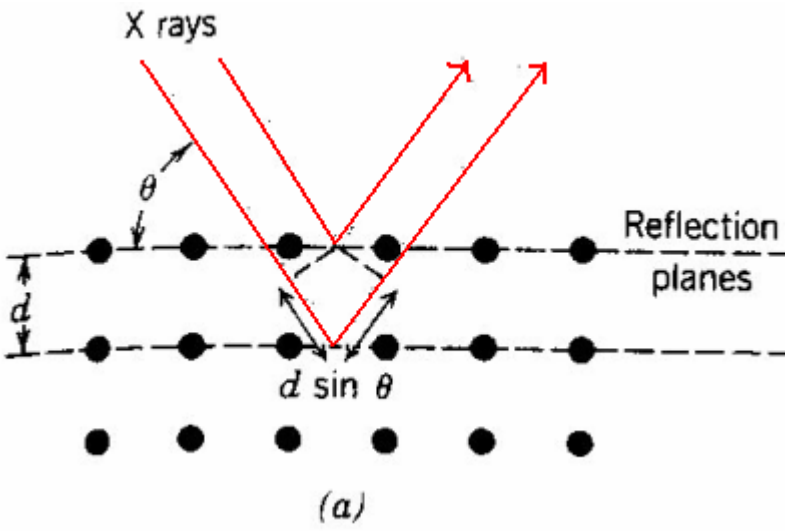

neutrons

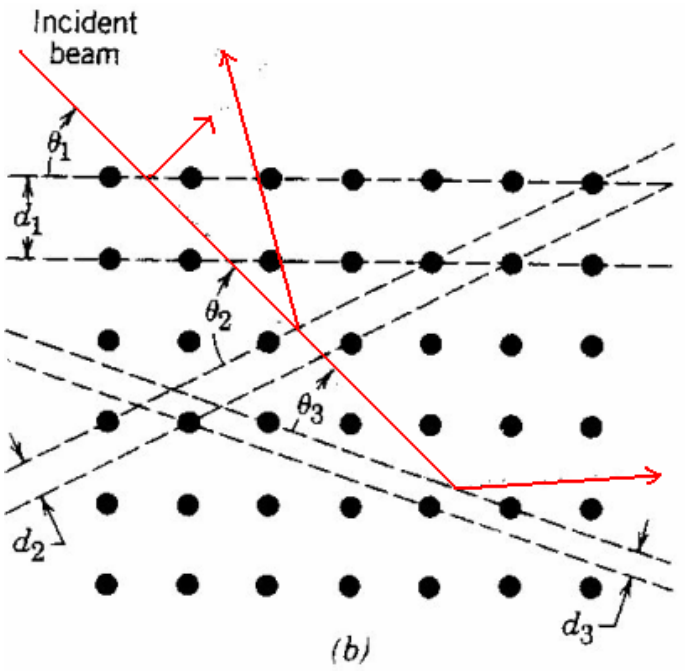

γ–ray energy Bragg's law $E_\gamma = \frac{nhc}{2d\ sin\theta}$

energy resolution angular resolution $\Delta E_\gamma = \frac{2d}{nhc} E_\gamma^2\ cos\theta\ \Delta\theta$

Order of diffraction *n*

$$\Delta E[\mathrm{eV}] \simeq 20\left(\frac{\mathrm{E[keV]}}{100}\right)^2 \frac{\Delta\theta[\mathrm{arcsec}]}{\mathrm{n}}$$

$$\Delta E_\gamma[\mathrm{keV}] = 2.5 \times 10^{-6}(E_\gamma[\mathrm{keV}])^2/n$$

Lifetime measurements	
GRID	Gamma Ray Induced Doppler
DS	Doppler Shift
DB	Doppler Broadening

High flux reactor & high resolution γ – ray spectroscopy

Laser interferometer for GAMS2/3 spectrometers. A rotation unit supports the diffraction crystal and a system of mirrors to generate Michelson diffraction fringes.

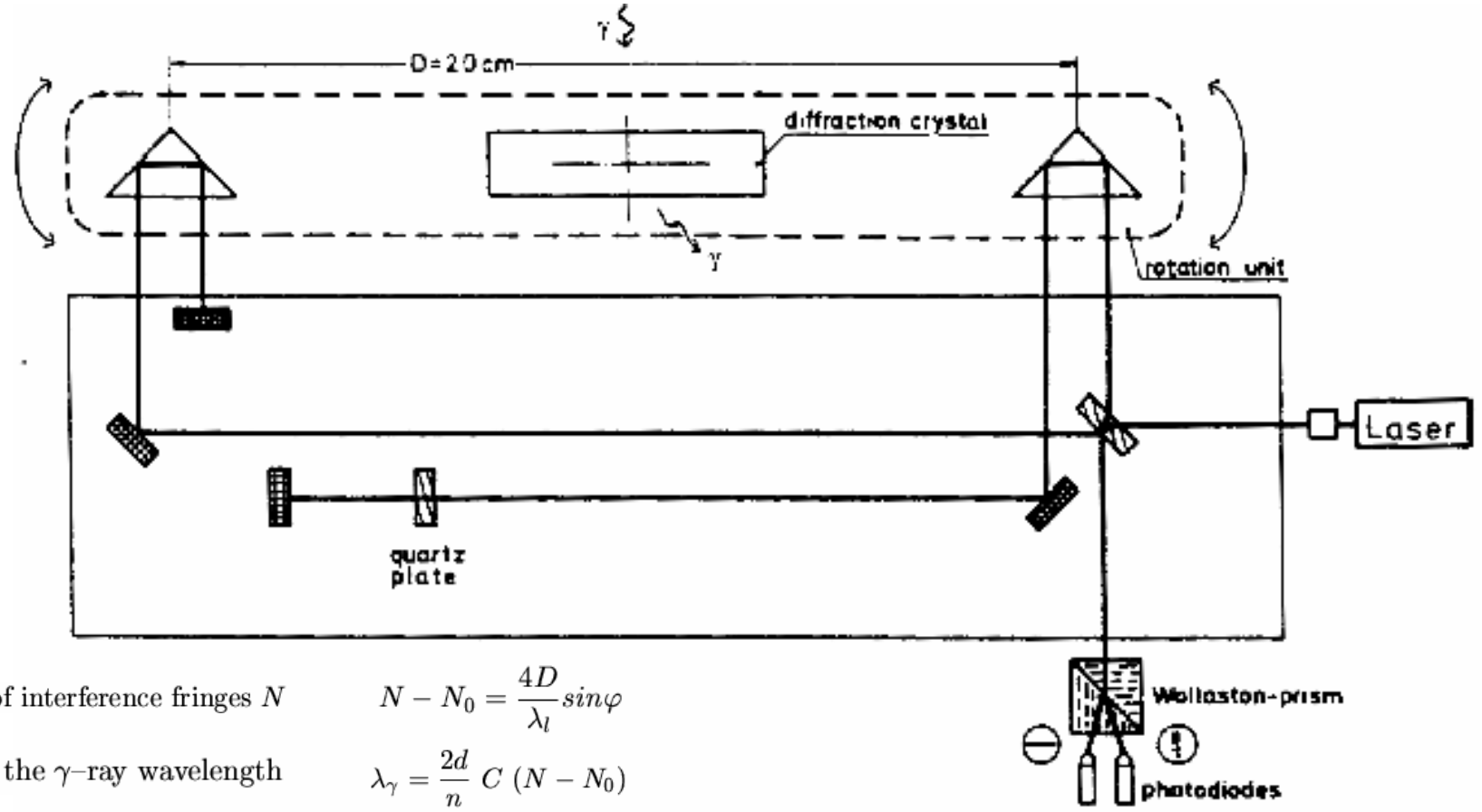

the number of interference fringes N $\quad N - N_0 = \frac{4D}{\lambda_l} sin\varphi$

the γ–ray wavelength $\quad \lambda_\gamma = \frac{2d}{n}\, C\, (N - N_0)$

Bent – crystal γ spectrometer

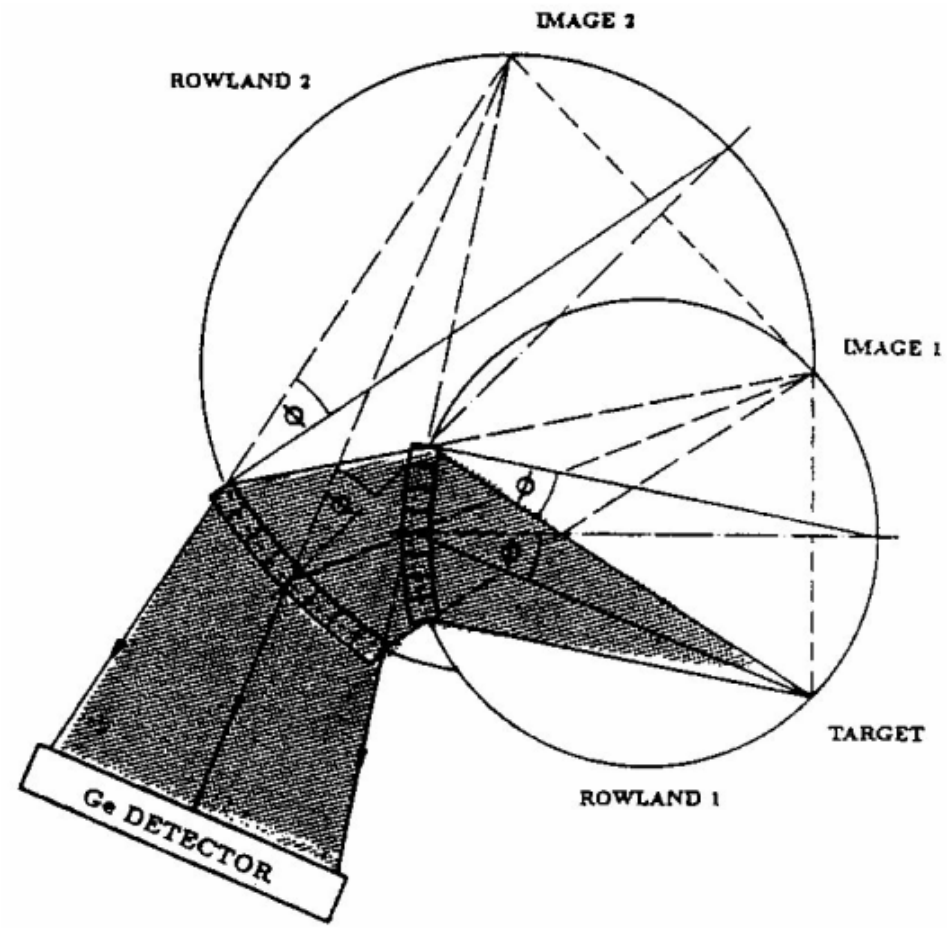

Schematic diagram describing the principle of operation of the two axes bent crystal spectrometer. The Bragg angle shown here is highly exagerated. In realistic measurements θ_B is typically in the order of several minutes to degrees.

Target burn up & γ – ray attenuation

burn up time is calculated from the condition

$$n_B \sigma_B \ll n_{158} \sigma_{158}$$

burn up time

$$t \gg \frac{1}{\sigma_B \phi_n} ln\left(\frac{\eta_f + 1}{\eta_i + 1}\right)$$

relative content

$$\eta_i \equiv \frac{n_i^{158}}{n_i^B} \quad , \qquad \eta_f \equiv \frac{n_f^{158}}{n_f^B}$$

attenuation of γ–rays in the sample target

$$I_\gamma = \int_0^l \frac{I_0}{l}\, e^{-\mu\rho x} dx = I_0 \frac{1 - e^{-\mu\rho l}}{\mu\rho l} \equiv I_0 A$$

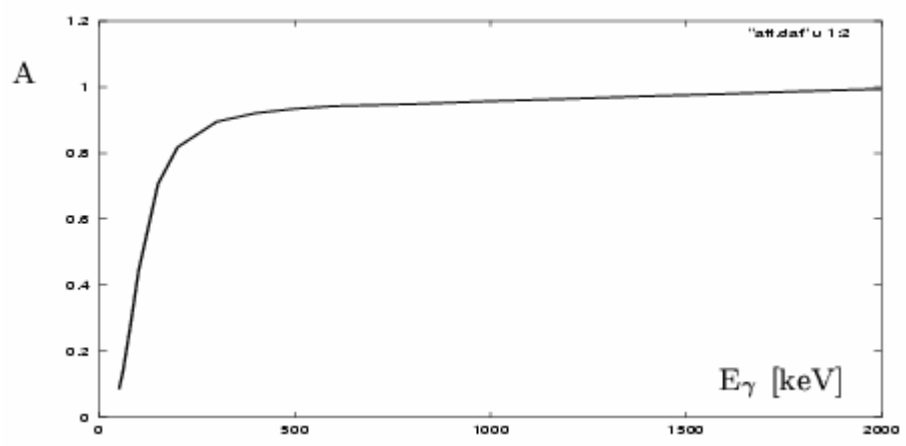

internal conversion

$$I = I_\gamma (1 + \alpha_{XL})$$

High resolution γ-ray spectra: GAMS2/3 @ ILL

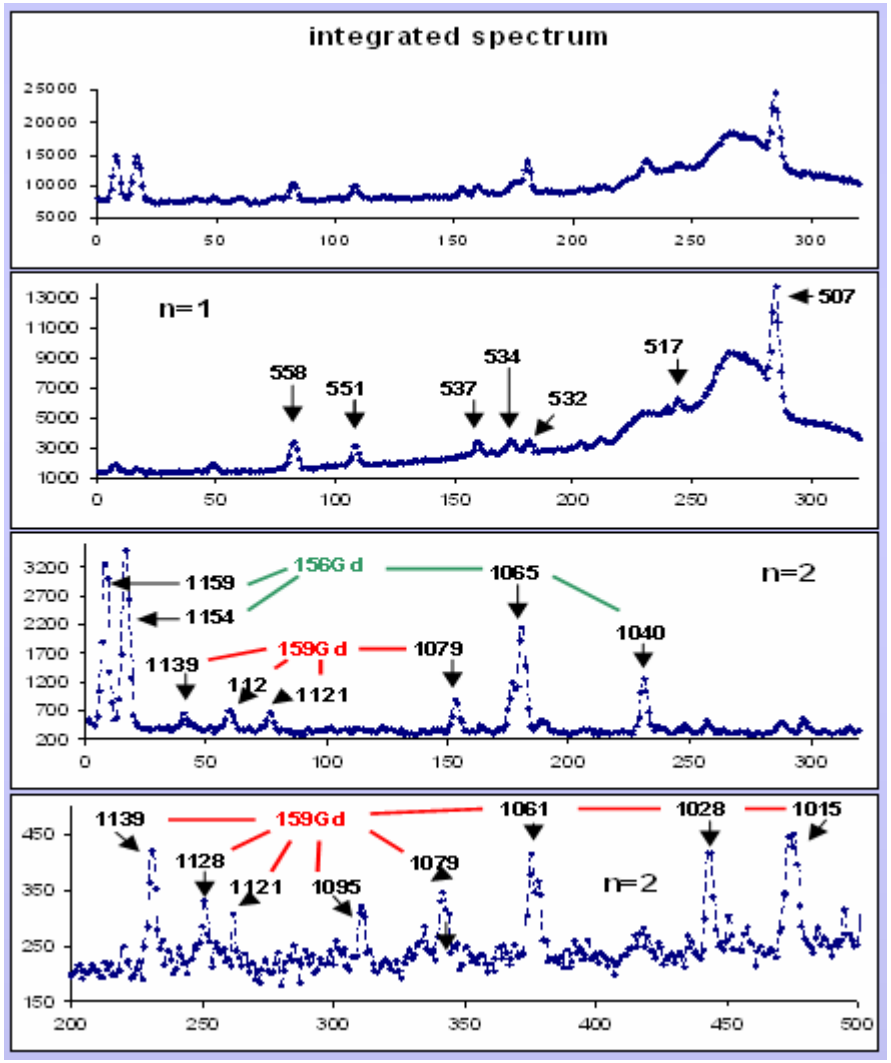

High resolution γ-ray spectra: GAMS2/3 @ ILL

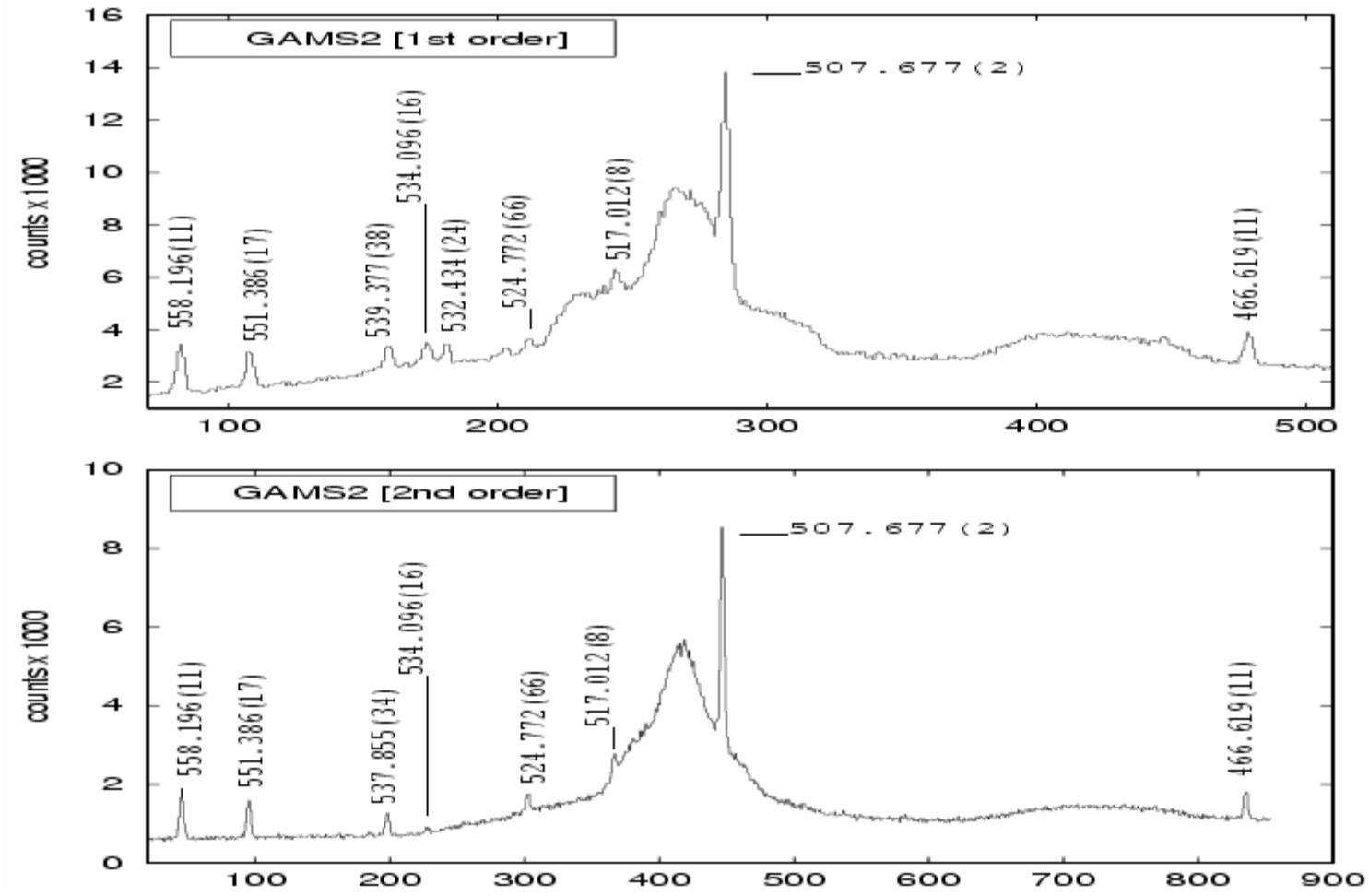

High resolution γ-ray spectra: GAMS2/3 @ ILL

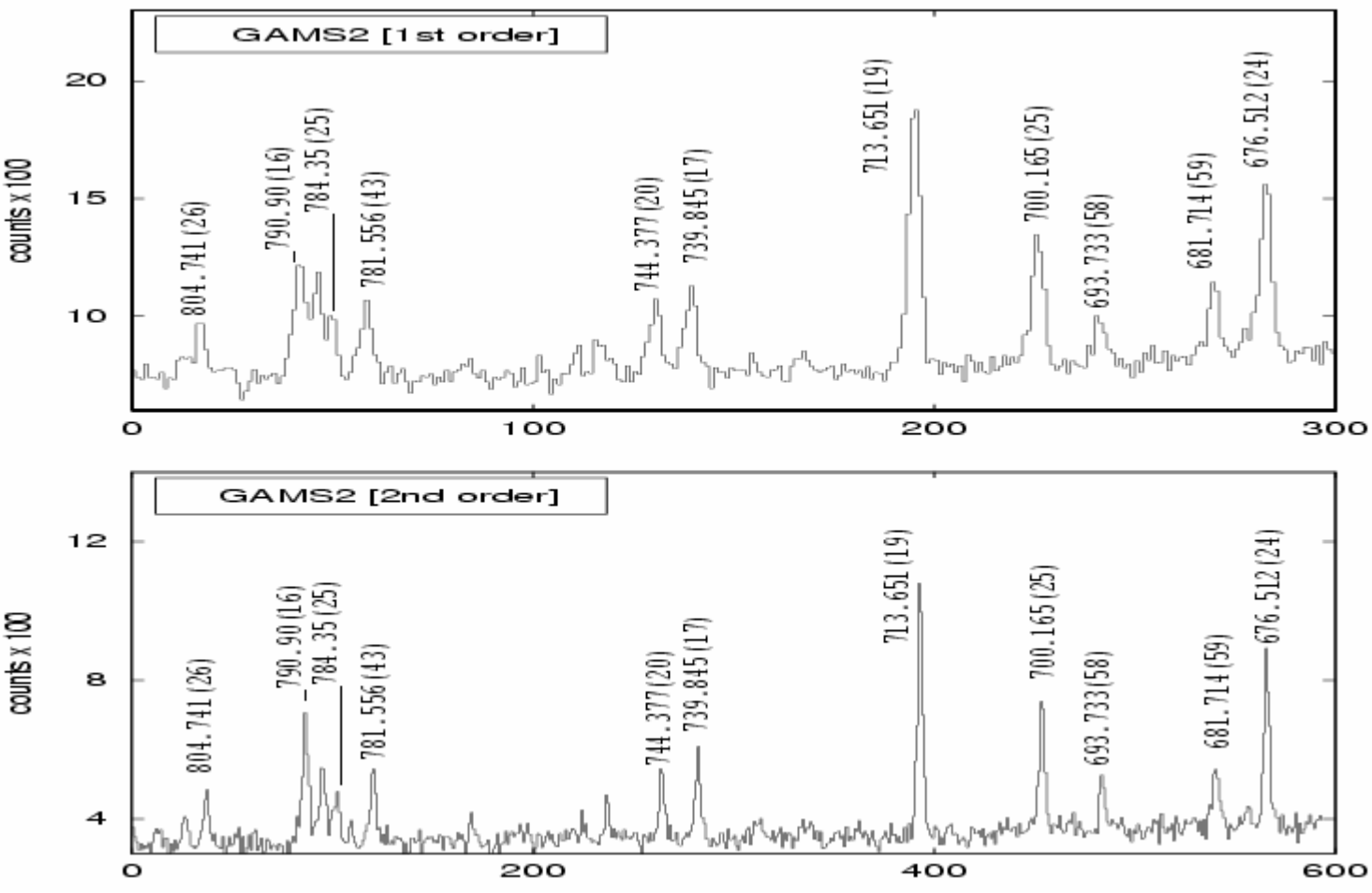

Neutron transfer experiments

EXPERIMENT Laboratory	E_d [MeV]	beam	Target [μg cm^2]	Enrich. [%]	Angle range [º]	FWHM Δ E [keV]
(d,p) TU-Munich	18	unpolarised	130	97.0	13 - 55	p ~ 3
(d,t) TU-Munich	22	polarised	125	98.2	12 - 50	t ~ 7

Nucleon transfer reactions

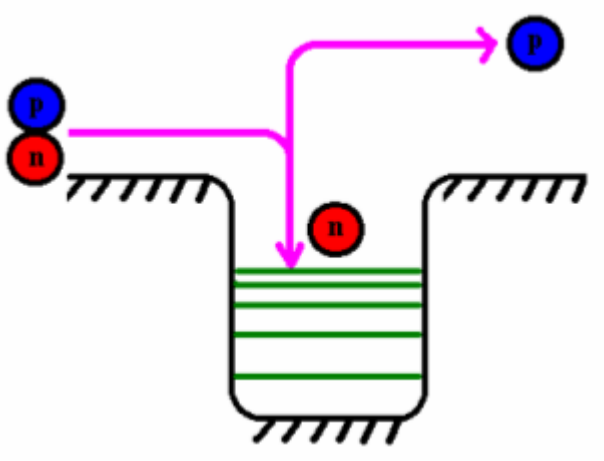

- population of single-quasiparticle states

STRIPPING: (d,p)	⇒ particle states
PICK-UP: (d,t)	⇒ hole states

- selective population of nuclear states. Level spin and parity result from the transferred angular momentum
- identification of quasiparticle Nilsson states and their associated rotational bands
- Spectroscopic factors relate to the spreading of single particle strength into Nilsson states.

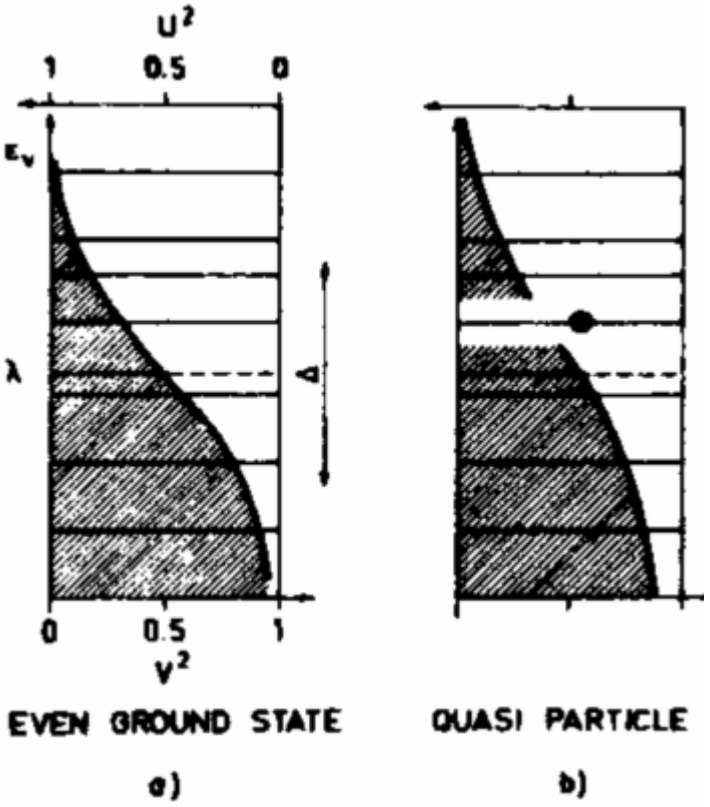

the pairing formalism (a) The occupation by pairs of the single particle levels near the Fermi surface is measured by the U^2 and V^2 factors. (b) An odd particle causes rearrangement in the distribution shown in (a). It is thus a "quasi particle."

Nucleon transfer reactions

conservation of *angular momentum* in a (d,p) reaction

$$\vec{p_l} = \vec{p_d} - \vec{p_p}$$

$$p_l^2 = p_d^2 + p_p^2 - 2p_d p_p cos\theta$$

transferred angular momentum l
projectile–target separation R

$$\hbar^2(l+\frac{1}{2})^2 \leq p_l^2 R^2$$

total transferred angular momentum

$$\vec{j} = \vec{l} + \vec{s}$$

The angular distribution and peak–maximum position are sensitive only to the *orbital* angular momentum transferred l

The two possible values $j = l \pm \frac{1}{2}$ are not distinguished.

using a **polarized** beam and measuring the **asymmetry** of the transition amplitude

In a polarized beam the nucleon spin is aligned either *up* or *down* along the direction normal to the scattering plane.

⟶ analyzing power $A_y = \frac{2}{3P_y}\frac{\sigma_+ - \sigma_-}{\sigma_+ + \sigma_-}$

Nucleon transfer reactions: Q

The reaction Q–values for the (d,p) and (d,t) reactions are

$$Q_{(d,p)} = T_p + T_{A+1} - T_d = \quad B_n(A+1) - E_x - B_n(d)$$
$$Q_{(d,t)} = T_t + T_{A-1} - T_d = \quad -B_n(A) - E_x + B_n(t)$$

$$Q_{(d,p)} = \quad 5943.1 - 2224.6 \quad = \quad 3718.6 \qquad (A_{\text{target}} = 158)$$
$$Q_{(d,t)} = \quad -7451.4 + 6257.3 = -1194.1 \qquad (A_{\text{target}} = 160)$$

parity of the level populated
even target

$$\pi = (-1)^l$$

Nucleon transfer reactions: Cross Section

spherical nucleus

$$\frac{d\sigma}{d\Omega}^{\pm} = (2j+1)\, N^{\pm} \sigma^{\pm}_{jl}(\theta)\, f^2_{(U,V)}$$

deformed nucleus
single nucleon transfer cross section
specific state of spin j
momentum transfer l

$$\frac{d\sigma}{d\Omega}^{\pm} = 2 \underbrace{N^{\pm}\sigma^{\pm}_{jl}(\theta)}_{kinem.} \underbrace{C^2_{jl} f^2_{(U,V)}}_{struct.}$$

determined by the incoming and outgoing waves

spectroscopic factors

$$S_{jl} \equiv C^2_{jl} f^2_{(U,V)} = \frac{\left(\frac{d\sigma}{d\Omega}\right)_{\rm exp}}{\left(\frac{d\sigma}{d\Omega}\right)_{\rm DWBA}}$$

$U^2 + V^2 = 1$

pairing factor
stripping reaction (U)
pickup reaction (V)

$$f^2_{(U,V)} = \left\{ \begin{array}{c} U^2 \\ V^2 \end{array} \right\} = \frac{1}{2}\left(1 \pm \frac{\varepsilon - \lambda}{\sqrt{(\varepsilon-\lambda)^2 + \Delta^2}}\right)$$

single–particle energy, Fermi energy and pairing energy are denoted by $\varepsilon,\ \lambda,\ \Delta,$

Van de Graaff accelerator

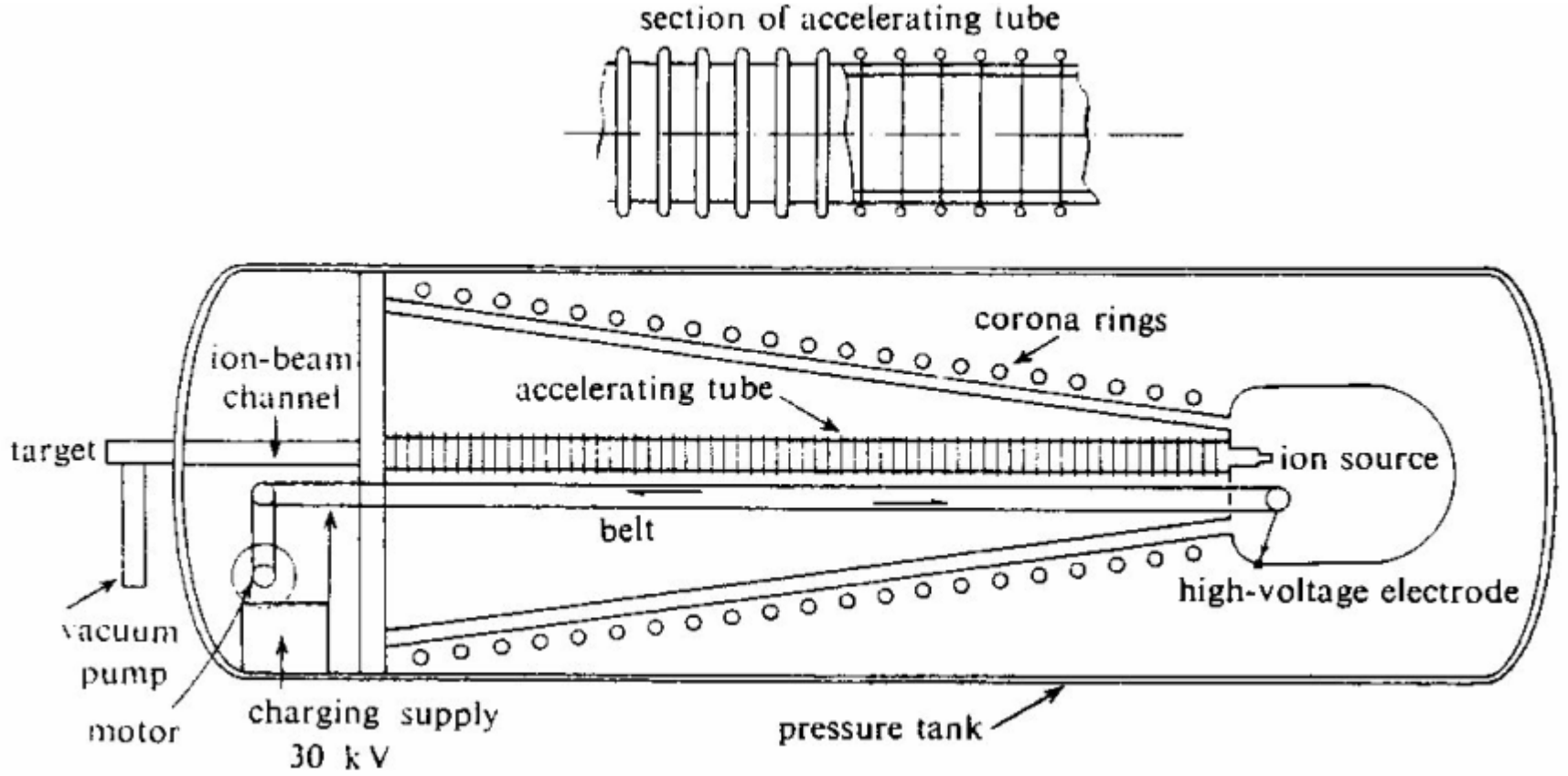

Schematic drawing of a Van de Graaff accelerator illustrating the principle of operation.

Tandem Van de Graaf: Doubles the accelerating potential → doubles the particle's kinetic energy.

Q3D Magnetic Spectrograph

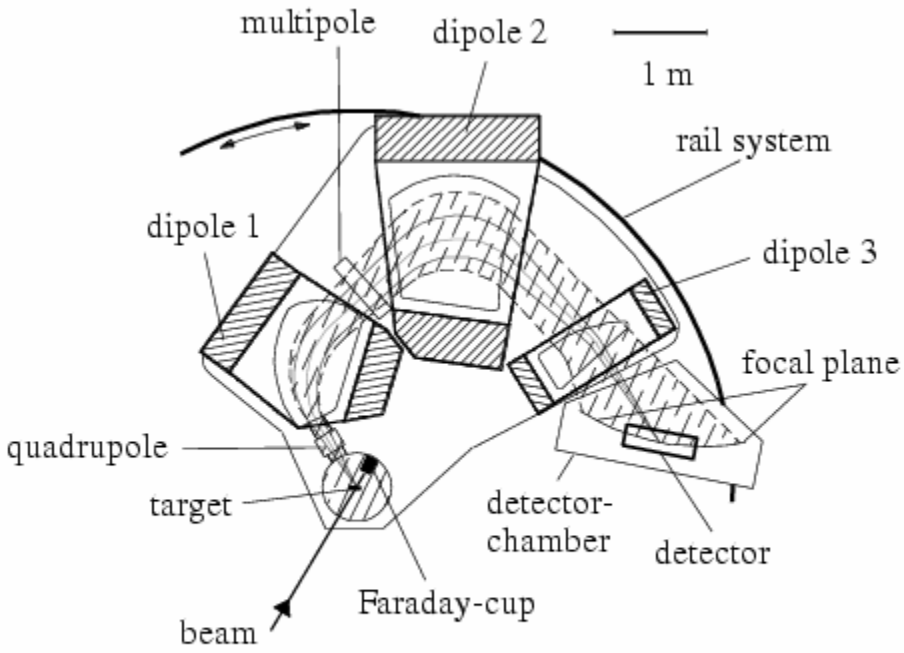

The Q3D magnetic spectrograph [85] at the Tandem van de Graaff accelerator of the University and the Technical University Munich [84].

particles are focused $r = \frac{p}{qB} = \frac{\sqrt{2mE}}{qB}$

Charged particle detection

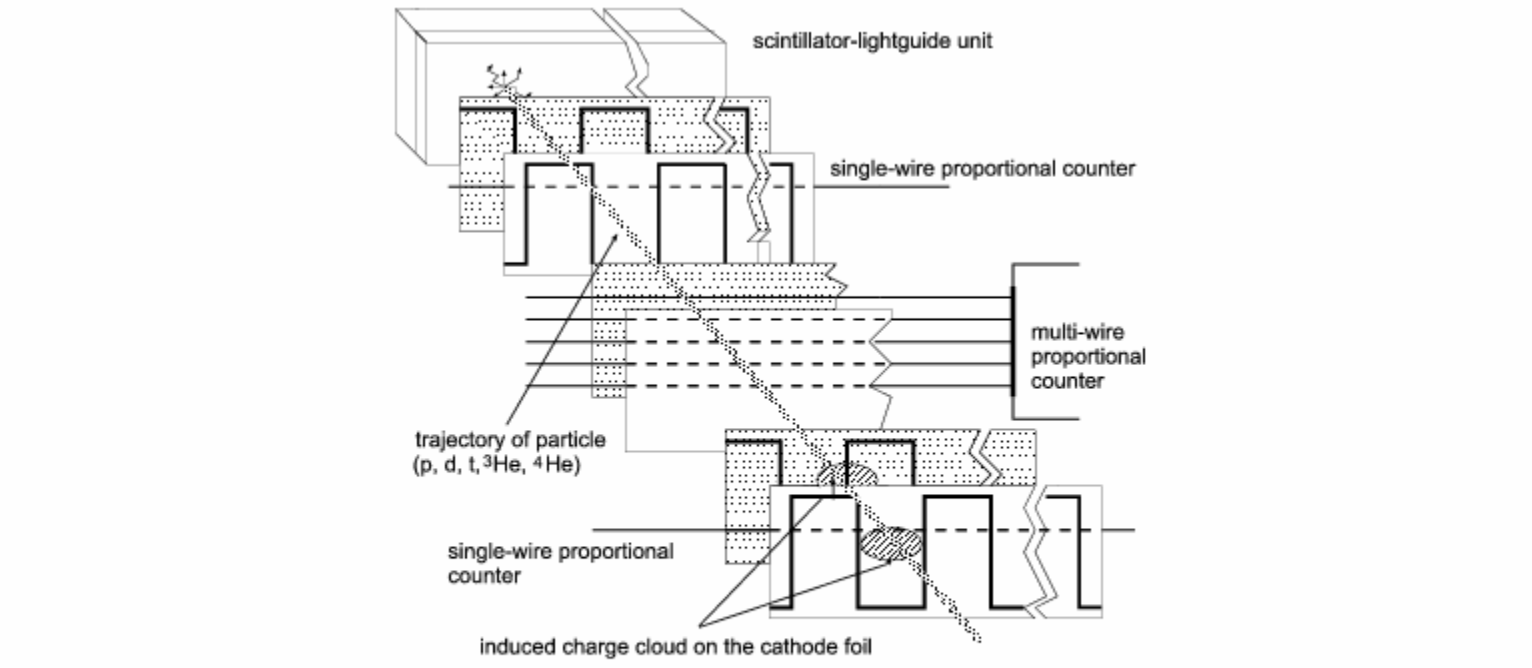

Long position sensitive detector [88] at the Q3D focal–plane. Particle position is determined in two dimensions by two single–wire and one multiwire proportional chambers. Energies of particles are determined in the plastic scintillator.

Charged particle detection

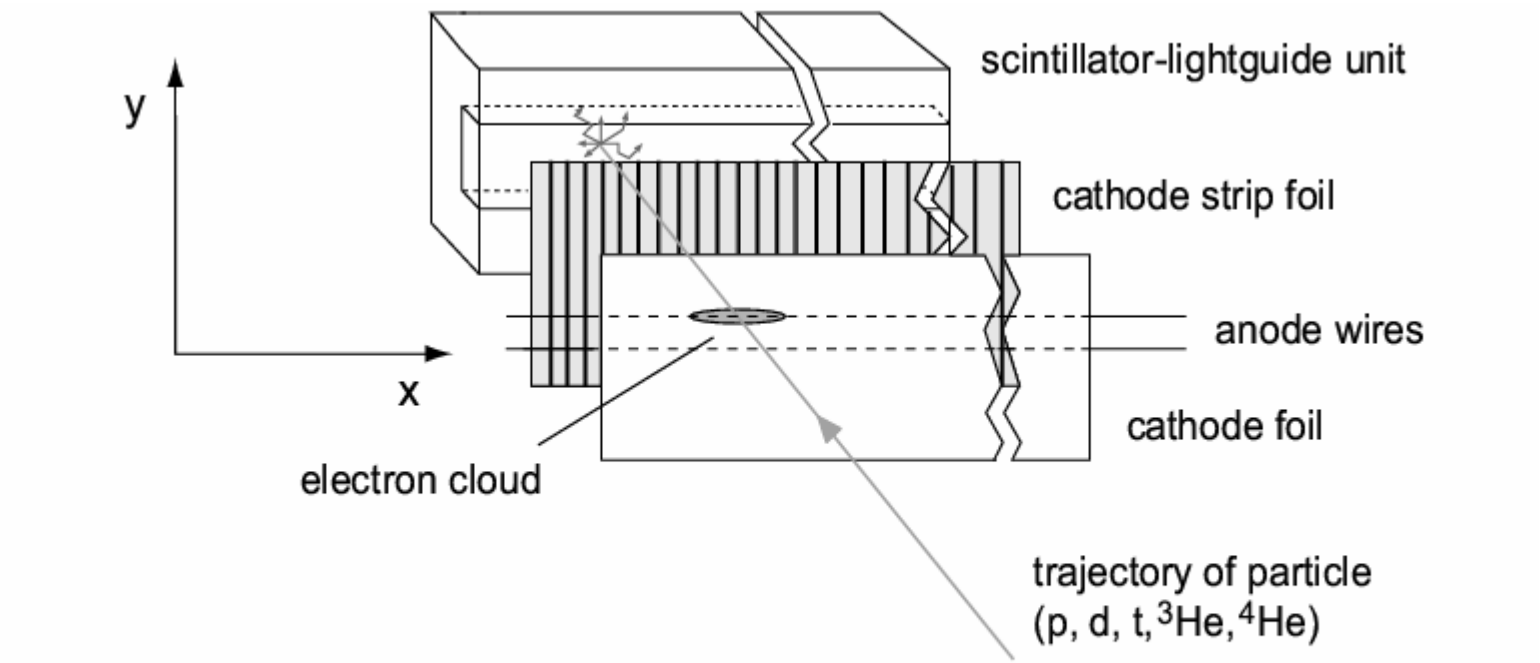

New position sensitive detector [93, 94] at the Q3D focal–plane. Particle position is determined in two–dimensions by a two–wire proportional gas chamber with cathode–strip readout. Additional particle identification is provided by the plastic scinitillator.

Charged particle detection

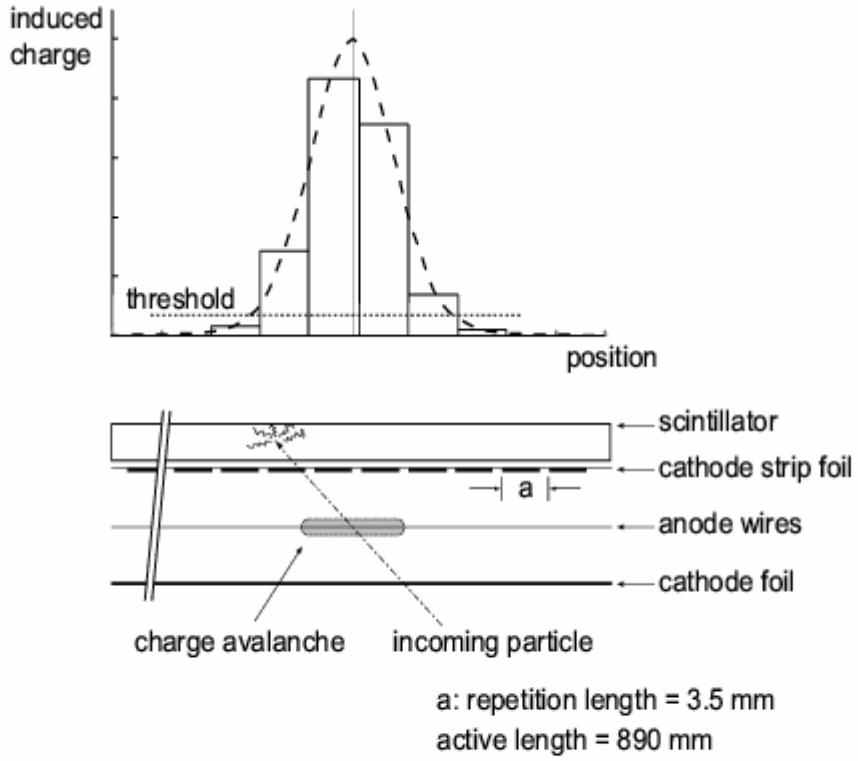

Working principle of the cathode strip read–out detector [93, 94] in Fig. 25. The particle's trajectory is determined by a gaussian fit of the charge distribution on several adjacent strips. Events recorded in fewer than 3 and more than 7 strips are rejected.

Proton spectra: unpolarized *d* beam

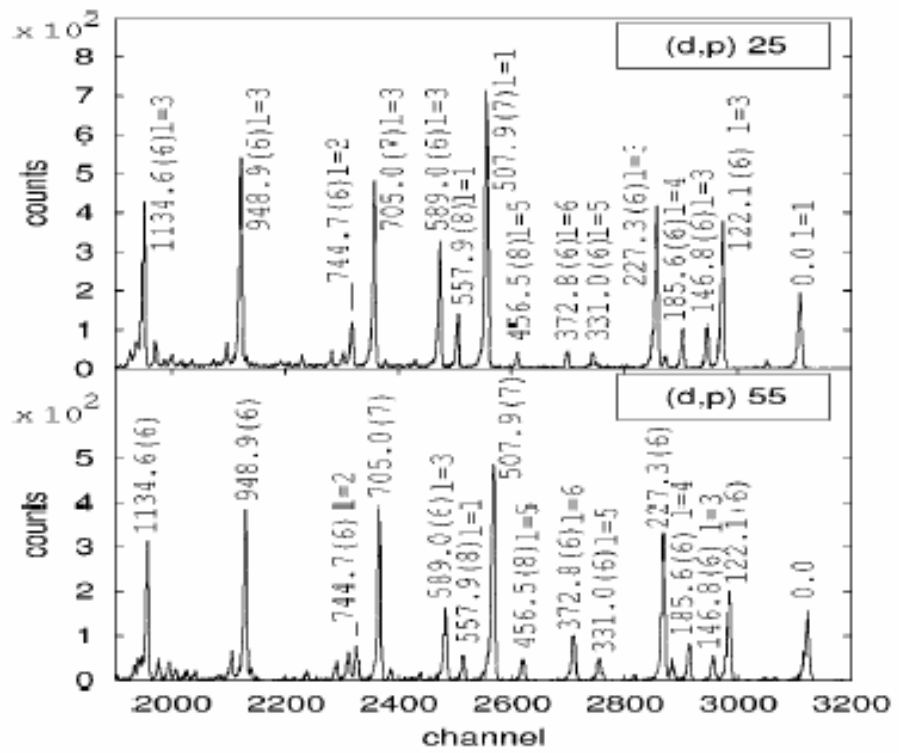

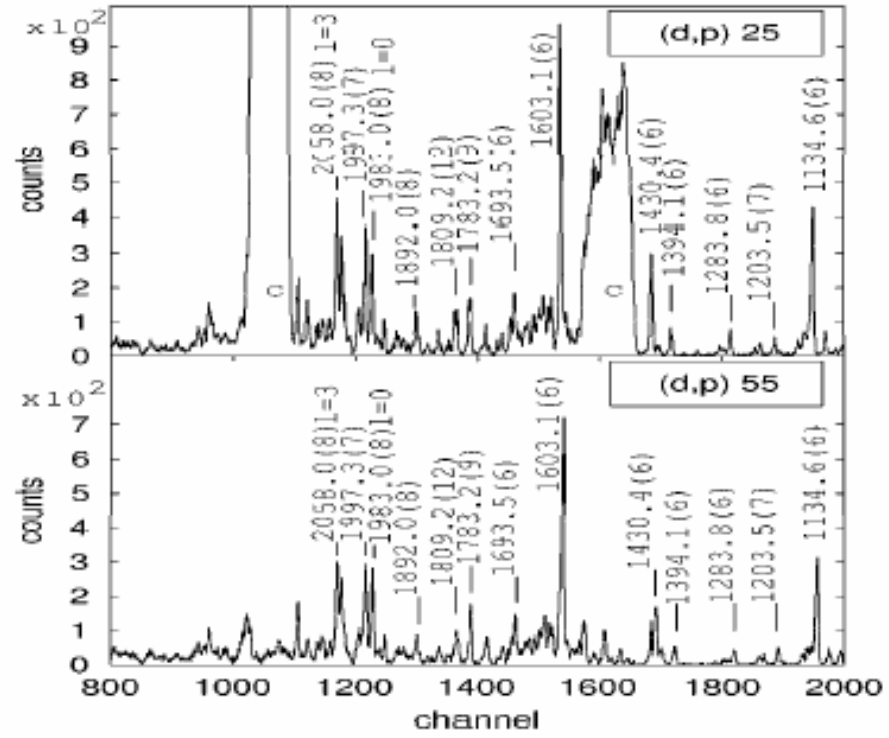

Triton spectra: polarized *d* beam

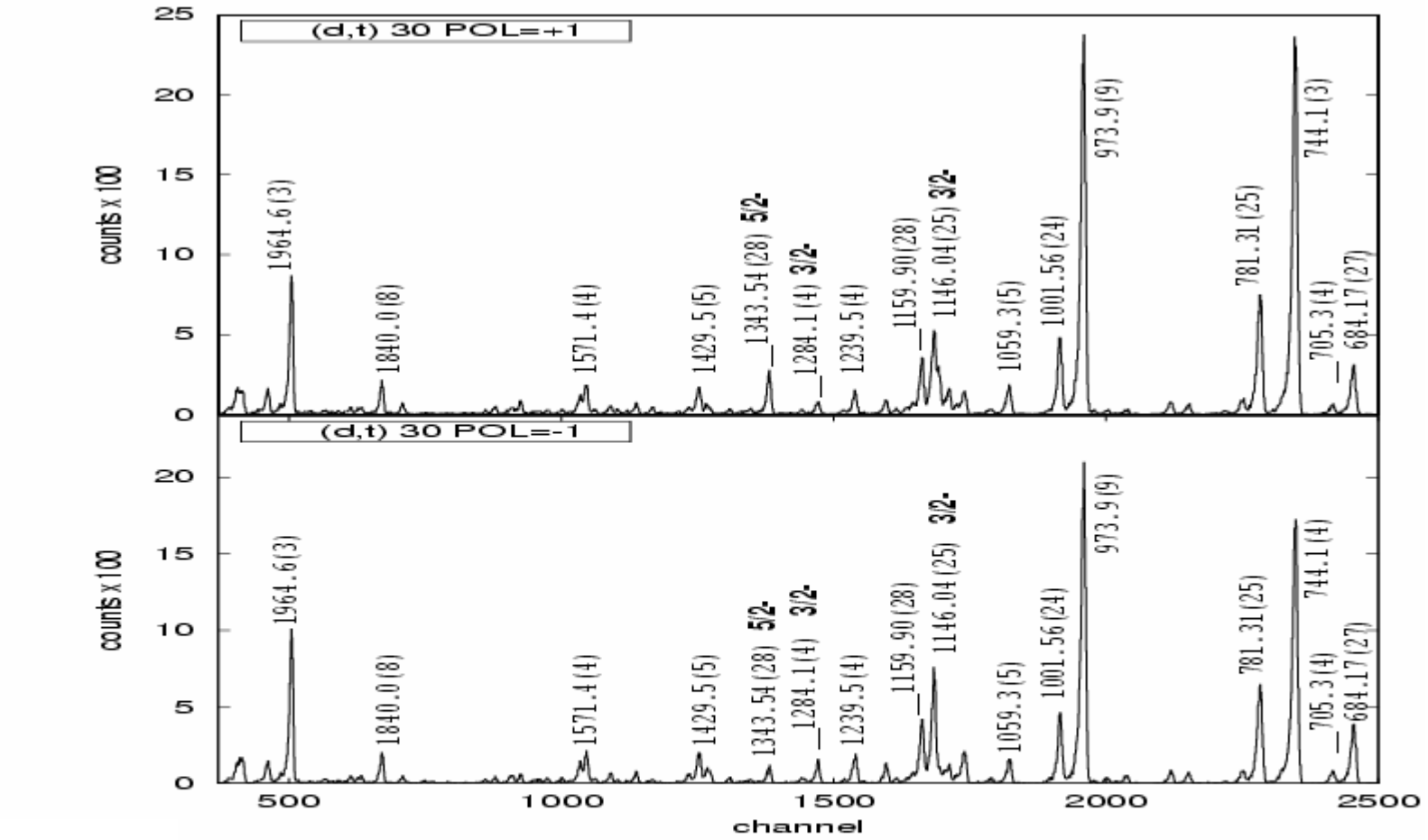

Portion of triton spectra at 30° in the ^{160}Gd($\vec{d}$,t)^{159}Gd reaction with spin up (+1) and down (−1) polarized 22 MeV deuterons. Note the peaks of indicated $3/2^-$ and $5/2^-$ levels. Some levels are labelled with their energy in keV.

Single neutron transfer

Neutron stripping

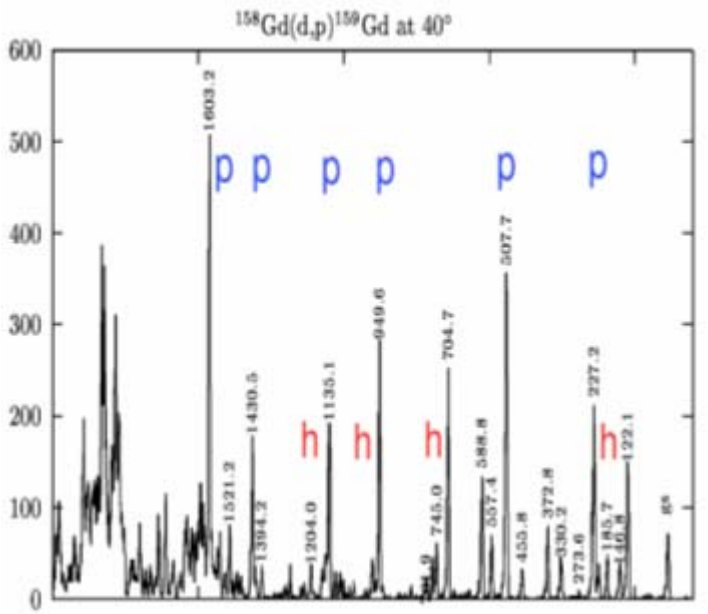

Neutron pick-up

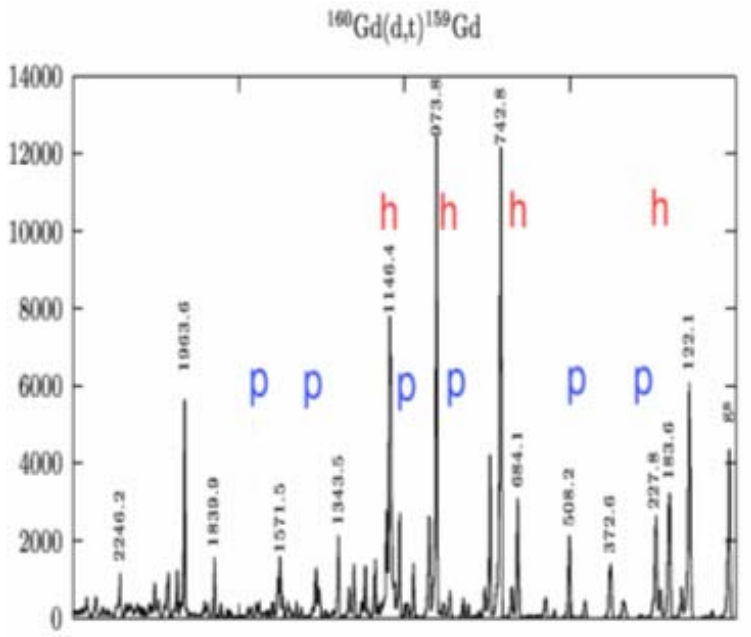

Cross Section angular distribution: (d,p)

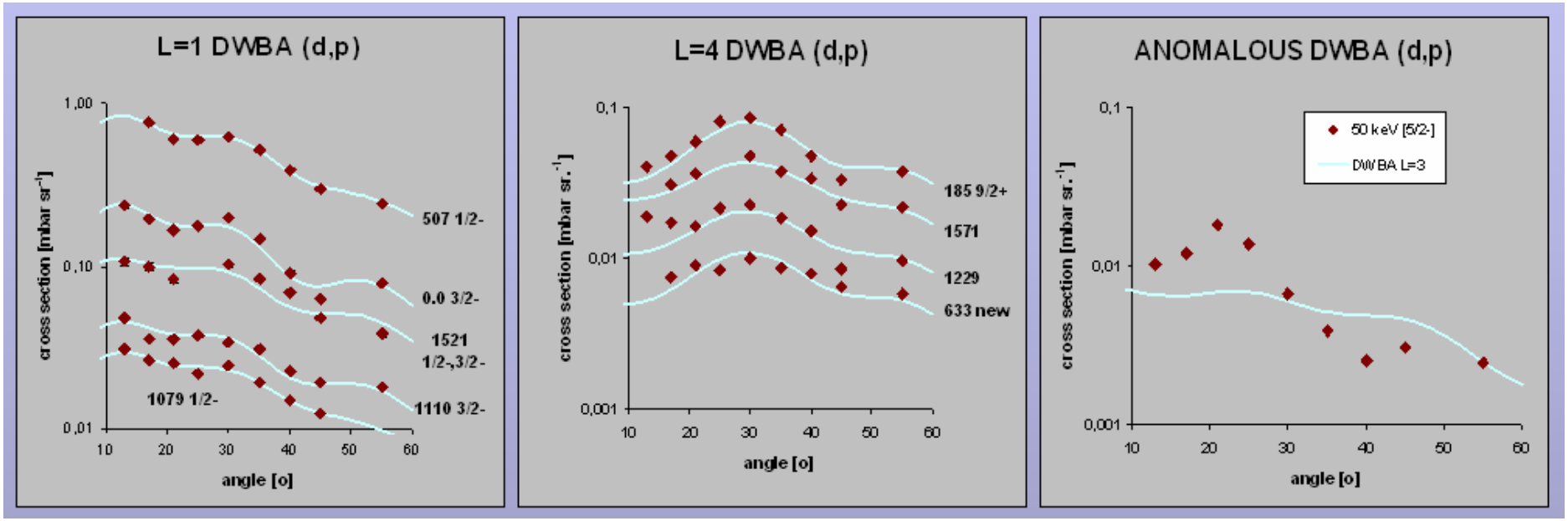

DWBA Distorted Waves Born Approximation

PWBA Plane Waves BA

CCBA Coupled Channels BA

Distorted Waves Born Approximation

[3]The optical potential is divided into a volume (I), surface (II), spin-orbit (III) and coulomb (IV) parts having the form [97, 98, 100]

$$
\begin{aligned}
V = \quad & -V_V \; f(r, r_R, a_R) - i \; W_V \; f(r, r_I, a_I) + && \text{(I)} \\
& i \; 4 \; a_I \; W_S \; \tfrac{d}{dr} f(r, r_I, a_I) + && \text{(II)} \\
& V_{LS} \; (\vec{L} \cdot \vec{S}) \left(\tfrac{\hbar}{mc}\right)^2 \; \tfrac{1}{r} \tfrac{d}{dr} f(r, r_{LS}, a_{LS}) + && \text{(III)} \\
& V_C \quad , && \text{(IV)}
\end{aligned}
$$

where the the potential well f is given by the Saxon-Woods form [97]. The potential parameters are:

V	...	real potential depth
W	...	imaginary absorption
a	...	diffuseness
r	...	interaction radius

Distorted Waves Born Approximation

Table 13: Optical parameters used in DWBA calculations.

		^{158}Gd(d,p)^{159}Gd			^{160}Gd(d,t)^{159}Gd		
		d	*p*	n	*d*	*t*	n
V_r	(MeV)	94.24	56.45	a	118.64	140.61	a
$4W_D$	(MeV)	49.46	34.84		50.29		
W_0	(MeV)					20.80	
V_{so}	(MeV)	6.81	12.40	$\lambda = 25$	7.30	9.50	$\lambda = 25$
r_r	(fm)	1.17	1.22	1.25	1.15	1.16	1.25
r_D	(fm)	1.33	1.32		1.29		
r_0	(fm)					1.20	
r_{so}	(fm)	1.07	1.01		0.88	1.10	
R_c	(fm)	1.30	1.25		1.30	1.40	
a_r	(fm)	0.74	0.75	0.75	0.83	0.75	0.75
a_D	(fm)	0.91	0.64		0.89		0.65
a_0	(fm)					0.82	
a_{so}	(fm)	0.66	0.75		1.00	0.80	
nlc		0.54	0.85	0.85	0.54	0.30	0.85

a Adjusted by CHUCK3.

The spectroscopic factor S_{lj}, in (d,p), and the spectroscopic strength G_{lj}, in (d,t), result from the measured and calculated cross sections as

$$\frac{d\sigma^{\exp}}{d\Omega} = S_{lj}\sigma_{lj}^{\mathrm{CHUCK3}} \quad \ldots \quad (\mathrm{d,p}) \quad ,$$

$$\frac{d\sigma^{\exp}}{d\Omega} = G_{lj}\sigma_{lj}^{\mathrm{CHUCK3}} \quad \ldots \quad (\mathrm{d,t}) \quad .$$

Cross Section angular distribution & Asymmetry: (d,t_{pol})

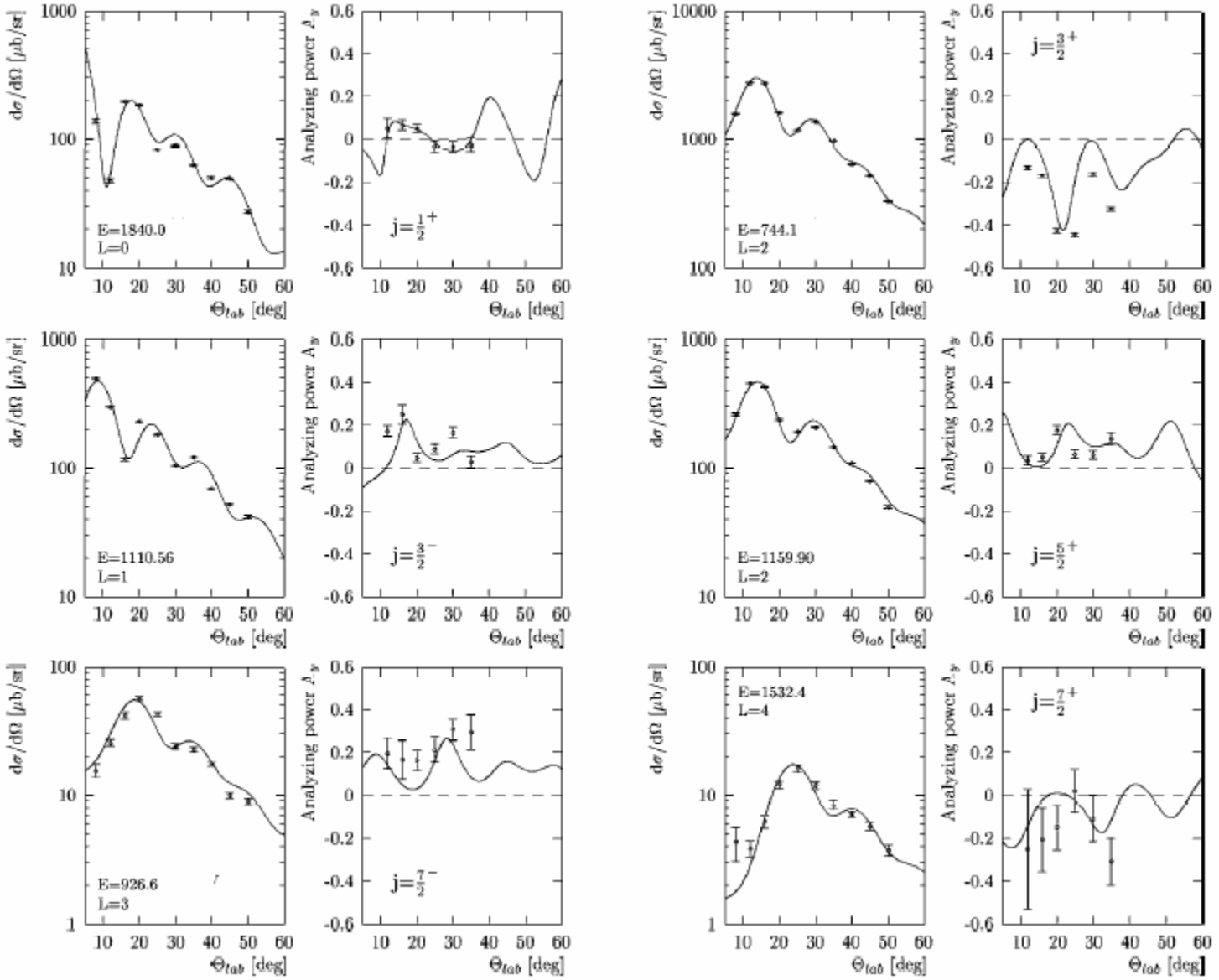

Cross Section angular distribution: (d,p)

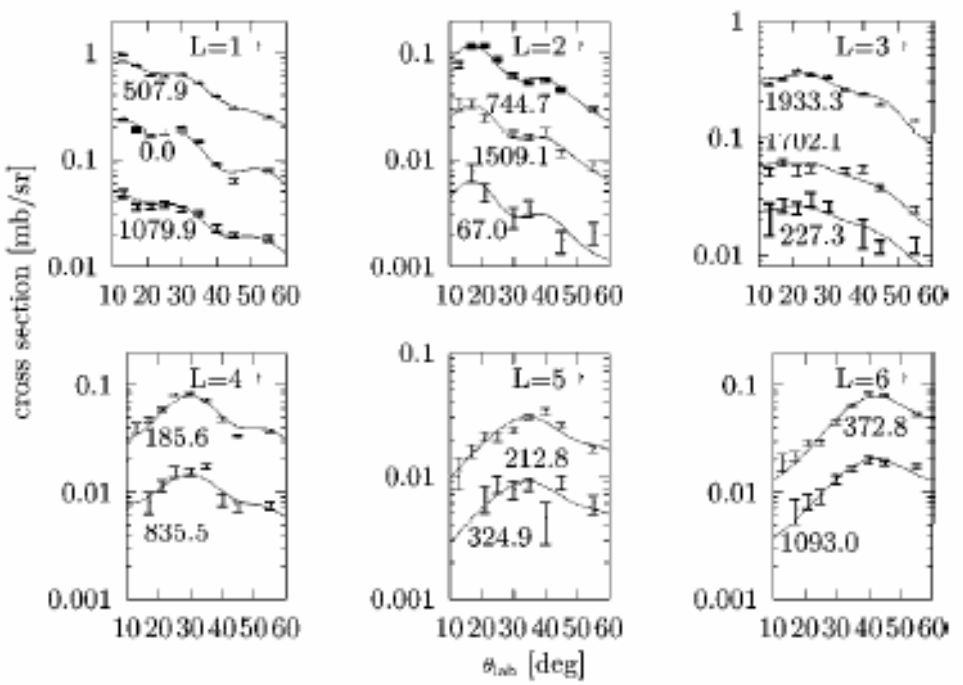

DWBA

?

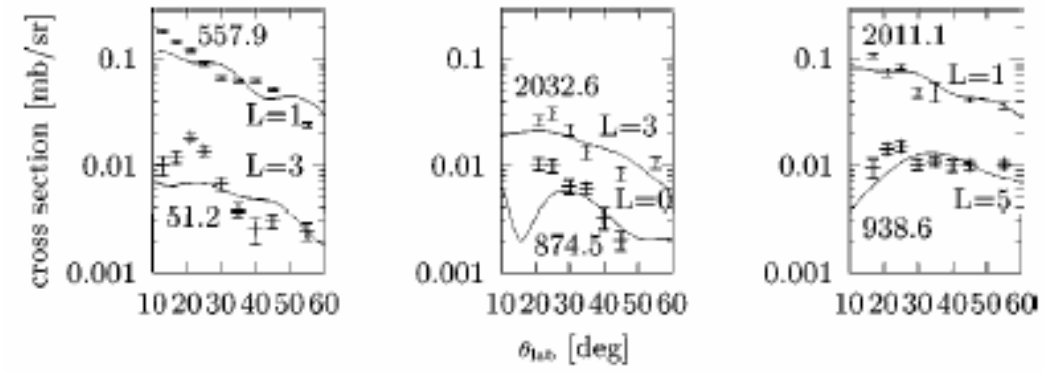

Spectroscopy information from Transfer Reactions

Spectroscopic information for ^{159}Gd from (d,p) and ($\vec{d}$,t) reactions. The level energies and spin–parity values deduced are given along with the cross section (at $\theta_{lab} = 30°$) and the corresponding spectroscopic factor or spectroscopic strength (see equations (2) and (3)). Uncertain assignments are given in parenthesis.

(d,p)				($\vec{d}$,t)			
E_x(keV)[a]	$d\sigma/d\Omega$(μb/sr)[b]	J^π	$S_{jl}(10^{-3})$[c]	E_x(keV)[d]	$d\sigma/d\Omega$(μb/sr)[b]	J^π	$G_{jl}(10^{-3})$
0.0	197	$1/2^-, 3/2^-$	62	0.0[&]	511[&]		66[&#]
51.2(9)	7	$(5/2^-, 7/2^-)^{\%}$	(3)	51.0(8)[&]	22[&]		8[&#]
67.0(7)	3	$3/2^+, 5/2^+$	2	66.2(9)[&]	6[&]		3[&#]
				119.2(9)[&]	63[&]		91[&i]
122.1(6)	242	$5/2^-, 7/2^-$	91	122.1(6)[&]	672[&]		184[&#]
146.8(6)	71	$5/2^-, 7/2^-$	27	145.4(6)[&]	106[&]		36[&#]
185.6(6)	85	$7/2^+, 9/2^+$	118	184.4(6)[&]	307[&]		90[&#]
212.8(6)	24	$9/2^-, 11/2^-$	70	212.3(6)[&]	55[&]		177[&#]
227.3(6)	328	$5/2^-, 7/2^-$	121	227.8(5)[&]	252[&]		66[&#]
274.0(7)	4	$11/2^+, 13/2^+$	27	273.7(9)[&]	6[&]		61[&#]
324.9(8)	8	$9/2^-, 11/2^-$	40	324.9(6)[&]	18[&]		33[&#]
331.0(6)	35	$9/2^-, 11/2^-$	70	330.6(8)[&]	22[&]		71[&#]
372.8(6)	44	$11/2^+, 13/2^+$	373	372.6(6)[&]	121[&]		756[&#]
456.5(8)	28	$9/2^-, 11/2^-$	78	456.4(6)[&]	26[&]		47[&#]
507.9(7)	626	$1/2^-, 3/2^-$	219	508.1(6)[&]	251[&]		30[&#]
557.9(8)	66	$(1/2^-, 3/2^-)^{\%}$	(58)	558.2(10)[&]	23[&]		2[&#]
589.0(6)	182	$5/2^-, 7/2^-$	67	588.6(7)[&]	63[&]		59[&#]
601.8(12)	1	$3/2^+, 5/2^+$	3	602.2(13)[&]	9[&]		4[&#]
632.9(10)	10	$7/2^+, 9/2^+$	12	633.4(7)[&]	4[&]		5[&#]
				646.5(10)[&]	7[&]		3[&#]

continu

$$\frac{d\sigma^{\exp}}{d\Omega} = S_{lj}\sigma_{lj}^{\mathrm{CHUCK3}} \quad \ldots \quad (\mathrm{d,p}) \ , \qquad (2)$$

$$\frac{d\sigma^{\exp}}{d\Omega} = G_{lj}\sigma_{lj}^{\mathrm{CHUCK3}} \quad \ldots \quad (\mathrm{d,t}) \ . \qquad (3)$$

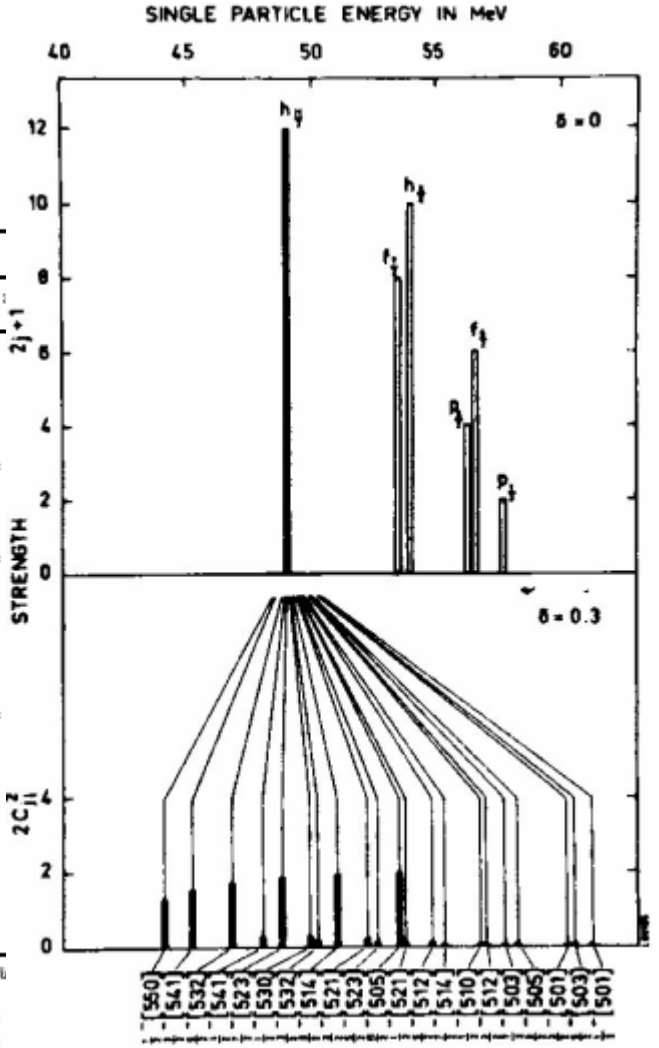

Distribution of the shell model strength on the various states in a deformed nucleus. In the example chosen, the *h* 11/2 state contributes to 21 Nilsson states covering a considerable interval of energy. The figure is based on theoretical expansion coefficients.

Spectroscopy information from Transfer Reactions

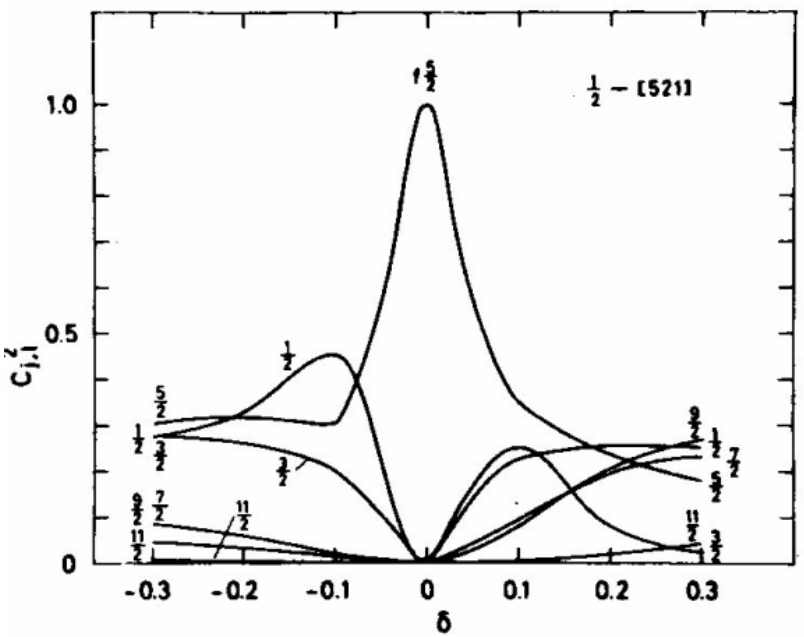

The composition of a deformed nucleus single particle wave function for various deformations. Already at a deformation of 0.1, the wave function has completely lost any resemblance to the spherical f 5/2 state. The figure is based on theoretical expansion coefficients.

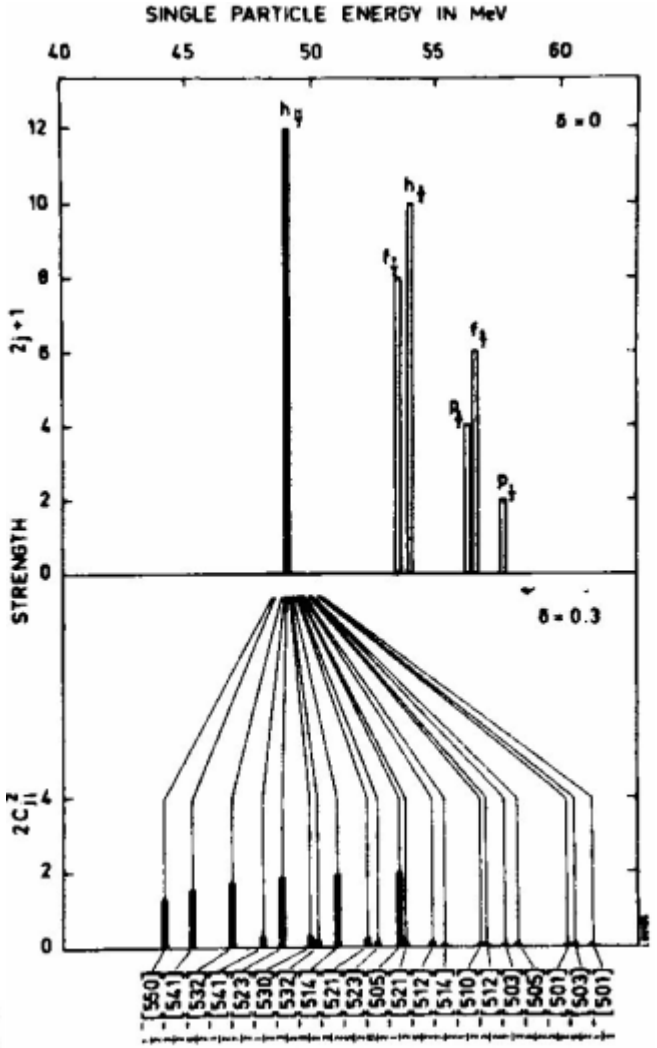

$$\frac{d\sigma^{\exp}}{d\Omega} = S_{lj}\sigma^{\mathrm{CHUCK3}}_{lj} \quad \ldots \quad (\mathrm{d,p}) \,, \qquad (2)$$

$$\frac{d\sigma^{\exp}}{d\Omega} = G_{lj}\sigma^{\mathrm{CHUCK3}}_{lj} \quad \ldots \quad (\mathrm{d,t}) \,. \qquad (3)$$

Distribution of the shell model strength on the various states in a deformed nucleus. In the example chosen, the h 11/2 state contributes to 21 Nilsson states covering a considerable interval of energy. The figure is based on theoretical expansion coefficients.

Spectroscopic results

EXPERIMENT (laboratory)	# Eγ PRI	# Eγ SEC	Range E_f [MeV]	# of levels	J^π
(n,γ) IRC DUBNA	80	14	0.0 – 2.4	80	$1/2^{\pm},3/2^{\pm}$
(n,γ) 2 keV ARC BNL	145	–	0.0 – 3.0	176	$1/2^{\pm},3/2^{\pm},5/2^{+}$
(n,γ) 24 keV ARC BNL	140	–	0.0 – 3.0		$1/2^{\pm},3/2^{\pm},5/2^{\pm}$
(n,γ) ILL	–	73	0.0 – 1.5	35	$1/2^{\pm},3/2^{\pm},5/2^{\pm},7/2^{\pm},9/2^{-}$
(d,p) TU-Munich			0.0 – 2.1	106	$1/2^{\pm},3/2^{\pm},5/2^{\pm},7/2^{\pm},9/2^{\pm},11/2^{\pm},13/2^{-}$
(d,t) TU-Munich			0.0 – 2.3	160	$1/2^{\pm},3/2^{\pm},5/2^{\pm},7/2^{\pm},9/2^{\pm}$

Level density

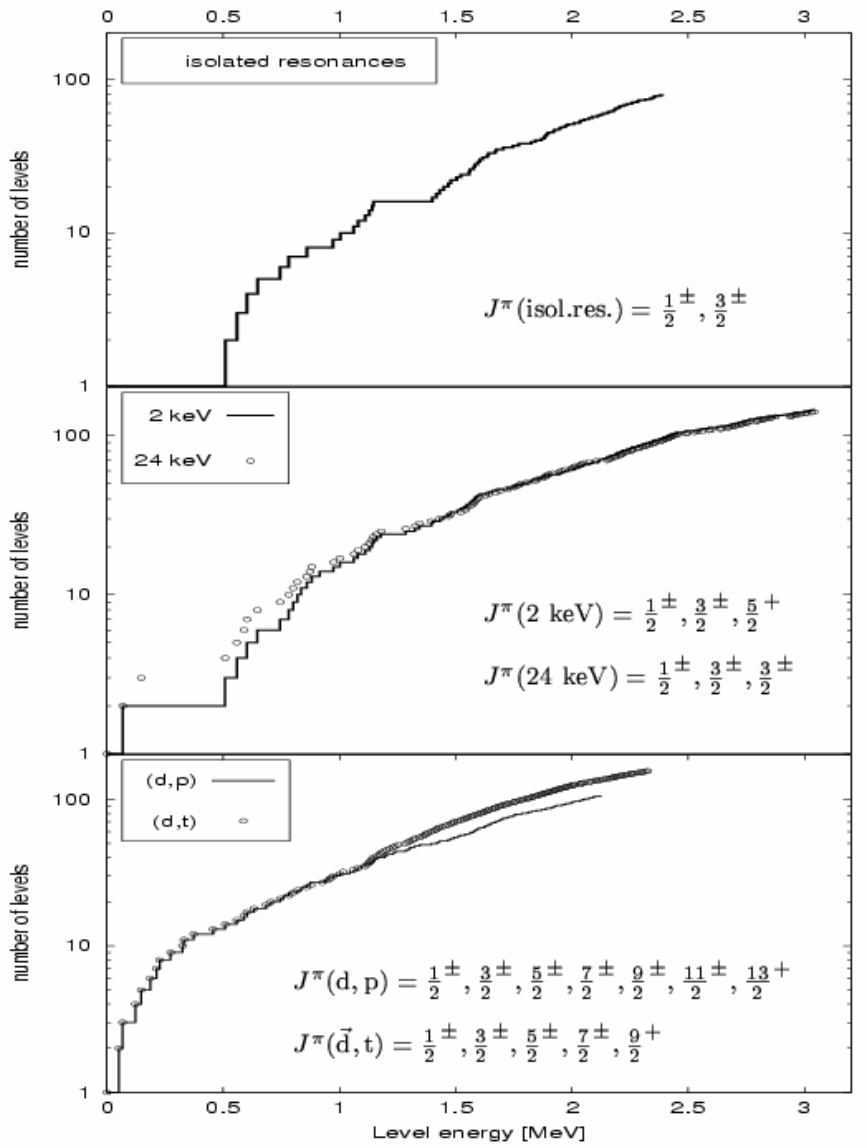

Level density

$$\rho(E,J) = S(J)\frac{1}{T}e^{(E-E_0)/T} \quad , \qquad S(J) = \frac{2J+1}{2\sigma^2}e^{-(J+1/2)^2/2\sigma^2}$$

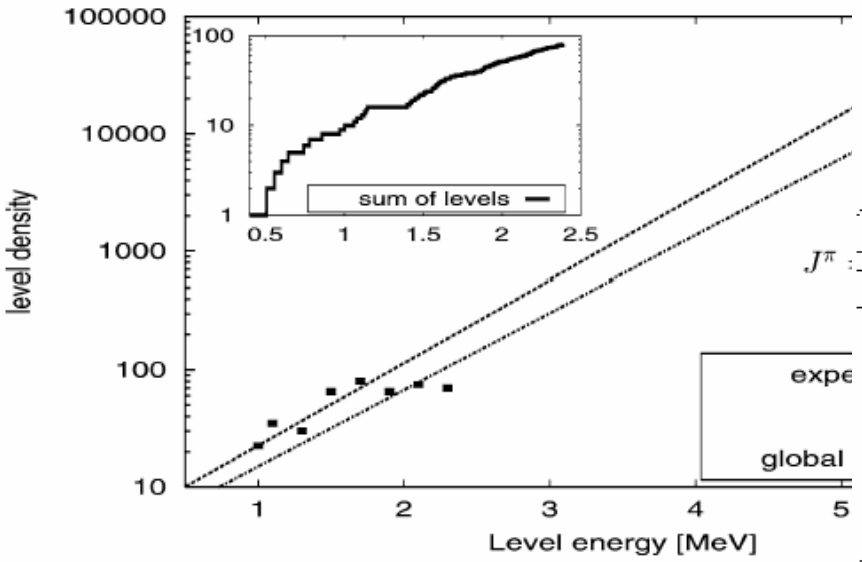

Density of $\frac{1}{2}^{\pm}$, $\frac{3}{2}^{\pm}$ levels in ^{159}Gd. The constant temperature Fermi gas mod
fitted to the experimental data and to a global survey [26].

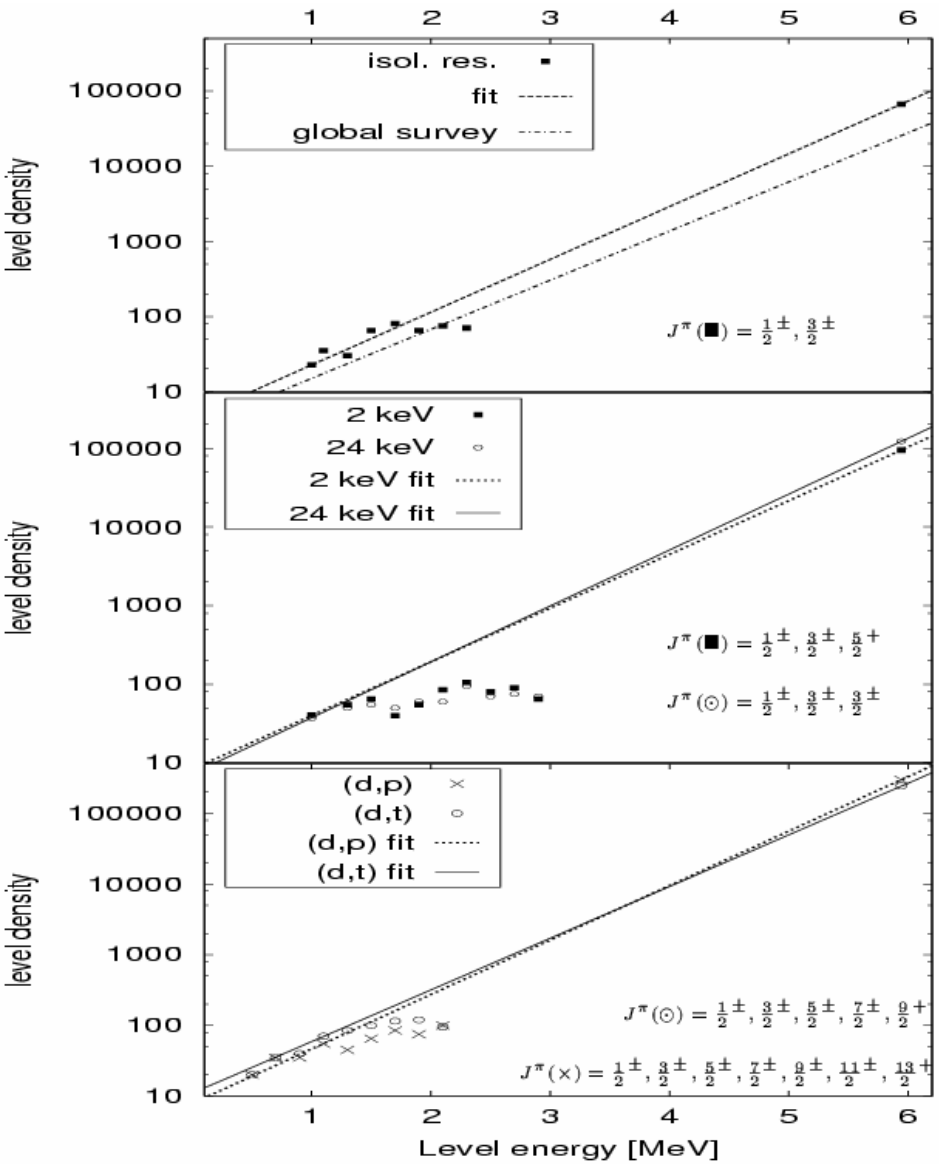

Levels: energy & spin-parity

Level scheme of ^{159}Gd. Final levels result as combination of levels observed in the transfer reactions and levels populated by primary γ-rays from our previous (n,γ) experiments [11, 12]. Levels reported in previous studies of (d,p), (d,t) [1] and (n,γ) [9] reactions are included for comparison.

final		(d,p), ($\vec{d}$,t)		(n,γ_{pri})		previous studies	
E_x(keV)	J^π	E_x(keV)	J^π	E_x(keV)	J^π	E_x(keV)	J^π
0.0	$3/2^-$ #	0.0	$1/2^-, 3/2^-$	0.0	$1/2^-, 3/2^-$	0.0	$3/2^-$
50.627(9)[a]	$5/2^-$ #	51.1(6)	$(5/2^-, 7/2^-)$[%]			50.66(9)	$5/2^-$
67.829(24)[a]	$5/2^+$ #	66.7(6)	$3/2^+, 5/2^+$	67.65(6)	$5/2^+$	67.79(7)	$5/2^+$
118.686(28)[a]	$7/2^+$ #	119.2(9)				118.92(15)	$7/2^+$
121.899(24)[a]	$7/2^-$ #	122.1(4)	$5/2^-, 7/2^-$			121.93(13)	$7/2^-$
146.316(6)[a]	$5/2^-$ #	146.1(4)	$5/2^-, 7/2^-$	146.94(23)	$5/2^-$	146.39(8)	$5/2^-$
185.0(4)	$9/2^+$ #	185.0(4)	$7/2^+, 9/2^+$			185.4(4)	$9/2^+$
212.6(6)	$9/2^-$ #	212.6(4)	$9/2^-, 11/2^-$			212.30(23)	$9/2^-$
227.412(21)[a]	$7/2^-$ #	227.6(4)	$5/2^-, 7/2^-$			227.49(10)	$7/2^-$
273.9(6)	$11/2^+$ #	273.9(6)	$11/2^+, 13/2^+$			273.(2)	$(11/2^+)$
324.9(5)	$11/2^-$ #	324.9(5)	$9/2^-, 11/2^-$				
330.479(13)[a]	$9/2^-$ #	330.8(5)	$9/2^-, 11/2^-$			328.(3)	$9/2^-, 11/2^-$

Gamma – ray decay: energy & intensity

Gamma–decay of levels in ^{159}Gd observed in the (n,γ) reaction. Several transitions reported in the β^-–decay of ^{159}Eu [10] are included. E_i, J_i^π and E_f, J_f^π denote the energy, spin and parity of the initial and final level, respectively. E_γ indicates the gamma–ray energy. Gamma–ray intensities I_γ are given per 100 neutrons captured or per 100 β^-–decay, the latter quantities are presented in parenthesis.

E_i (keV)	J_i^π	E_f (keV)	J_f^π	E_γ (keV)	I_γ	E_i (keV)	J_i^π	E_f (keV)	J_f^π	E_γ (keV)	I_γ
50.627	$\frac{5}{2}^-$	0.0	$\frac{3}{2}^-$	50.7[&]		858.51	$\frac{3}{2}^+$	0.0	$\frac{3}{2}^-$	858.39	0.8
67.829	$\frac{5}{2}^+$	0.0	$\frac{3}{2}^-$	67.8[&#]	(19.2)			50.627	$\frac{5}{2}^-$	807.60	0.4
		50.627	$\frac{5}{2}^-$	17.1[&]	(1.6)			67.829	$\frac{5}{2}^+$	790.90	1.5
118.686	$\frac{7}{2}^+$	50.627	$\frac{5}{2}^-$	67.8[&#]	(19.2)			118.686	$\frac{7}{2}^+$	739.847	0.7
		67.829	$\frac{5}{2}^+$	51.0[&]		872.64	$\frac{5}{2}^-$	0.0	$\frac{5}{2}^-$	871.4[&]	(0.21)
121.899	$\frac{7}{2}^-$	0.0	$\frac{5}{2}^-$	121.9[&]	(0.4)			67.829	$\frac{5}{2}^+$	804.743[$]	0.7
		50.627	$\frac{5}{2}^-$	71.4[&]	(1.1)			118.686	$\frac{7}{2}^+$	754.03[$]	0.3
146.316	$\frac{5}{2}^-$	0.0	$\frac{5}{2}^-$	146.324[$]	1.4			146.316	$\frac{5}{2}^-$	726.47[$]	0.20

Level scheme

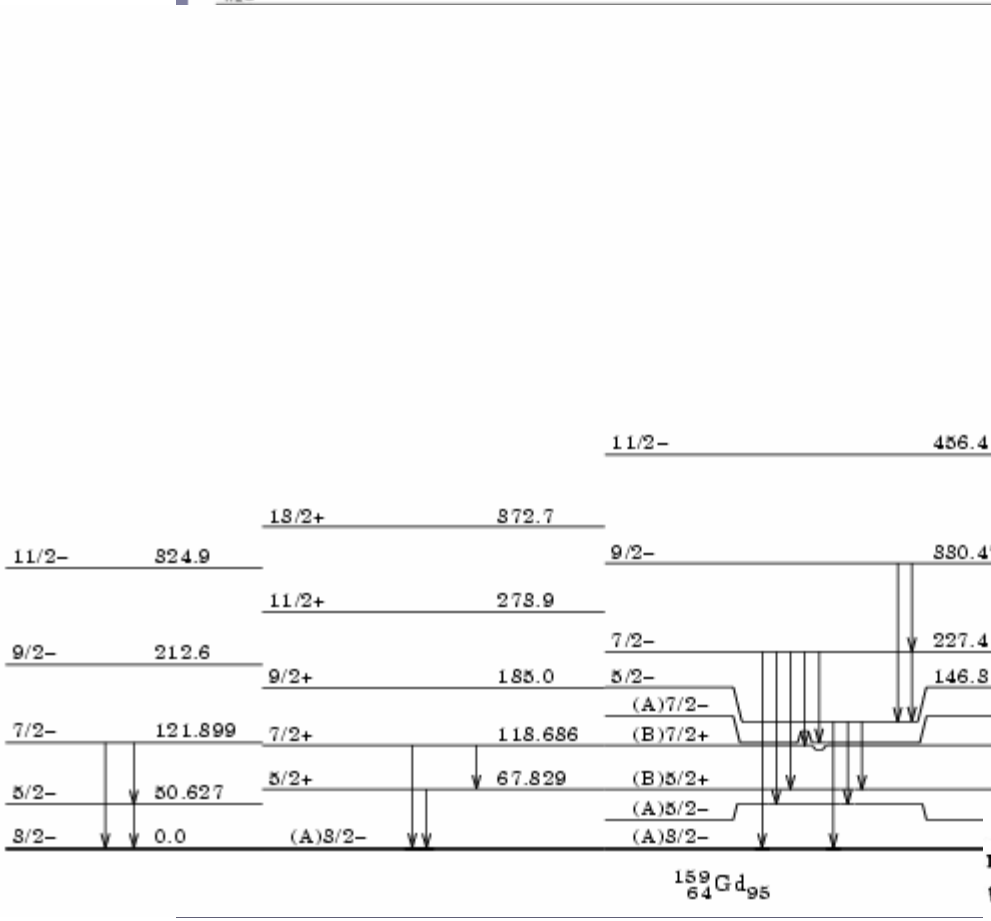

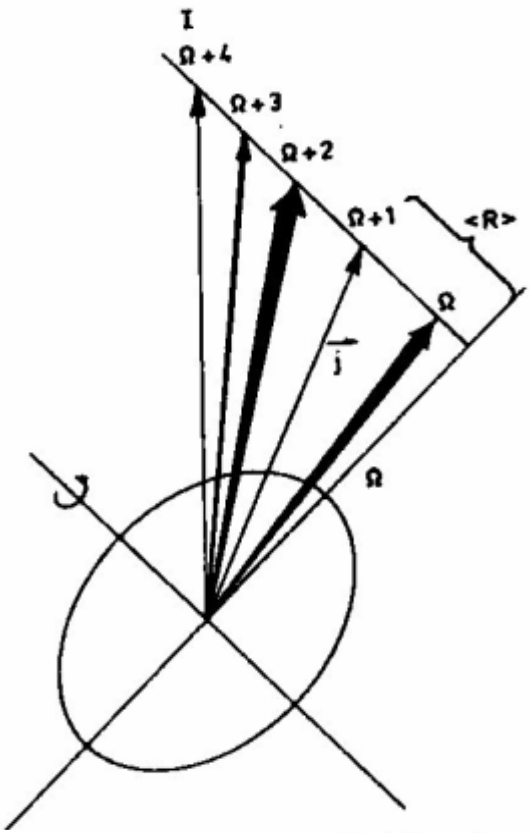

Stripping leading to an odd deformed nucleus. The neutron enters with a definite total angular momentum j into a Nilsson state where the projection of j must be Ω. The nucleus must have $I = j$ and must therefore, in order to accommodate j, acquire rotational angular momentum R.

Rotational bands: odd-*A* deformed nucleus

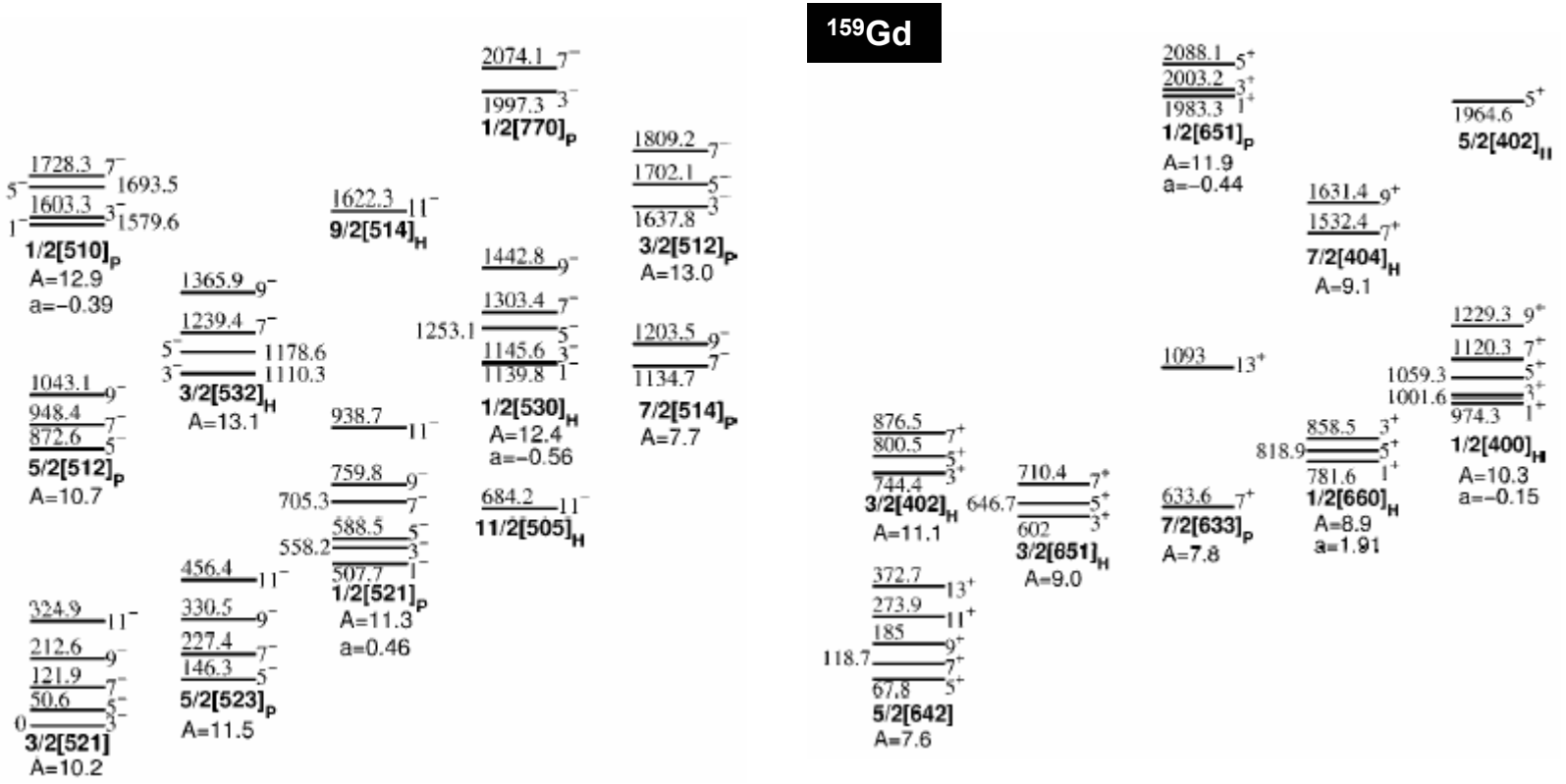

$$E = E_0 + A\{J(J+1) + (-1)^{J+1/2} a(J+1/2)\}$$

Rotational bands: odd-*A* deformed nucleus

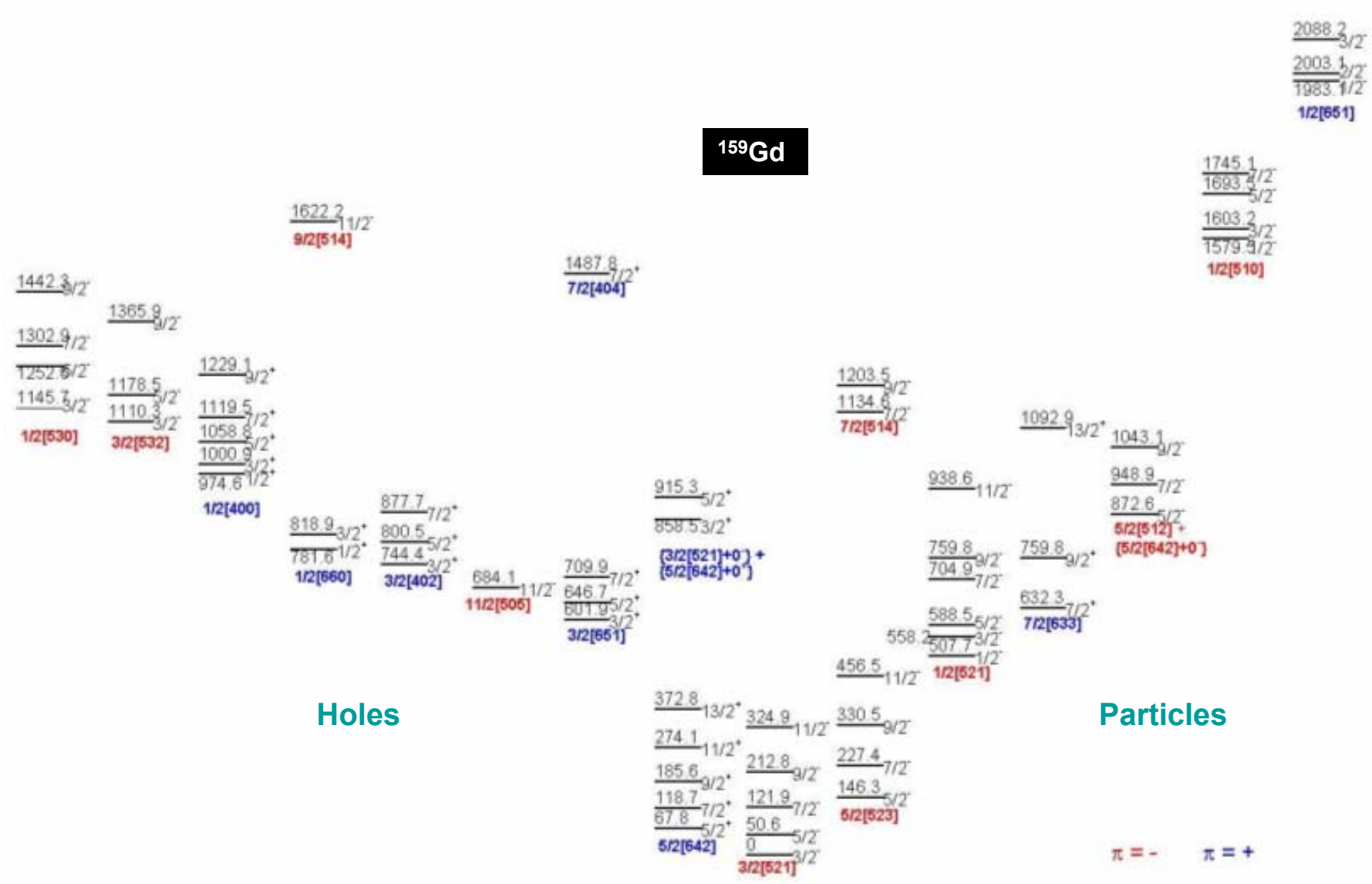

Rotational band parameters

Evolution of the experimental effective rotational parameters A and decoupling parameters a of rotational bands in ^{159}Gd. Corresponding values obtained in the model calculation with the Coriolis interaction included (see Section VI) and the pure Nilsson a–values are given in the two rightmost columns.

band	energy	A–values (in keV) and a–parameters							
$K[Nn_z\Lambda]$	(keV)	$\frac{1}{2}-3/2(-5/2)$	$3/2-5/2(-7/2)$	$5/2-7/2(-9/2)$	$7/2-9/2(-11/2)$	$9/2-11/2$	$11/2-13/2$	Coriolis	Nilsson
$\frac{3}{2}[521]$	0.0		10.12	10.18	10.10	10.19		12.1	
$\frac{5}{2}[642]$	67.829			7.27	7.43	8.05	7.59	14.9	
$\frac{5}{2}[523]$	146.316			11.58	11.45	11.45		12.3	
$\frac{1}{2}[521]$	507.724	11.42 (0.47)	11.31 (0.47)	11.35 (0.46)	11.2 (0.45)			11.6 (0.37)	(0.37)
$\frac{3}{2}[651]$	601.977		8.96					8.8	
$\frac{7}{2}[633]$	633.60				14.16	13.87		11.5	
$\frac{3}{2}[402]$	744.378		11.22	11.02				11.6	
$\frac{1}{2}[660]$	781.556	8.85 (1.91)						7.0 (3.50)	(5.05)
$\frac{5}{2}[512]$	872.64			10.85	10.55			10.6	
$\frac{1}{2}[400]$	974.29	10.22 (-0.14)	10.15 (-0.14)	10.44 (-0.16)				9.6 (-0.35)	(-0.35)
$\frac{3}{2}[532]$	1110.25		13.64	11.71	14.04			11.2	
$\frac{7}{2}[514]$	1134.7				7.66			6.9	
$\frac{1}{2}[530]$	1139.84	11.80 (-0.83)	14.24 (-0.49)	11.30 (-0.36)				9.9 (-0.45)	(1.24)
$\frac{1}{2}[510]$	1579.6	13.03 (-0.38)	12.76 (-0.41)					10.1 (-0.53)	(-5.90)
$\frac{3}{2}[512]$	1637.8	12.88						9.2	
$\frac{1}{2}[651]$	1983.3	11.86 (-0.44)						11.8 (-0.44)	(1.58)

Nuclear structure models

Odd – *A* heavy deformed nuclei

• **Nilsson Model** (intrinsic Hamiltonian, deformed mean field, pairing, multipole - multipole interaction)

• **Quasiparticle – phonon model** (nuclear mean – field, pairing interactions, multipole (e.g., quadrupole and octupole vibrations "*microscopically*"), spin – multipole and charge – exchange interactions, phonon – quasiparticle coupling (fragmentation), ...)

• **Particle – rotor** and the **Coriolis** interaction.

• **Rotational bands** built on intrinsic **quasi – particle states** with **phonon** admixtures

⇒ low-lying spectra, electromagnetic transitions, spectroscopic factors, phonon admixtures

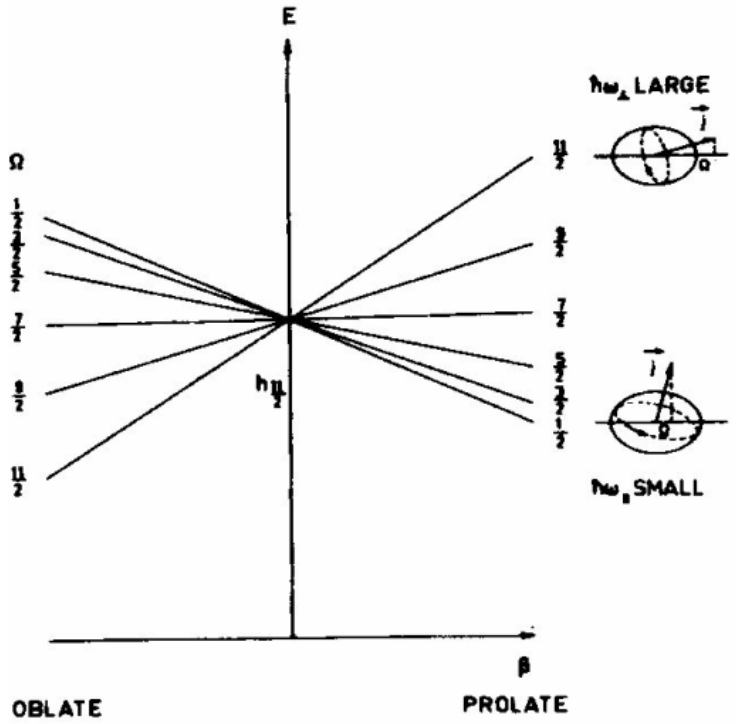

Splitting of a shell model state under the influence of nuclear deformation. The $2j + 1$ fold degenerate spherical state is split into $(2j + 1)/2$ doubly degenerate deformed states. The ordering of the states with the high Ω-values highest for prolate deformation, is preserved in the general Nilsson model.

PHONON: a quantum of **vibration** of nucleons in nuclei. Understood as a **collective** process.

FRAGMENTATION: the distribution (**spreading**) of one –, two –, three –, ... single particle or collective strength into various other states.

QUASI – PARTICLE An entity used in the description of a system of many interacting particles which has **particle – like properties** such as mass, energy, and momentum but which **does not exist as a free particle** such as the single – particle (with **pairing**) excitations in nuclei.

Low – lying non – rotational states and high – lying collective states of the giant resonance – type are well describabed within **microscopic models** based on **mean – field**, **pairing** and the **effective interactions** between **quasi – particles**.

The **states lying below and above the neutron resonances** are well described **microscopically non – statistically**.

Rotational bands: odd-*A* deformed nucleus

Experiment

Theory

^{159}Gd

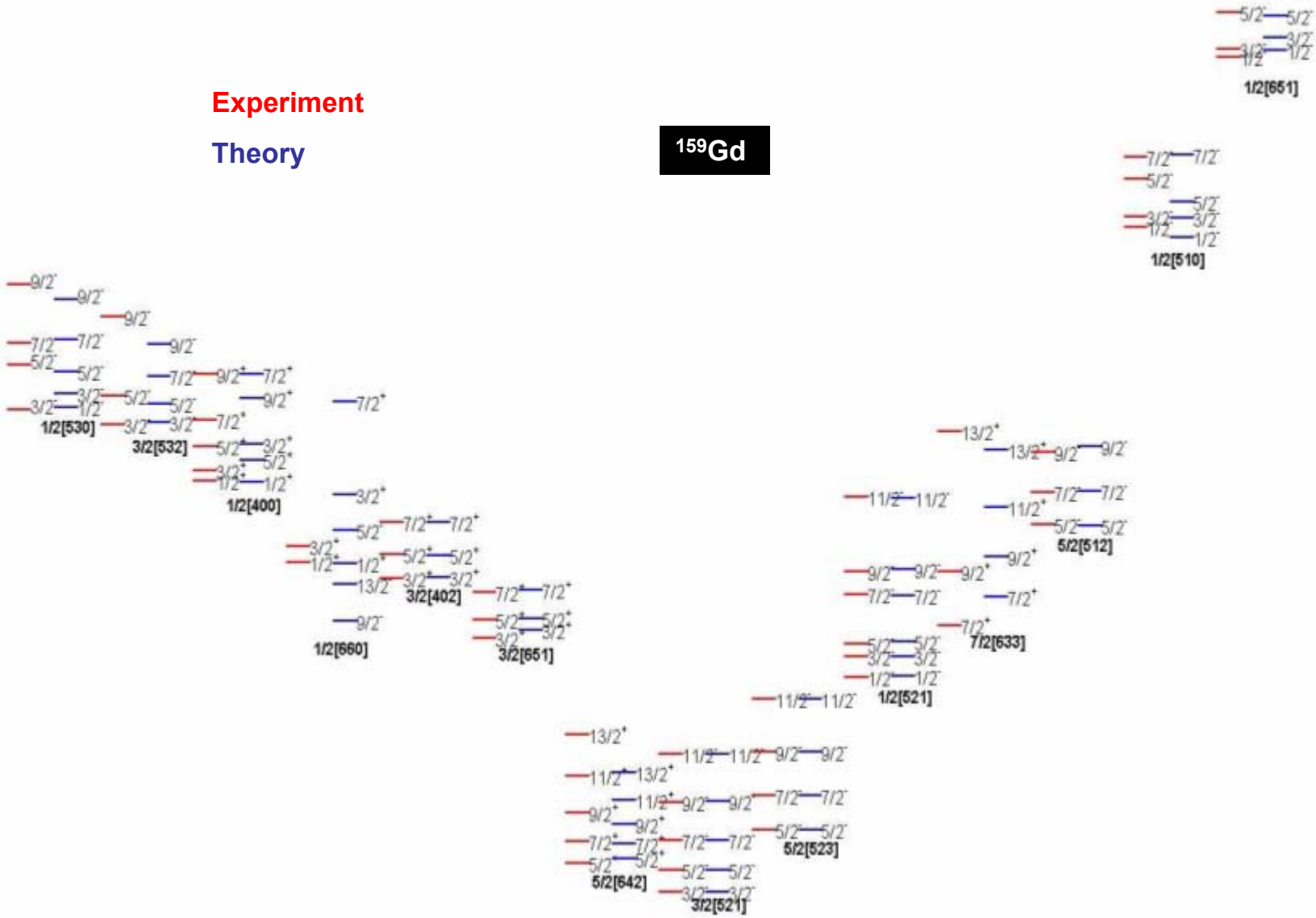

Structure intrinsic states: quasiparticle – phonon model

Structure of low–lying intrinsic states in ^{159}Gd. Experimental band head energies are compared with values obtained in QPM calculations. Percentages of the main components of the quasiparticle–phonon admixtures are given. Only components greater than 5% are included. Level energies are given in keV.

J^π	E_{exp}	E_{th}	Structure $K[Nn_n\Lambda]Q_{\lambda\mu}$
$\frac{3}{2}^-$	0.0	0	$\frac{3}{2}[521]$ 83%
$\frac{5}{2}^+$	67.829	89	$\frac{5}{2}[642]$ 84%
$\frac{5}{2}^-$	146.316	93	$\frac{5}{2}[523]$ 42% + $\frac{5}{2}[512]$ 30% + $\{\frac{5}{2}[642]Q_{30}\}$ 8% + $\{\frac{11}{2}[615]Q_{33}\}$ 7%
$\frac{1}{2}^-$	507.724	497	$\frac{1}{2}[521]$ 71%
$\frac{3}{2}^+$	601.977	578	$\frac{3}{2}[651]$ 77%
$\frac{7}{2}^+$	633.60	672	$\frac{7}{2}[633]$ 68% + $\{\frac{3}{2}[521]Q_{32}\}$ 16%
$\frac{11}{2}^-$	684.16	695	$\frac{11}{2}[505]$ 85% + $\{\frac{5}{2}[402]Q_{33}\}$ 9%
$\frac{3}{2}^+$	744.378	755	$\frac{3}{2}[402]$ 81% + $\{\frac{1}{2}[400]Q_{22}\}$ 8%
$\frac{1}{2}^+$	781.556	799	$\frac{1}{2}[660]$ 81%
$\frac{5}{2}^-$	872.64	1088	$\frac{5}{2}[512]$ 41% + $\frac{5}{2}[523]$ 45%
$\frac{1}{2}^+$	974.29	989	$\frac{1}{2}[400]$ 70% + $\{\frac{3}{2}[402]Q_{22}\}$ 13% + $\{\frac{3}{2}[521]Q_{31}\}$ 7%
$\frac{3}{2}^-$	1110.25	1126	$\frac{3}{2}[532]$ 73% + $\{\frac{3}{2}[402]Q_{30}\}$ 12%
$\frac{7}{2}^-$	1134.7	1177	$\frac{7}{2}[514]$ 47% + $\frac{7}{2}[503]$ 21% + $\{\frac{13}{2}[606]Q_{33}\}$ 12% + $\{\frac{7}{2}[633]Q_{30}\}$ 8%
$\frac{1}{2}^-$	1139.84	1172	$\frac{1}{2}[530]$ 82% + $\{\frac{1}{2}[400]Q_{30}\}$ 6%
$\frac{5}{2}^+$		1186	$\frac{5}{2}[402]$ 22% + $\{\frac{11}{2}[505]Q_{33}\}$ 55% + $\{\frac{1}{2}[400]Q_{22}\}$ 5%
$\frac{7}{2}^+$	1532.4	1526	$\frac{7}{2}[404]$ 68% + $\{\frac{3}{2}[402]Q_{22}\}$ 22%
$\frac{1}{2}^-$	1579.6	1714	$\frac{1}{2}[510]$ 39% + $\{\frac{5}{2}[642]Q_{33}\}$ 20% + $\{\frac{5}{2}[642]Q_{32}\}$ 8% + $\{\frac{5}{2}[512]Q_{22}\}$ 5%
$\frac{9}{2}^-$	1622.3%	1643	$\frac{9}{2}[514]$ 83% + $\{\frac{3}{2}[411]Q_{33}\}$ 6%
$\frac{3}{2}^-$	1637.8	1770	$\frac{3}{2}[512]$ 63% + $\{\frac{7}{2}[514]Q_{22}\}$ 8%
$\frac{3}{2}^+$		1785	$\{\frac{3}{2}[521]Q_{32}\}$ 83% + $\{\frac{3}{2}[521]Q_{30}\}$ 5%

% Energy of rotational band level (see Section IV).

Structure intrinsic states: Quasiparticle-Phonon Model

Energies and structure of intrinsic states in ^{159}Gd from quasiparticle–phonon model calculations. Components greater than 5% are included.

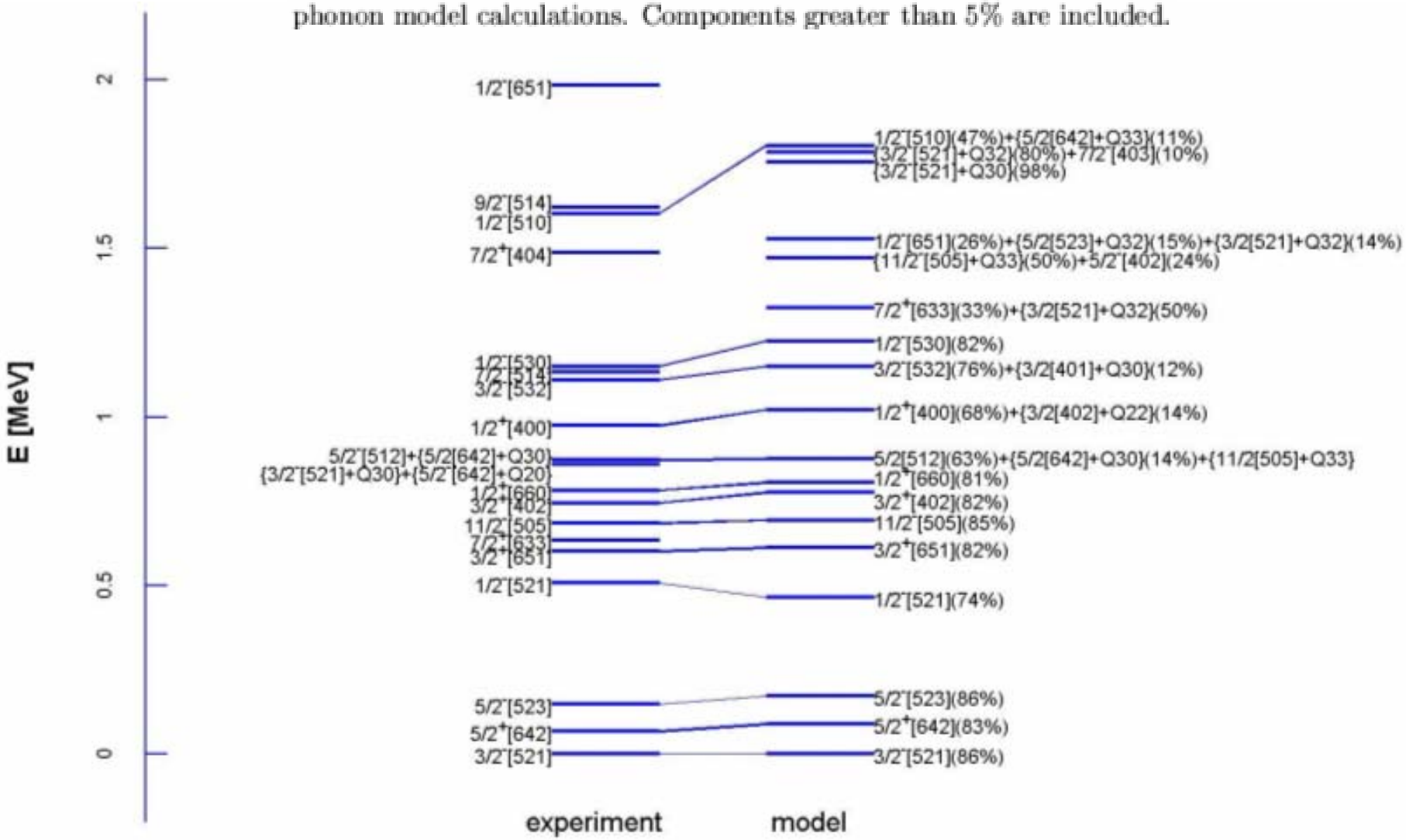

Spectroscopic Factors: Experiment & Model

: Spectroscopic factors ($\times 10^{-3}$) of negative and positive parity bands in ^{159}Gd. Experimental values are compared with predictions of the Coriolis band mixing calulations. Only absolute values of the factors $S_{lj}(N = N_{state})$ with main quantum number of the dominant Nilsson assignment of a state are listed. Level energies derived in the model calculations are included.

State	I^π	E^{exp}(keV)	E^{th}(keV)	(d,p) S_{lj}^{exp}	(d,p) S_{lj}^{th}	($\vec{d}$,t) S_{lj}^{exp}	($\vec{d}$,t) S_{lj}^{th}	State	I^π	E^{exp}(keV)	E^{th}(keV)	(d,p) S_{lj}^{exp}	(d,p) S_{lj}^{th}	($\vec{d}$,t) S_{lj}^{exp}	($\vec{d}$,t) S_{lj}^{th}
$\frac{3}{2}^-[521]$	$\frac{3}{2}^-$	0.0	0	31	75	68	296	$\frac{5}{2}^+[642]$	$\frac{5}{2}^+$	67.829	74	1	2	3	24
	$\frac{5}{2}^-$	50.627	50	3	25	6	73		$\frac{3}{2}^+$	118.686	119		25	124	70
	$\frac{7}{2}^-$	121.899	121	59	149	186	860		$\frac{1}{2}^+$	185.0	184	64	105	115	417
	$\frac{9}{2}^-$	212.6	214	70	259	293	977		$\frac{11}{2}^+$	273.9	272	27	40	91	128
	$\frac{11}{2}^-$	324.9	325	24	12	65	223		$\frac{13}{2}^+$	372.7	368	149	352	969	1449
$\frac{5}{2}^-[523]$	$\frac{5}{2}^-$	146.316	146	27	86	30	101	$\frac{3}{2}^+[651]$	$\frac{3}{2}^+$	601.977	624	3	6	4	73
	$\frac{7}{2}^-$	227.412	227	78	252	67	506		$\frac{5}{2}^+$	646.697	621		14	3	239
	$\frac{9}{2}^-$	330.479	331	70	333	119	267								
	$\frac{11}{2}^-$	456.4	456	41	108	95	280								
$\frac{1}{2}^-[521]$	$\frac{1}{2}^-$	507.724	509	219	407	28	171	$\frac{7}{2}^+[633]$	$\frac{7}{2}^+$	633.60	623	12	17	8	40
	$\frac{3}{2}^-$	558.211	558	29	153	2	80		$\frac{5}{2}^+$	835.5	814	3	34		175
	$\frac{5}{2}^-$	588.517	589	67	255	15	179		$\frac{11}{2}^+$		1038		19		26
	$\frac{7}{2}^-$	705.3	704	71	240	117	236		$\frac{13}{2}^+$	1093.0	1147	35	180		60
	$\frac{9}{2}^-$	759.8	759	74	188		206								
	$\frac{11}{2}^-$	938.7	939	15	67		108								
$\frac{11}{2}^-[505]$	$\frac{11}{2}^-$	684.16	684	17	98	978	1507	$\frac{7}{2}^+[404]$	$\frac{7}{2}^+$	1488.2	1488		46	79	1400
$\frac{5}{2}^-[512]$	$\frac{5}{2}^-$	872.64	873		22		18	$\frac{3}{2}^+[402]$	$\frac{3}{2}^+$	744.378	745	31	115	920	1379
	$\frac{7}{2}^-$	948.35	948	462	419	47	131		$\frac{5}{2}^+$	800.45	800		16	36	237
	$\frac{9}{2}^-$	1043.2	1044	26	222		8		$\frac{7}{2}^+$	876.5	878	3	19	163	330
$\frac{3}{2}^-[532]$	$\frac{3}{2}^-$	1110.25	1116	6	5	194	24	$\frac{1}{2}^+[660]$	$\frac{1}{2}^+$	781.556	756	12	6	126	71
	$\frac{5}{2}^-$	1178.6	1176		41	55	628		$\frac{3}{2}^+$	858.51	868	2	4	27	63
	$\frac{7}{2}^-$	1303.4	1310	2	16	75	763		$\frac{5}{2}^+$	818.89	835		7	15	146
	$\frac{9}{2}^-$	1365.9	1348		48	121	1238								
$\frac{1}{2}^-[530]$	$\frac{1}{2}^-$	1139.84	1142		9	170	70	$\frac{1}{2}^+[400]$	$\frac{1}{2}^+$	974.29	975	20	90	359	983
	$\frac{3}{2}^-$	1145.60	1158	4	34	615	476		$\frac{3}{2}^+$	1001.62	1000	3	49	173	783
	$\frac{5}{2}^-$	1253.1	1251		7	58	112		$\frac{5}{2}^+$	1059.6	1060	4	14	78	249
	$\frac{7}{2}^-$	1239.4	1220	2	3	135	92		$\frac{7}{2}^+$	1120.3	1120		14	92	325
	$\frac{9}{2}^-$	1442.8	1455		10	190	42		$\frac{9}{2}^+$	1229.3	1229	13	3	68	77

Quasi-particle systematics

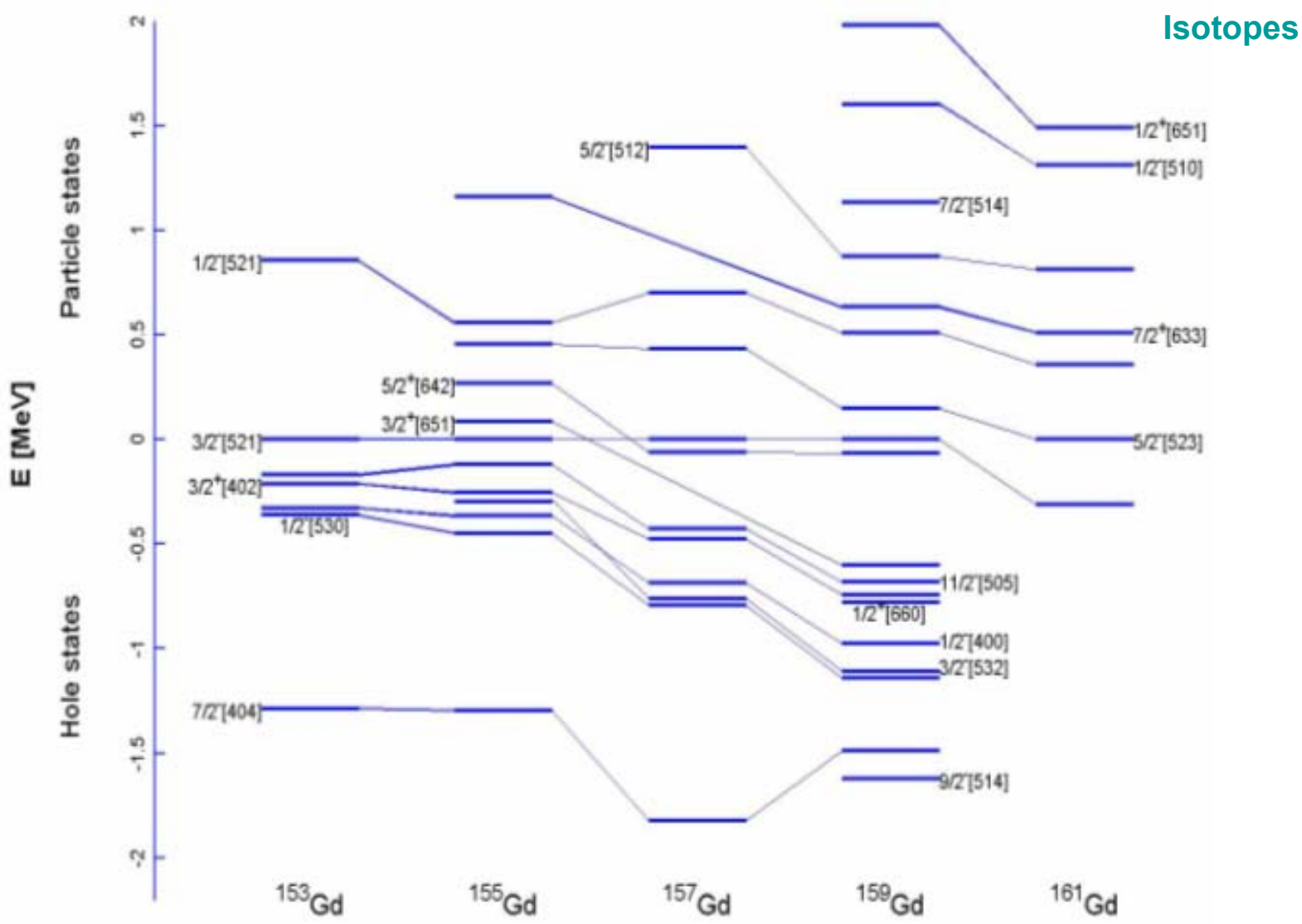

Quasi-particle systematics

Isotones

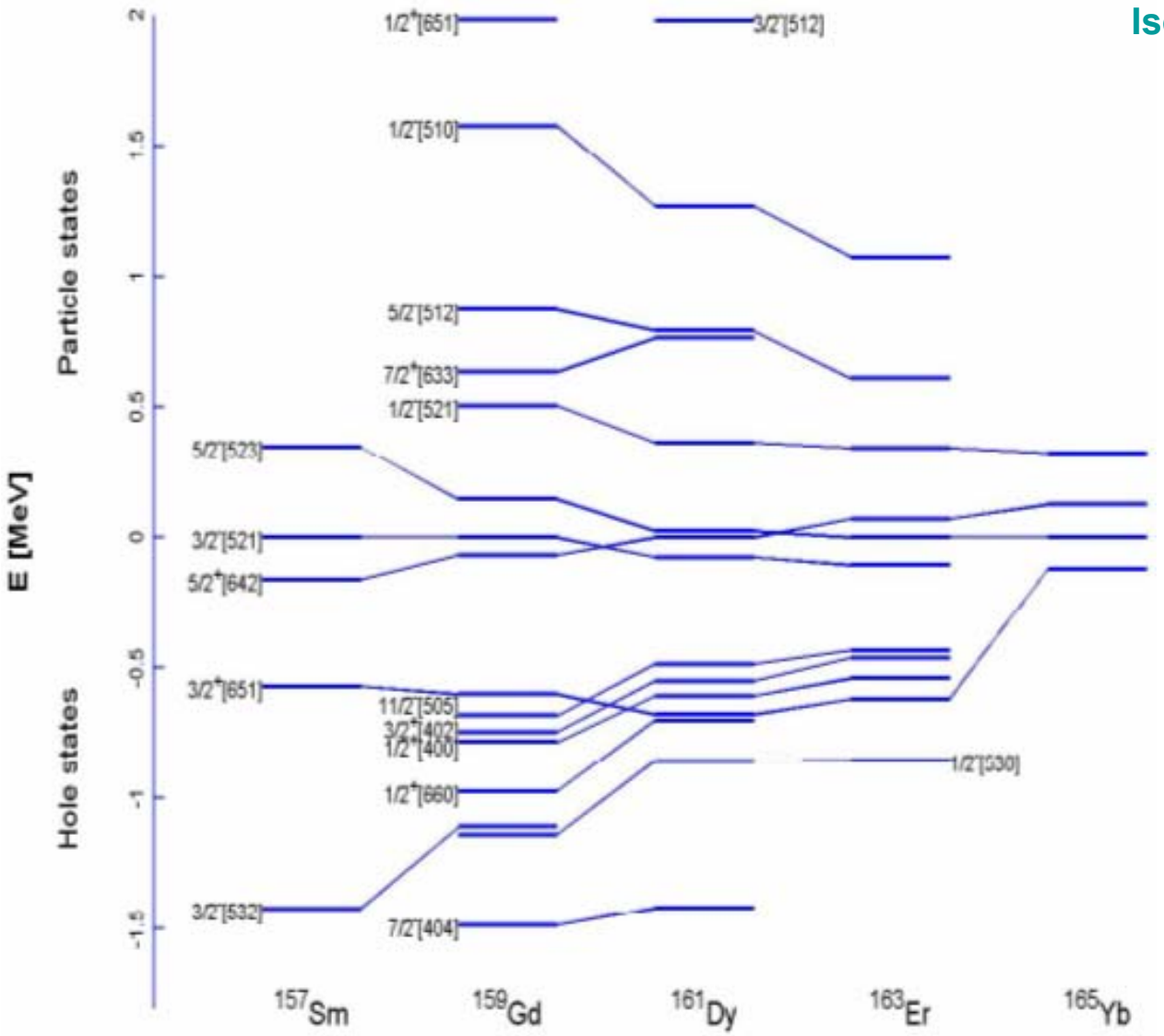

Quasi-particle systematics

Isotopes

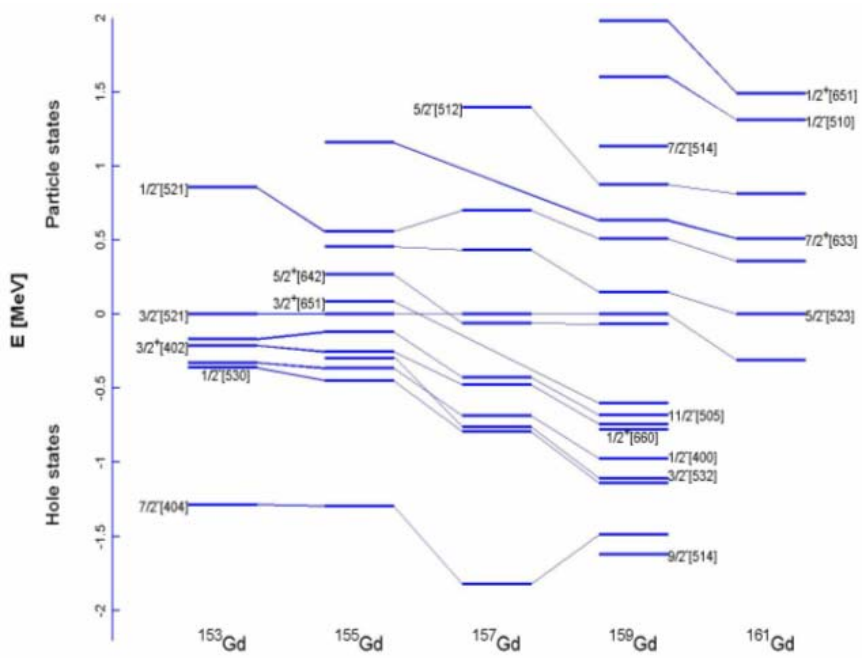

Isotones

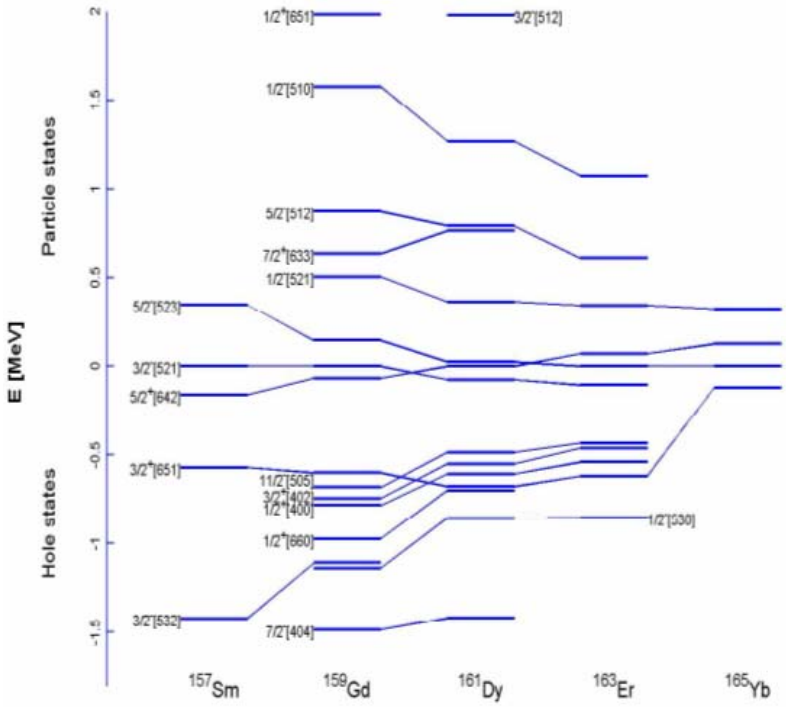

Nuclear spectroscopy with neutrons

Nuclear structure of ^{159}Gd

C. Granja* and S. Pospíšil
Institute of Experimental and Applied Physics, Czech Technical University in Prague, CZ–12800 Prague 2, Czech Republic

A. Aprahamian
Department of Physics, Notre Dame University, South Bend, IN–46556, USA

H. Börner and H. Lehmann
Institut Laue–Langevin, BP 156, F–38042 Grenoble, France

T. von Egidy and H.–F. Wirth
Physik–Department, Technische Universität München, D–85748 Garching, Germany

G. Graw, R. Hertenberger, and Y. Eisermann
Sektion Physik, Ludwig–Maximilians–Universität München, D–85748 Garching, Germany

D. Nosek
Faculty of Mathematics and Physics, Charles University, CZ–18000 Prague 8, Czech Republic

L. Rubáček†
Faculty of Nuclear Sciences and Physical Engineering,
Czech Technical University in Prague, CZ–11519 Prague 1, Czech Republic

S. A. Telezhnikov
Joint Institute for Nuclear Research, 141–980 Dubna, M.R. Russia
(Dated: September 23, 2003)

Physical Review C (2004) in print

Literature

TEXTBOOKS

Elements of Neutron Physics, K. Wirtz and K. H. Beckurts, Springer – Verlag (1958)

Neutron Radiative Capture, Ed. R. E. Chrien, Pergamon Press (1984)

Neutron Sources for Basic Physics and Applications, Ed. S. Cierjacks, Pergamon Press (1983)

Neutron Physics, L. Koester and A. Steyerl, Springer – Verlag (1977)

Radiation Detection and Measurement, G. F. Knoll, North – Holland (2000)

Introduction to Nuclear Physics, K. Krane, Springer (1998)

Elements of Nuclear Physics, Mayerhof, Mc. Graw – Hill (1974)

PROCEEDINGS

Proceedings of the ***International Conference on Nuclear Structure Study with Neutrons***, Budapest, Ed. J. Ero, Akademia Kiado Budapest (1974)

All Proceedings of the ***International Symposium on Capture Gamma – Ray Spectroscopy and Related Topics***: last held in Prague (2001), next: to be held in Notre Dame (2005)

Proceedings of the "***Europhysics Topical Conference on Neutron Induced Reactions***", Ed. P. Oblozinsky, Smolenice, Czechoslovakia (1982)

Proceedings of the "***4th International Symposium on Neutron Induced Reactions***", Eds. J. Kristiak, E. Betak, Smolenice, Czechoslovakia (1985)

Proceedings of "***Joint Summer School JINR – Romania on Neutron Physics for Investigation of Nuclei, Condensed Matter and Life Sciences***", Baia Mare, Romania, July (2002)

Proceedings of the ***Symposium on Neutron Physics*** at Rensselaer Polytechnic Institute, Ed. M. L. Yeater, Ac. Press New York (1962)

Contributions of the ***Conference on Nuclear Structure Study with Neutrons***, Budapest, Ed. L. Janossy, Central Research Institute for Physics, Budapest (1972)

Proceedings of the Workshop on ***Nuclear Physics and Fundamental Physics with Neutrons II***, KEK, Tsukuba, Ed. Y. Masuda (1996)

User Guide for ***Neutron Experimental Facilities at JINR***, Ed. A. V. Belushkin, Dubna (1991)

Neutron Experimental Facilities for Nuclear Research Investigations, Ed. V. V. Sikolenko, Frank Laboratory of Neutron Physics, JINR Dubna (1997)

Proceedings of the ***4th Workshop on Radiative Capture***, Berkeley, Ed. S. A. Wender, Los Alamos (1990)